



City Research Online

City, University of London Institutional Repository

Citation: Annibal, P. S. (1990). Statistical analysis and Kalman filtering applied to nuclear materials accountancy. (Unpublished Doctoral thesis, City, University of London)

This is the accepted version of the paper.

This version of the publication may differ from the final published version.

Permanent repository link: <https://openaccess.city.ac.uk/id/eprint/29031/>

Link to published version:

Copyright: City Research Online aims to make research outputs of City, University of London available to a wider audience. Copyright and Moral Rights remain with the author(s) and/or copyright holders. URLs from City Research Online may be freely distributed and linked to.

Reuse: Copies of full items can be used for personal research or study, educational, or not-for-profit purposes without prior permission or charge. Provided that the authors, title and full bibliographic details are credited, a hyperlink and/or URL is given for the original metadata page and the content is not changed in any way.

STATISTICAL ANALYSIS AND KALMAN FILTERING
APPLIED TO
NUCLEAR MATERIALS ACCOUNTANCY

A thesis by

Peter Stewart Annibal

for the degree of

Doctor of Philosophy

submitted to

City University, London

Control Engineering Centre

Department of Electronic, Electrical and Information Engineering

in

August 1990

CONTENTS

TABLE OF CONTENTS	i
LIST OF TABLES	v
LIST OF FIGURES	vi
ACKNOWLEDGEMENTS	x
PREVIOUS PUBLICATION OF MATERIAL	xi
DECLARATION	xii
ABSTRACT	xiii
NOTATION	xiv
Statistical tests	
Pneumerators	
Subscripts	
Expansion coefficients	
Main variables	
MVUE notation	
Correlation notation	
Kalman Filter notation	
1. Introduction	1-1
2. Nuclear Material Accountancy	2-1
2.1 Introduction	2-1
2.2 Material Unaccounted For	2-1
2.3 Sources of MUF	2-2
2.4 Near Real Time Materials Accountancy	2-3
2.5 Test procedure	2-5
2.5.1 Comparison with a threshold	2-5
2.5.2 Application to Page's CUSUM Test	2-7
2.6 Test statistics proposed for NRTMA	2-10
2.6.1 MUF, CUMUF & ACUMUF	2-10
2.6.2 Filters	2-13
2.6.3 Smoothers	2-18
2.7 Choice of thresholds	2-20
2.8 Choice of performance benchmarks	2-25

3. Plant description	3-1
3.1 Introduction	3-1
3.2 Techniques and problems in nuclear material determination	3-1
3.3 Description of the Dounreay Fast Reactor Fuel Reprocessing Plant	3-2
3.4 Plant measurements in the head-end	3-5
3.5 Determination of liquor height by the pneumaticator system	3-6
3.6 Modelling the head-end MBA	3-8
3.7 Summary	3-8
4. A minimum variance estimate of the transfer from an accountancy tank	4-1
4.1 Introduction	4-1
4.2 Mass transfer measurement and instrumentation	4-2
4.2.1 The basis of mass transfer calculation	4-2
4.2.2 Laboratory measurements	4-2
4.2.3 The pneumaticator systems	4-3
4.3 Equations of Mass Transfer Calculation	4-4
4.4 Sensitivity of the weighting coefficients	4-11
4.5 Analysis of the sensitivity to measurement bias	4-13
4.6 Results	4-15
4.7 Summary	4-16
5. Analysis of correlations in the MUF sequence	5-1
5.1 Introduction	5-1
5.2 Derivation of the covariance between successive MUF values	5-2
5.3 Correlations over more than one interval	5-4
5.4 Application to the Fast Reactor Fuel Reprocessing Plant	5-5
5.4.1 Plant measurements in the head-end MBA	5-5
5.4.2 Plant measurements in the solvent extraction MBA	5-6
5.5 Application of the MUF-residuals transformation	5-8
5.6 Results	5-9

5.7 Summary	5-36
6. Application of a Kalman Filter	6-1
6.1 Introduction	6-1
6.2 The basic Kalman Filter	6-1
6.3 Application to the Fast Reactor Fuel Reprocessing Plant	6-4
6.3.1 Introduction	6-4
6.3.2 Modelling the 'ideal' plant	6-6
6.3.3 Augmentation of the state vector to describe plant conditions	6-7
6.3.4 Calculation of the progression matrix and progression noise vector	6-10
6.3.5 Kalman Filter equations	6-14
6.4 Performance of the Kalman Filter	6-17
6.5 Results	6-19
6.6 The use of a 'twin' test	6-21
6.7 Summary	6-32
7. Conclusions & suggestions for future work	7-1
7.1 Accountancy tank MVUE	7-1
7.2 Modelling the plant measurement system	7-1
7.3 Future work	7-4
8. References & Bibliography	8-1
APPENDIX I - Liquor height in a tank from pneumericator readings	I-1
APPENDIX II - Derivation of the components of Table 4.1	II-1
APPENDIX III - General derivation of MVUE coefficients	III-1
APPENDIX IV - Calculation of accountancy tank transfer MVUE coefficients	IV-1
APPENDIX V - Comparison of the sensitivity to measurement bias	V-1

of the MVUE with the existing four methods

APPENDIX VI - Setting the alarm thresholds	VI-1
APPENDIX VII - A method of generating the residuals sequence from a general covariance matrix	VII-1
APPENDIX VIII - Derivation of the Kalman Filter	VIII-1

TABLES

Table 4.1	Terms used in forming the accountancy tank transfer estimate	4-5
Table V.1	Percentage change in estimate of accountancy tank transfer for a 3σ bias	V-1
Table V.2	Percentage change in estimate of accountancy tank transfer for a 1% bias	V-2

FIGURES

2.1	Sample probability density, MUF data	2-3
2.2	Setting thresholds to achieve the required credibility	2-6
2.3	Continuous plot of CUSUM with V-mask	2-8
2.4	Plot of S^+ and S^-	2-9
2.5	Effect of unaccounted negative correlation on the credibility	2-11
2.6	Cumulative false alarm probabilities with fixed CUMUF thresholds, Threshold test	2-24
3.1	Schematic of the Fast Reactor Fuel Reprocessing Plant	3-3
3.2	The basic pneumaticator system	3-7
3.3	Schematic of the accountancy tank	3-8
5.1	Sample data, old accountancy system (independent dissolver assessment)	5-10
5.2	Cumulative alarm probs. for abrupt loss, old system: Threshold test with MUF, MUFR, ITMUF	5-13
5.3	Cumulative alarm probs. for abrupt loss, old system: Page's Test with MUF, MUFR, ITMUF	5-14
5.4	Cum. alarm probs. for protracted loss, old system: Threshold test with MUF, MUFR, ITMUF	5-15
5.5	Cum. alarm probs. for protracted loss, old system: Page's Test with MUF, MUFR, ITMUF	5-16
5.6	Cum. alarm probs. for loss over 5 periods, old system: Threshold test with MUF, MUFR, ITMUF	5-17
5.7	Cum. alarm probs. for loss over 5 periods, old system: Page's Test with MUF, MUFR, ITMUF	5-18
5.8	Cumulative alarm probabilities for alternate loss with fractional replacement, old system:	5-19

	Threshold test with MUF, MUFR, ITMUF	
5.9	Cumulative alarm probabilities for alternate loss with fractional replacement, old system: Page's Test with MUF, MUFR, ITMUF	5-20
5.10	Absolute power for abrupt loss on period 30, old sys: Threshold test with MUF, MUFR, ITMUF	5-21
5.11	Absolute power for abrupt loss on period 30, old sys: Page's Test with MUF, MUFR, ITMUF	5-21
5.12	Absolute power for protracted loss, old system: Threshold test with MUF, MUFR, ITMUF	5-22
5.13	Absolute power for protracted loss, old system: Page's Test with MUF, MUFR, ITMUF	5-22
5.14	Sample data, new accountancy system (dissolver assumed from sub-assembly burn-up calculation)	5-23
5.15	Cumulative alarm probs. for abrupt loss, new system: Threshold test with MUF, MUFR, ITMUF	5-27
5.16	Cumulative alarm probs. for abrupt loss, new system: Page's Test with MUF, MUFR, ITMUF	5-28
5.17	Cum. alarm probs. for protracted loss, new system: Threshold test with MUF, MUFR, ITMUF	5-29
5.18	Cum. alarm probs. for protracted loss, new system: Page's Test with MUF, MUFR, ITMUF	5-30
5.19	Increase in power for a protracted loss due to incorrect assumption of negative correlation	5-31
5.20	Cumulative alarm probabilities for alternate loss with fractional replacement, new system: Threshold test with MUF, MUFR, ITMUF	5-32
5.21	Cumulative alarm probabilities for alternate loss with fractional replacement, new system: Page's Test with MUF, MUFR, ITMUF	5-33
5.22	Absolute power for abrupt loss on period 30, new sys:	5-34

	Threshold test with MUF, MUFR, ITMUF	
5.23	Absolute power for abrupt loss on period 30, new sys: Page's Test with MUF, MUFR, ITMUF	5-34
5.24	Absolute power for protracted loss, new system: Threshold test with MUF, MUFR, ITMUF	5-35
5.25	Absolute power for protracted loss, new system: Page's Test with MUF, MUFR, ITMUF	5-35
6.1	Cumulative alarm probs. for abrupt loss, old system: Threshold test with MUF, MUFR, KALR, KALMUF, CUMUF	6-22
6.2	Cumulative alarm probs. for abrupt loss, old system: Page's Test with MUF, MUFR, KALR, KALMUF	6-23
6.3	Cum. alarm probs. for protracted loss, old system: Threshold test with MUF, MUFR, KALR, KALMUF, CUMUF	6-24
6.4	Cum. alarm probs. for protracted loss, old system: Page's Test with MUF, MUFR, KALR, KALMUF	6-24
6.5	Cumulative alarm probabilities for alternate loss with fractional replacement, old system: Threshold test with MUF, MUFR, KALR, KALMUF, CUMUF	6-25
6.6	Cumulative alarm probabilities for alternate loss with fractional replacement, old system: Page's Test with MUF, MUFR, KALR, KALMUF	6-25
6.7	Absolute power for abrupt loss on period 30, old sys: Threshold test with MUF, MUFR, KALR, KALMUF, CUMUF	6-26
6.8	Absolute power for abrupt loss on period 30, old sys: Page's Test with MUF, MUFR, KALR, KALMUF	6-26
6.9	Absolute power for protracted loss, old system: Threshold test with MUF, MUFR, KALR, KALMUF, CUMUF	6-27
6.10	Absolute power for protracted loss, old system: Page's Test with MUF, MUFR, KALR, KALMUF	6-27
6.11	Cum. alarm probs. for protracted loss, new system: Threshold test with MUF, MUFR, KALR, KALMUF, CUMUF	6-28

6.12	Cum. alarm probs. for protracted loss, new system: Page's Test with MUF, MUFR, KALR, KALMUF	6-28
6.13	Absolute power for abrupt loss on period 30, new sys: Threshold test with MUF, MUFR, KALR, KALMUF, CUMUF	6-29
6.14	Absolute power for abrupt loss on period 30, new sys: Page's Test with MUF, MUFR, KALR, KALMUF	6-29
6.15	Absolute power for protracted loss, new system: Threshold test with MUF, MUFR, KALR, KALMUF, CUMUF	6-30
6.16	Absolute power for protracted loss, new system: Page's Test for with MUF, MUFR, KALR, KALMUF	6-30
6.17	Effect of varying H-K pair in Page's Test: Abrupt loss, new system	6-31
6.18	Effect of varying H-K pair in Page's Test: Protracted loss, new system	6-31
I.1	Conversion of pneumatic readings to pressures	I-2
VI.1	CUMUF threshold curves to maintain constant false alarm probability	VI-2
VI.2	Cumulative false alarm probabilities: Varying CUMUF thresholds, new accountancy system	VI-3
VI.3	Page's Test H-K curve for MUF, old accountancy system	VI-4
VI.4	Page's Test H-K curve for MUFR	VI-4
VI.5	Page's Test H-K curve for ITMUF, old accountancy system	VI-4
VI.6	Page's Test H-K curve for KALR	VI-4
VI.7	Page's Test H-K curve for MUF, new accountancy system	VI-5
VI.8	Page's Test H-K curve for ITMUF, new accountancy system	VI-5

ACKNOWLEDGEMENTS

The author wishes to express his gratitude to the Atomic Energy Authority for funding this work under the AEA Technology Safeguards R & D Project, and for providing computing and other facilities at Winfrith Technology Centre, Dorset. He would like to thank Mr T L Jones, Dounreay Nuclear Power Development Establishment, Mr A Hopkinson, Winfrith Technology Centre, and Mr R Gale, formerly of Winfrith Technology Centre, for their assistance with practical and theoretical aspects, and Professor P D Roberts of City University for supervising the project.

PREVIOUS PUBLICATIONS OF MATERIAL

P S Annibal & Prof P D Roberts; Improvements in statistical techniques for Nuclear Materials Accountancy. Published at the 11th Annual Symposium on Safeguards and Nuclear Material Management, organised by the European Safeguards Research and Development Association, May/June 1989.

P S Annibal & Prof P D Roberts; The application of statistical techniques to Nuclear Materials Accountancy. AEA Technology Safeguards R & D Report, SRDP-166, 1990.

DECLARATION

The author grants discretionary powers to the University Librarian to allow the thesis to be copied in whole or in part without further reference to the author.

ABSTRACT

It is important for political, commercial, security and safety reasons to be assured that all nuclear material is accounted for at all times. However, measurement and accessibility problems mean that there will always be a degree of uncertainty, which can be minimized but not eliminated by careful design of nuclear plants and instruments.

Much theoretical research has been carried out on the development of statistical methods for nuclear material accountancy. In practice, physical, financial and time constraints mean that the techniques must be adapted to give an optimal performance in plant conditions. This thesis aims to bridge the gap between theory and practice, to show the benefits to be gained from a knowledge of the facility operation.

Four different aspects are considered; firstly, the use of redundant measurements to reduce the error on the estimate of the mass of heavy metal in an 'accountancy tank' is investigated. Secondly, an analysis of the calibration data for the same tank is presented, establishing bounds for the error and suggesting a means of reducing them. Thirdly, a plant-specific method of producing an optimal statistic from the input, output and inventory data, to help decide between 'material loss' and 'no loss' hypotheses, is developed and compared with existing general techniques. Finally, an application of the Kalman Filter to materials accountancy is developed, to demonstrate the advantages of state-estimation techniques.

The results of the analyses and comparisons illustrate the importance of taking into account a complete and accurate knowledge of the plant operation, measurement system, and calibration methods, to derive meaningful results from statistical tests on materials accountancy data, and to give a better understanding of critical random and systematic error sources.

The analyses were carried out on the head-end of the Fast Reactor Reprocessing Plant, where fuel from the prototype fast reactor is cut up and dissolved. However, the techniques described are general in their application.

NOTATION

Statistical tests

NRTMA	Near Real Time Material Accountancy
MUF	Material Unaccounted for
CUMUF	Cumulative MUF
ACUMUF	Average Cumulative MUF
ITMUF	Independently Transformed MUF
MUFR	MUF-Residual
KALR	Kalman-Residual
KALMUF	Kalman-MUF
REMUF	Retrospective-MUF
GEMUF	Geschätzter-MUF (Estimated-MUF)

Pneumercators

A	"Overall" gauge reading (tank full) (mm H ² O)
a	"Heel" reading (from "Overall" gauge) (mm H ² O)
P	"Neck" gauge reading (mm H ² O)
s	in tank specific-gravity meter reading (mm H ² O)
d	distance between dip-tubes on 's' (mm)
D	distance between 'overall' and 'neck' dip tubes (mm)

Subscripts

T	"at tank temperature"
t	"at laboratory temperature"
20	"at 20°C"
L	"of liquor"
w	"of water"
a	"of air"

Expansion coefficients

α	expansion coefficient of 5M nitric acid at 20°C
δ	volume expansion coefficient of stainless steel tank at 20°C

Main variables

T tank temperature ($^{\circ}\text{C}$)
t laboratory temperature ($^{\circ}\text{C}$)
L mass of heavy metal (g)
 ρ density (g/l)
Z concentration of heavy metal, weight for weight (g/g)
Y concentration of heavy metal, weight for volume (g/l)

MVUE notation

[L] Minimum Variance Unbiased Estimate of the mass transfer (g)

V Volume of transfer (l)

$C_{w/V}$ Concentration, weight for volume (g/l)

$C_{w/W}$ Concentration, weight for weight (g/g)

C_1, V_1 $C_{w/V}$, V calculated from lab. determined density

C_2, V_2 $C_{w/V}$, V calculated from in-tank density estimate 's'

C_3, V_3 $C_{w/V}$, V calculated from hydrostatic pressure difference ('A' - 'P')

C_4 $C_{w/V}$ using plant control determination 'Y'

[L₁] Minimum variance estimate of mass transfer, using lab. determined density to calculate volume

[L₂] Minimum variance estimate of transfer using in-tank density determination 's' to calculate volume

[L₃] Minimum variance estimate of transfer using hydrostatic pressure difference (A - P) to determine volume

ψ Functional relationship representing the tank calibration process relating liquor height to volume

v_1, v_2, v_3, v_4 Coefficients for [L₁]

$\gamma_1, \gamma_2, \gamma_3, \gamma_4$ Coefficients for [L₂]

$\eta_1, \eta_2, \eta_3, \eta_4$ Coefficients for [L₃]

ω_{1-12}	MVUE weighting coefficients for [L]
Σ	Summation operator
i, j	Summation indices
σ	Standard deviation
λ	Lagrangian undetermined multiplier
Λ	Matrix to be inverted to obtain minimum variance coefficients

Correlation notation

Inv	Inventory
U	Net input
IP	Input
OP	Output
Cor	Correlation
Cov	Covariance
$\sigma^2(x)$	Variance of x

Subscripts refer to the balance period number

Kalman Filter notation

\underline{x}	State vector
A	Progression matrix
\underline{u}	Input vector
$\underline{\omega}$	Progression model error vector
\underline{z}	Measurement vector
H	Observation matrix
\underline{v}	Measurement error vector
Q	Progression model error covariance matrix
R	Measurement model error covariance matrix
$\tilde{\underline{x}}$	Predicted state vector
P	Covariance matrix of predicted state
$\hat{\underline{x}}$	Estimated state vector
G	Covariance matrix of estimated state
K	Kalman gain matrix

1. Introduction

In any field dealing with valuable or dangerous materials, the operator will want assurance that all quantities in his care are secure and accounted for. In many cases the risk will be clearly defined: for example, theft for precious metals, or leakage to the environment for toxic or radio-active chemicals.

For the nuclear fuel cycle there is the additional need related to international agreements covering the restriction placed on the use of fissile plutonium and uranium. The processes of verifying the use of these materials, which are implemented by the International Atomic Energy Agency (IAEA) and Euratom, are collectively known as international safeguards. Safeguards are essential to encourage public confidence and assure the international forum of the integrity of the nuclear fuel cycle.

The aim of the Safeguards Inspectors is to establish with a high degree of confidence that no material has been diverted from civil use. In designing a safeguards system, the task must be viewed as a non-cooperative two-person game. The political consequences of the inspectors decision are significant; if history proves his declaration of confidence in the integrity of the declared material cycle false, the value of safeguards is severely weakened. If, on the other hand, the available data points mistakenly to a misappropriation, the operator may question his involvement in a treaty entered voluntarily.

There is thus good reason to take all necessary steps to minimize the uncertainty on measurements of nuclear materials. While instrumentation is continuously improving, in certain parts of a nuclear plant

transducers cannot be changed after installation. Thus there will always be limits to the accuracy with which determinations can be made, which leave a 'grey area' in which it is difficult to decide whether the discrepancies are due to measurement error or diversion. This is where statistical tools play their part; calculating the standard deviations, conditioning the data, and applying decision criteria.

The task of material accountancy is essentially a control problem, using information from inputs, outputs and inventories to decide whether the process is 'in control', that is, no loss of material is taking place. Much general theoretical work has been carried out on different aspects of material accountancy, but as yet no standard techniques have been adopted. Suggestions pertaining to the research carried out here are discussed in the next chapter.

This thesis demonstrates the application of statistical and control theory to materials accountancy in a practical nuclear facility, to either improve accuracy or knowledge of the errors. The benefits have been quantified either by theoretical calculation, or by statistical simulation.

An introduction to the principles and practices of nuclear material accountancy is given in chapter 2, together with a summary of the research already carried out in this field.

In bridging the gap between the theoretical developments and practical application, an understanding of the plant under consideration is required. Chapter 3 contains a general introduction to the techniques and problems of assaying nuclear materials, and a description of the operation and instrumentation of part of the Fast Reactor Fuel Reprocessing Plant at Dounreay, Caithness. The impact of this on the

material accountancy is also considered.

The research carried out for this thesis falls into two areas of materials accountancy. The first is concerned with applying statistical techniques to improve the quality of the accountancy data. Currently, the most accurate process quantification of nuclear material is carried out in an accountancy tank, with the material in solution. Chapter 4 describes a technique for minimizing the random variance of the estimate of material in an accountancy tank, by utilizing parallel, redundant measurements.

The second area involves the use of plant data to quickly and accurately identify a material diversion. In Chapter 5, a plant-specific method of producing an optimal statistic from the input, output and inventory data, to help decide between 'material loss' and 'no loss' hypotheses, is developed and compared with existing general techniques.

Paralleling this, Chapter 6 illustrates the use of state-estimation techniques in the form of a Kalman Filter as an alternative means of producing an optimal test statistic.

The conclusions, and suggestions for further work, are presented in chapter 7.

2. Nuclear material accountancy

2.1 Introduction

To set the context of the research described in this thesis, and explain the methods and terminology of nuclear materials accountancy, this chapter comprises a summary of the fundamental definitions and the data-processing techniques suggested for the quantitative application of nuclear material safeguards.

2.2 Material Unaccounted For

An important aspect of nuclear safeguards involves accurate knowledge of the whereabouts and quantities of all nuclear materials. This is termed 'material accountancy'. As even small quantities of some nuclear materials, particularly plutonium and uranium-235, are of strategic value, careful checks are kept on the discrepancy between expected and measured quantities.

Thus the fundamental statistic in nuclear material accountancy is 'Material Unaccounted For' (MUF), which can be defined as [1]:

$$\text{Material Unaccounted For} = \text{Book inventory} - \text{Physical inventory}$$

A boundary is drawn around the accountancy area, and all transactions of material through this boundary are recorded. At regular intervals, a 'balance' is struck, comparing the expected inventory with the plant measurements. The difference is the MUF for that 'balance period'. Thus for balance period k ;

$$\text{MUF}_k = (\text{Inv}_{k-1} + U_k) - \text{Inv}_k \quad (2.1)$$

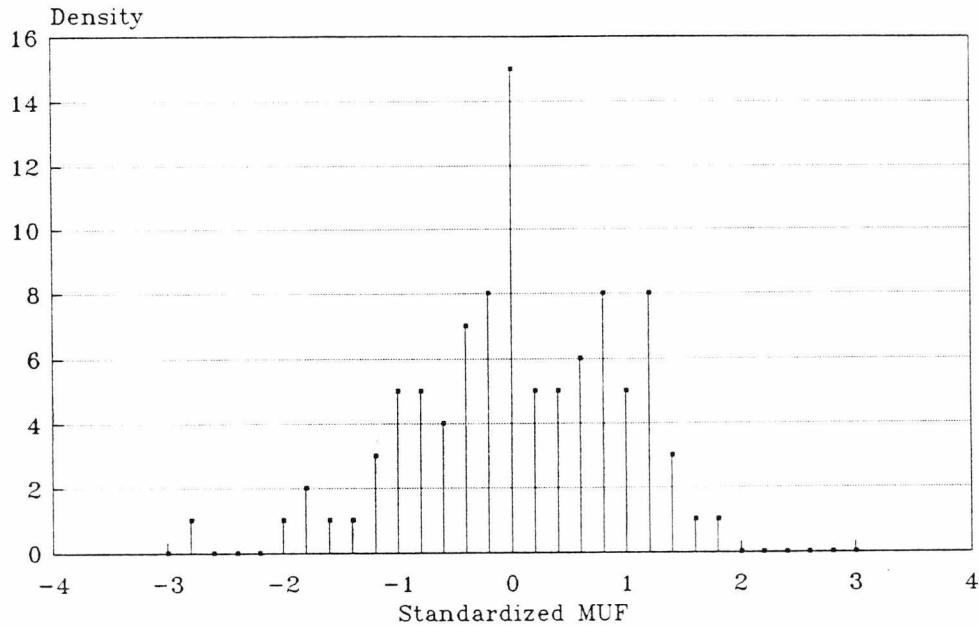
where Inv_k is the measured inventory of the area at the end of balance period k , and U_k is the measured net input to the area during the balance period.

2.3 Sources of MUF

MUF can result either from a real loss (or gain) of material, from measurement errors [2], or from errors in recording or processing the data. Statistical tests are used to identify anomalies which require further investigation.

Analysis of the MUF over a number of balance periods can help identify systematic errors in any of the estimates, and indicate transcription faults by showing an inconsistency.

As each MUF statistic comprises several measurements, it is generally assumed (by the central limit theorem) to be approximately normally distributed. Little reliable real data exists to confirm this; figure 2.1 shows a rough probability density distribution of the standardized MUF for 100 balance periods in part of the Fast Reactor Fuel Reprocessing Plant at Dounreay. The distribution is distorted by the fact that the mean of each MUF value is not necessarily zero - this is discussed in more detail later. However, it does indicate that the normal assumption is reasonably valid.



MUF data from PFR Reprocessing Plant
100 balance periods

Figure 2.1 Sample probability density, MUF data

2.4 Near Real Time Material Accountancy

In 'traditional' material accountancy, a material balance is struck relatively infrequently - typically twice a year. Intermediate inventories are only approximations, used for plant control purposes. Improvements in the accuracy and speed with which measurements can be made has led to 'Near Real Time Material Accountancy' (NRTMA), where balances are calculated perhaps once per day. This reduces the time taken to detect a diversion (an important consideration if the material could be quickly converted to military purposes), but careful consideration must be given to minimizing the false alarm rate, to avoid unnecessary time and expense in investigation.

Much discussion and development of NRTMA has taken place over the last

decade; the first experiments at commercial reprocessing plants were instigated in 1980 at Tokai, Japan [3,4], and Dounreay, Scotland [5]. A summary of the status of the NRTMA theory in 1982 is described by Lovett et al [6] and Gupta et al [7].

Disputes over the relative ability of NRTMA to ultimately detect a diversion of a given amount of material, compared to traditional accountancy, were addressed by Jones [8]; he demonstrated that in a 'worst case' of protracted loss carefully designed NRTMA was only marginally inferior, and was likely to 'alarm' much earlier.

The performance of a test against any loss in conventional accountancy can be compared with the 'optimal' Neyman-Pearson test for that scenario. The Neyman-Pearson lemma assumes that the diversion scenario is known, and enables the maximum possible detection probability to be calculated [9,10]. The test can be expressed:

$$NP_k = \underline{M}_k^T \cdot \Sigma_k^{-1} \cdot \underline{MUF}_k \quad (2.2)$$

where \underline{M}_k is the loss vector up to period k. In practice, this is not applicable, as the loss is unknown.

The introduction of NRTMA has greatly broadened the range of statistical treatment that can be carried out on the data. The loss pattern, as well as the loss magnitude, is now an unknown variable, so no single equivalent of the Neyman-Pearson tests exists as a guide to the design of an optimal detector for all diversion scenarios. This problem is discussed by Leitner et al [11], who conclude that a sensible NRTMA strategy must be evolved from a consideration of likely diversion scenarios, acceptable detection/timeliness/false alarm compromises, and

plant specific considerations. No standard method has yet been adopted; a review of proposals is given in the next section.

In general, the test statistic (either the MUF or a quantity derived from it) can either be compared with a threshold linked to its variance [12], or submitted to Page's Cumulative Sum (CUSUM) test, which is described in the next section.

2.5 Test procedure

The MUF figures for a sequential set of balance periods are used as the basis for statistical tests, to detect material loss scenarios ranging from one large diversion to small diversions over a number of balance periods. The tests are designed to be as sensitive as possible, while attempting to ignore 'loss' due to measurement errors. The 'power' of a test is defined as its probability to alarm a diversion; the 'credibility' is the probability of not alarming if there is no diversion. A useful figure is the 'false alarm rate' (FAR), which is equal to (1-Credibility).

2.5.1 Comparison with a threshold

On balance period k , the test statistic for that period (denoted e_k) is compared to a predetermined threshold h_k . The test can be expressed

$$\text{Alarm if } e_k \geq h_k \quad (2.3)$$

While material losses are the main concern, an apparent gain that is 'out of bounds' also requires investigation. The test can thus be

written

$$\text{Alarm if } |e_k| \geq h_k \quad (2.4)$$

If e_k is zero-mean, with a standard normal distribution (calculated by dividing the source statistic by its standard deviation), for each application of the test the choice of ' h_k ' determines the credibility:

h_k	<u>Credibility</u>	<u>False alarm rate</u>
1.5	86.64%	13.36%
2.0	95.45%	4.55%
2.5	98.76%	1.24%
3.0	99.73%	0.27%

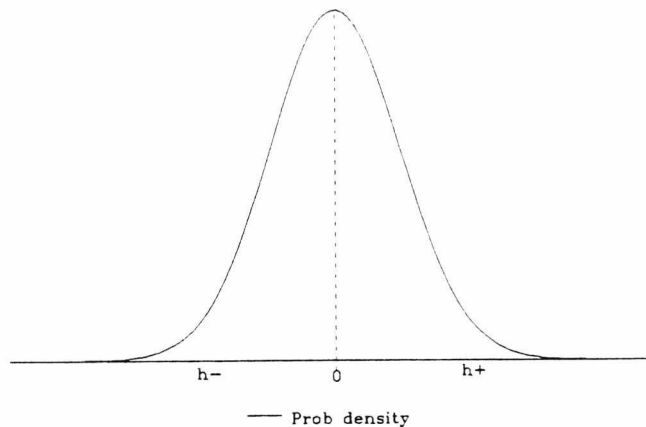


Figure 2.2 Setting thresholds to achieve the required credibility

A false alarm rate of 5% is generally regarded as acceptable. This is easy to apply in conventional accountancy, by choosing $h=2$. However, if the test statistics are independent, a campaign of 20 balance periods with the same threshold will give an overall credibility of $(0.9545)^{20}$, giving a false alarm rate of 60%, for NRTMA. To maintain the false

alarm rate at 5%, 'h' will have to be increased to 3.

This is covered in greater detail by Russell [13]. The same author also describes a method for calculating overall credibilities where the test statistics are correlated, by evaluating multinormal probability densities [14].

The power of a test is dependent on the loss scenario.

A time plot of a non-cumulative statistic is analogous to the Shewhart control chart [15].

2.5.2 Application to Page's CUSUM test

Page's CUSUM test [16] is a development of the sequential control chart, and has proved useful in process and quality control. At each step, a value S is attributed to the process; this is calculated from a plant parameter x , and is defined by

$$S_k^+ = \max (0, S_{k-1}^+ + x_k - K), \quad k=1, \dots, n \quad S_0^+ = 0 \quad (2.5)$$

An alarm is signalled if

$$S_k^+ \geq H \quad (2.6)$$

A second statistic is calculated to check for the negative 'out of control' condition:

$$S_k^- = \min (0, S_{k-1}^- + x_k + K), \quad k=1, \dots, n \quad S_0^- = 0 \quad (2.7)$$

This alarms if

$$S_k^- \leq H \tag{2.8}$$

In simple terms, the test allows a bias of K per balance period, and sums the drift away from the zero mean. By constraining $S^+ \geq 0$, and $S^- \leq 0$, the test responds quickly to a drift above the bias K . Figure 2.3 shows the test plotted in terms of x , using a V-mask. The slope of the mask is K ($\tan \theta = K$), and the mask is positioned such that the mouth of the V-mask on the point of application of the test is $2H$. If any point of the plot crosses the lower line, a positive 'out-of-control' signal is given. If it crosses the upper line, that alarm is negative. This representation gives a clear visual indication of the performance of the test parameter; if the bias alters, the point at which it occurs can be easily deduced.

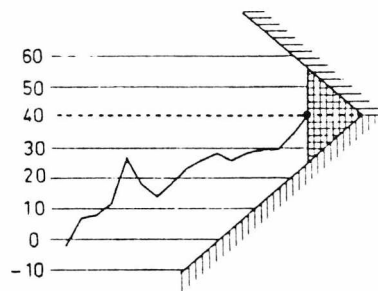


Figure 2.3 Continuous plot of CUSUM with V-mask

However, to contain the height of the graph, it is often more convenient to plot S . As S^+ is never less than zero, and S^- is never greater than zero, the two can be plotted on the same axes without conflict, as illustrated in figure 2.4. The equivalence of the two forms is demonstrated by De Bruyn [17].

2.6 Test statistics proposed for NRTMA

The test statistics currently used or proposed for NRTMA fall into three categories. Firstly, the MUF data may be interpreted directly or summed. Secondly, a technique may be adopted to remove the serial correlation from the MUF sequence, giving a set of zero-mean 'filtered' statistics. Thirdly, the latter technique can be extended to smooth the data, producing an estimate retrospectively with later information. The methods, advantages, and problems of each are set out below.

2.6.1 MUF, CUMUF & ACUMUF

The power and credibility of the tests are adversely affected by serial correlation in the test data.

There is an inherent covariance between successive MUF values due to the appearance of Inv_{k-1} in both MUF_k and MUF_{k-1} of

$$\text{Cov}(MUF_{k-1}, MUF_k) = -\sigma^2(Inv_{k-1}) \quad (2.11)$$

After the first balance period, the MUF values are not zero-mean. Assuming each MUF value has an approximately normal distribution, figure 2.5 illustrates that maintaining the 'decision thresholds' (to maintain the power) will result in an reduction of the credibility (a higher false alarm rate).

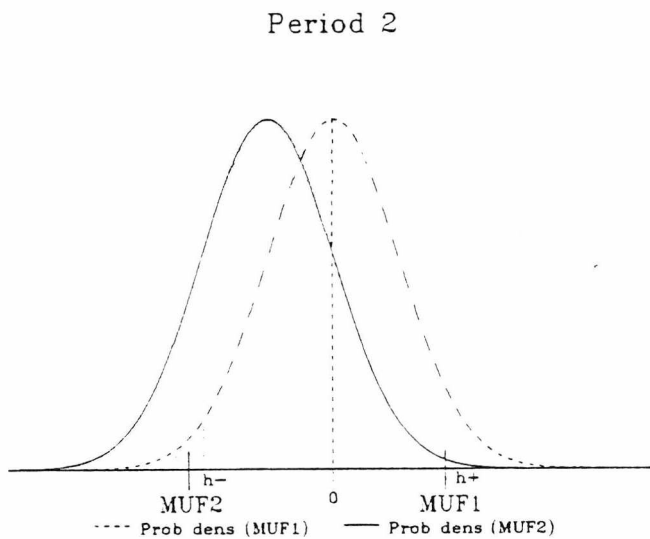
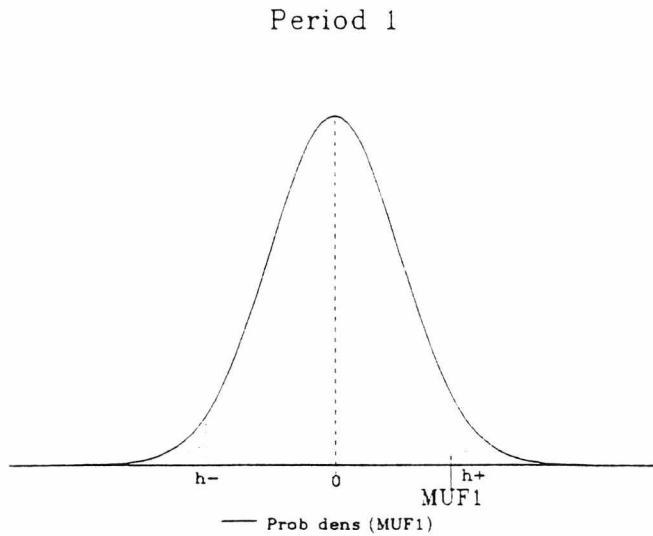


Figure 2.5 Effect of unaccounted negative correlation on the credibility

The MUF sequence is thus not the best indicator upon which to base decisions. Two basic approaches to ameliorate this effect may be adopted. Firstly, summing the MUF values over a number of balance periods (to give Cumulative MUF or CUMUF) will tend to reduce the significance of the correlation:

$$\text{CUMUF}_k = \sum_{i=1}^k \text{MUF}_i \quad (2.12)$$

This gives an unbiased estimate of the total loss for any diversion scenario. However, the variance increases with the number of balance periods:

$$\sigma^2(\text{CUMUF}_k) = \sum_{i=1}^k \left(\sigma^2(\text{IP}_i) + \sigma^2(\text{OP}_i) \right) + \sigma^2(\text{Inv}_0) + \sigma^2(\text{Inv}_k) \quad (2.13)$$

The sensitivity thus decreases as the campaign progresses, and the later statistics are highly correlated. The final CUMUF figure is equivalent to MUF in conventional accountancy, and gives an easily-interpretable insight. It is the Neyman-Pearson test for the whole campaign, and gives a minimum variance unbiased estimate of the total loss.

Similarly, Average CUMUF (ACUMUF) is defined as:

$$\text{ACUMUF}_k = \frac{1}{k} \text{CUMUF}_k \quad (2.14)$$

The scaling has no effect on the absolute performance of the test; ACUMUF behaves in the same manner as CUMUF. Both offer a high power/credibility compromise to detect losses early in a campaign, but the ratio decreases with an increasing number of balance periods. This weakness greatly reduces their effectiveness as safeguards deterrents - a potential diverter can easily plan an optimal theft strategy to minimize the risk of detection.

2.6.2 Filters

Given the same 'measurement model', which in this case translates to the MUF covariance matrix, all filters will generate the same results in the no-loss scenario. Three different approaches to obtaining a set of independent data from a correlated sequence have been developed. Stewart [25,26] described a method of diagonalizing the covariance matrix. In the nuclear safeguard field, Pike & Woods [27] took conditional expectations, calling the result Independently Transformed MUF (ITMUF). Using a plant model in which all inventories, inputs and outputs are determined independently on each balance period, and assuming constant variances on all the measurements, the errors on the MUF sequence can be described by a fixed, tri-diagonal covariance matrix:

$$F = \begin{bmatrix} \sigma^2 & \rho\sigma^2 & 0 & 0 & 0 & 0 \\ \rho\sigma^2 & \sigma^2 & \rho\sigma^2 & 0 & 0 & 0 \\ 0 & \rho\sigma^2 & \sigma^2 & \rho\sigma^2 & 0 & 0 \\ 0 & 0 & \rho\sigma^2 & \sigma^2 & \rho\sigma^2 & 0 \\ 0 & 0 & 0 & \rho\sigma^2 & \sigma^2 & \rho\sigma^2 \\ 0 & 0 & 0 & 0 & \rho\sigma^2 & \sigma^2 \end{bmatrix}$$

The correlation factor ρ will in general be in the range 0 (for a throughput-error dominated plant) to $-\frac{1}{2}$ (for an inventory error dominated plant) [13]. As all the variances are assumed fixed, ρ is also fixed. This covariance matrix can be used as the basis of a matrix transformation to yield the ITMUF sequence.

Calculation of the transformation matrix

Given a serially correlated vector \underline{x} , representing a MUF sequence with covariance matrix F , a transformation matrix to remove the serial

correlation can be calculated [13]. This matrix, B, is lower triangular with leading diagonal elements all '1'. The transformation can be stated as

$$\underline{y} = B \cdot \underline{x} \quad (2.15)$$

where each element of \underline{y} is independent of the others.

The matrix B has the property that

$$D = B \cdot F \cdot B^T \quad (2.16)$$

is diagonal. This is effected with a matrix of the form [13]:

$$B = \begin{bmatrix} 1 & 0 & 0 & \cdot & \cdot & 0 \\ B_{21} & 1 & 0 & & & \cdot \\ B_{31} & B_{32} & 1 & \cdot & & \cdot \\ \cdot & & & \cdot & \cdot & \cdot \\ \cdot & & & & \cdot & 0 \\ B_{n1} & \cdot & \cdot & \cdot & B_{n \ n-1} & 1 \end{bmatrix}$$

Thus,

$$ITMUF_1 = MUF_1$$

$$ITMUF_2 = B_{21} \cdot MUF_1 + MUF_2$$

$$ITMUF_3 = B_{31} \cdot MUF_1 + B_{32} \cdot MUF_2 + MUF_3$$

$$ITMUF_4 = B_{41} \cdot MUF_1 + B_{42} \cdot MUF_2 + B_{43} \cdot MUF_3 + MUF_4$$

Pike & Woods extended the covariance matrix to include calibration bias [28], and Beegden et al [29] also take systematic errors into account. The assumptions of independent measurements and constant covariances are still held.

For the 'ideal' plant generally considered [23,30,31], with a complete set of independent measurements taken on each balance period and a constant ratio of inventory:throughput, this technique will indeed be fairly effective.

Sellinschegg [32] derived a recursive algorithm for the same purpose, also based on conditional expectations. He termed the resulting sequence MUF-residuals, or MUFR.

$$\text{MUFR}_k = \text{MUF}_k - E(\text{MUF}_k | \text{MUF}_1, \dots, \text{MUF}_{k-1}) \quad (2.17)$$

Visualizing the same measurement model as Pike & Woods, he comments that this is identical to ITMUF. However, his derivation is expressed in more general terms and can be applied to different models.

To make the distinction clear, ITMUF will be used to describe the transformation with a fixed, tri-diagonal correlation matrix, the off-diagonal term being the average correlation between successive MUF figures, while MUFR will refer to a sequence with all the serial correlation removed. The principle of the calculation is identical to that of ITMUF; Sellinschegg describes an efficient recursive algorithm for effecting the transformation in the same paper [32].

The third method centres on the use of state estimation techniques, or the Kalman Filter [33,34]. A recursive matrix equation describing the plant parameters of interest in terms of the last determined state is drawn up; this will in general include an 'uncertainty' element reflecting the known range of deviation from the model progression. A measurement model describes the plant parameters in terms of the determinations that are made on the plant; these measurements will also

have an uncertainty associated with them. The Kalman Filter weights the predicted progression and the measurements according to their reliability, to produce optimal linear estimates of the parameters. A derivation of the Kalman Filter is given in Appendix VIII.

The application of Kalman Filtering to nuclear material accountancy was first suggested by Pike, Morrison & Westley [35]. They suggested a filter with the state vector comprising the inventory and the loss:

$$I_{k+1} = I_k + T_k - L_k \quad (2.18)$$

$$L_{k+1} = L_k + \alpha_k \quad (2.19)$$

where

I_k = True inventory at start of period k

T_k = True net transfers during period k

L_k = Material loss during period k

α_k = zero-mean random variable denoting modelling error

Using simulation, they demonstrated the improvements in performance offered by this technique over MUF and, to a lesser extent, ACUMUF. Stewart [25,26] developed a method for producing an optimal linear inventory estimate by weighting a progression model of the inventory and the measurements according to their accuracies, by minimum-variance techniques. This should give the same results as Pike et al's Kalman Filter when the loss is zero; however, by including the loss as a parameter, the Kalman Filter can adapt to be optimal for a loss scenario that fits the progression model - in this case, a constant loss on each

balance period.

Sellinschegg [32] demonstrates that the Kalman Filter can be used to generate approximate MUF-residuals. The Filter is built around a model of the MUF:

$$\tilde{MUF}_{k+1} = \tilde{MUF}_k \quad (\tilde{\text{ denotes an expected quantity)} \quad (2.20)$$

The measurement of the MUF can be expressed:

$$MUF_{k+1} = \tilde{MUF}_{k+1} - \eta_{k+1} - v_{k+1} + \varepsilon_{k+1} + \delta_{k+1} + \eta_k + v_k \quad (2.21)$$

- where η = random error in inventory determination
- v = systematic error in inventory determination
- ε = random error in transfer determination
- δ = systematic error in transfer determination

The key element of the state vector is the MUF, but it is augmented to allow for the correlations introduced by the systematic errors and the links with errors on other balance periods. The state vector is thus

$$\begin{pmatrix} \tilde{MUF} \\ \eta \\ v \\ \delta \end{pmatrix}$$

The approximate MUF-residual is calculated by subtracting the predicted value of the MUF from the measured value - as this is a Kalman Filter residual, it will be termed KALR:

$$KALR_{k+1} = MUF_{k+1} - \tilde{MUF}_{k+1} \quad (2.22)$$

In addition, the Kalman Filter produces a minimum variance unbiased linear estimate of the true mean MUF - a constant-loss estimator.

Shipley [36] uses a similar implementation in 'DECANAL', a software package for materials accountancy. Several progression models for the MUF can be invoked, giving optimal performance against constant, random or deterministic diversions.

The 'CIMA CT' material accountancy software package written at Winfrith Technology Centre [37] includes the Pike et al Filter and a two-state version of the Sellinschegg/Shipley Filter, with the systematic terms excluded. This package was originally written specifically for materials accountancy at the Fast Reactor Fuel Reprocessing Plant, and no data concerning systematic errors was available. These are described by Russell [19].

Just as the transformation techniques rely on the accuracy of the MUF covariance matrix, the Kalman Filter implementations require an accurate model of the process. Another illustration of the links between the covariance matrix approach and the Kalman Filter is provided by Nakamori & Hataji [38], who demonstrate the application of a Kalman Filter using the measurement error covariance matrix in place of the state-space progression model.

2.6.3 Smoothers

The correlation links to each MUF value go forward in time as well as back. By taking advantage of this, it is possible to smooth the MUF sequence. Pike et al describe how this can be effected with their

Kalman Filter [35]. Russell et al [39] developed a smoothed estimate based on an extension of ITMUF. The resulting statistic, termed Retrospective-MUF or REMUF, can be expressed:

$$\text{REMUF}_{k,d} = \text{MUF}_{k-d} - E\left(\text{MUF}_{k-d} \mid \text{MUF}_i; i=1, \dots, k; i \neq k-d\right) \quad (2.23)$$

where the test is applied on period k with a delay of d . Thus $\text{REMUF}_{k,d}$ is the smoothed estimate for period $(k-d)$. Russell demonstrates that this gives a significant improvement in performance over ITMUF. His analysis is restricted to a tri-diagonal covariance matrix, which means that the set

$$\text{MUF}_i ; i \leq k-d-1$$

is independent of the set

$$\text{MUF}_i ; i \geq k-d+1$$

Extending this to a fuller covariance matrix introduces substantial complications.

Seifert [31] has suggested an alternative smoothed statistic, called Geschätzter-MUF (Estimated-MUF) or GEMUF. Echoing the Neyman-Pearson test, the statistic is calculated from:

$$\text{GEMUF}_k = \underline{\text{MS}}_k^T \cdot \underline{\Sigma}_k^{-1} \cdot \underline{\text{MUF}}_k \quad (2.24)$$

MS_k is an estimate of the loss pattern, and has been chosen by experimentation as:

$$MS_k = \frac{1}{k} \cdot (MUF_{k-2} + MUF_{k-1} + 3 \cdot MUF_k + MUF_{k+1} + MUF_{k+2}) \quad (2.25)$$

Seifert compares the absolute power of this statistic with CUMUF, Page's Test, and the theoretical optimal Neyman-Pearson test. While not as powerful as CUMUF for protracted diversions starting on period one, GEMUF offers a robust performance against a number of diversion scenarios, a desirable facility for safeguards assurance.

Again, this test is dependent on the quality of the covariance matrix, or measurement model. Recognizing this, Beegden, Seifert and others working at the Kernforschungszentrum Karlsruhe with data from the Wiederaufarbeitungsanlage Karlsruhe reprocessing facility, progressed from a 'one-block model' (fixed covariance matrix with allowance for systematic errors) [40,41], to a full analysis of each measurement variance with flow-chart information [42]; this follows a similar approach to the MUF-residuals calculation detailed in this thesis, and was published at the same conference [43].

2.7 Choice of thresholds

The only control that can be pre-set for any test are the 'alarm' thresholds; these govern both the power and the credibility. The cost of investigating false alarms, in both money and resources, means that these must be constrained; the test must thus be carefully selected to maximize the power.

Several methods of comparing tests have been proposed. As illustrated above, the false alarm rate is dependent on the number of balance periods; results can only be interpreted with information about the

model. To circumvent this, the concept of the 'Average Run Length' (ARL) has been proposed, as it requires no qualification. L^0 , the ARL with no loss, is set to the required value (calculated from $1/\alpha$). For a given diversion, the test with the shortest L^1 (the ARL after the loss) is the most powerful. It also gives a direct indication of timeliness, appealing in NRTMA. Leitner et al [30] use this measure, but they comment that it is difficult to justify from first principles.

The run length distribution may be highly skewed, and is affected by correlation in the test data [44]. Thus, comparing tests on the basis of a fixed ARL may not indicate that they have an equi-probable chance of false alarming. For example, setting the ARL much longer than the campaign length will result in a disproportionately large number of CUMUF false alarms, because of the strong positive correlation in the sequence.

Leitner et al [11] demonstrated this effect by comparing performance on a 23-balance-period campaign, setting $L^0 = 100$. Uncorrelated statistics (MUF-residuals) have an overall FAR of

$$[1-(1-\alpha)^{23}] = 0.206$$

The CUMUF sequence has the best performance, but has a FAR of 0.74. Clearly this does not offer a fair comparison, as the cost is related to the FAR, and the ARL is a secondary measure.

Pike & Woods [45] proposed a refinement using run length percentiles, defining $P_j(L)$ by

$$\text{Prob} \{ \text{run length} \leq P_j(L) \} = j/100$$

where L is the loss occurring per balance period. Thus $P_{10}(0)$ is the run length below which 10% of runs end under no diversion. The authors suggest taking 10%, 50% and 90% run lengths for comparison.

This method does offer a solution to the above problem, but in generating three 'figures of merit' for each test under each loss scenario, it is rather more difficult to interpret the results, and has not been widely adopted. Again, it does not offer a direct indication of the cost of false alarms.

Thus, several authors writing on the practical aspects of implementing material accountancy have favoured the FAR route [22,23], typically working with the IAEA recommendation of a 5% FAR. This still leaves an ambiguity in interpretation; it could be taken as 5% per test, an overall of 5% per reprocessing campaign, or 5% of campaigns. The last is the most stringent, and matches the traditional accountancy goal; this is the standard by which the tests are compared in this thesis.

For the purpose of comparison, a campaign length of 40 balance periods is used. The thresholds are set such that 5% of these campaigns have one or more false alarms. There will be a 0.25% probability that, having alarmed once, a campaign will suffer a second false alarm, and a 0.01% chance of a third. This definition thus gives an effective false alarm rate of 5.26%. For the threshold test, if the statistics are uncorrelated (MUFR), the threshold values to achieve this are easily calculable from normal-distribution area tables. Each campaign must have an effective credibility of 0.9474, so each individual test in the campaign must have a credibility of

$$0.9474^{0.025} = 0.99865$$

This lies well into the tail of the normal distribution, it is difficult to place exactly. With 4 sig. fig. tables, this places the thresholds in the range 3.19-3.21.

If the statistics are correlated, the calculation of the thresholds becomes much more difficult. Russell [14] suggests a way of evaluating multinormal densities, but the lengthy calculation is only practical for up to about eight balance periods.

The correlations in the CUMUF sequence, leading to the exaggerated skew in the run length distribution, also mean that fixed thresholds will lead to a highly unequal probability of false alarming over the campaign. The cumulative false alarm probability of an independent sequence will tend asymptotically to 1; for the conditions described above the effective ARL (50% false alarms) is about 760 balance periods, and the curve will not be detectable over 40 balance periods. However, as the graph in figure 2.8 shows, the CUMUF FAR rises rapidly towards the 5% level and levels off. To overcome this, the thresholds must be set to decrease as the campaign progresses, maintaining a constant false alarm rate of about 0.13% per balance period.

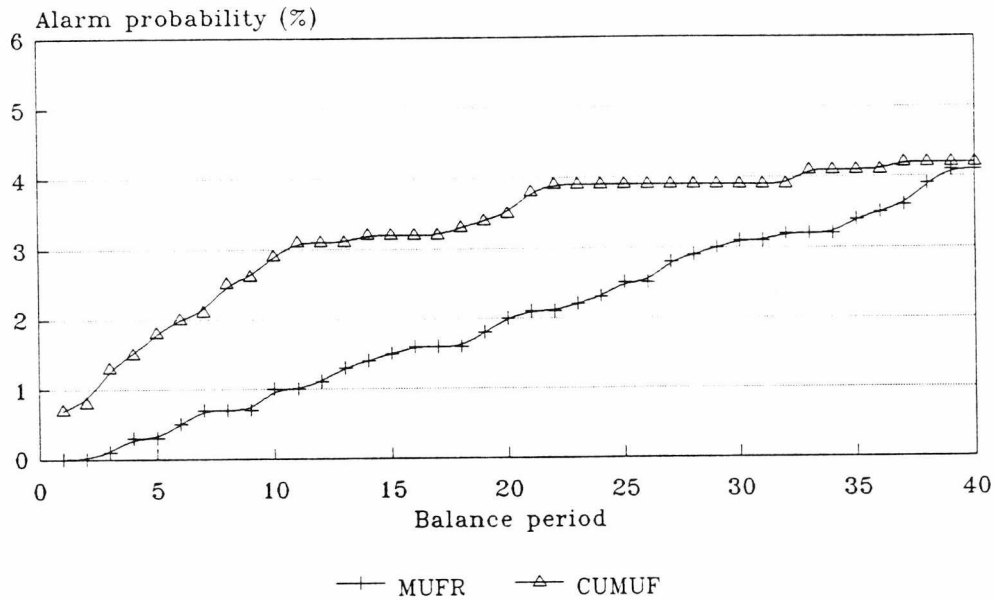


Figure 2.6 Cumulative false alarm probabilities with fixed CUMUF thresholds: Threshold test

In practice, it is likely that several tests will be used. To maintain the desired FAP, the thresholds must be raised. As the tests are based on the same data, the results will be highly correlated; the only practical way to find the new thresholds will be by simulation.

Improvements in data availability and timeliness will reduce the effort involved in investigating a suspected anomaly. A higher false alarm rate may thus be tolerable. A system of tiered thresholds could also be implemented, allowing low-significance alarms to be investigated quickly, while the evidence is still readily available without disrupting plant operation, to see if the cause is easily traceable [46].

2.8 Choice of performance benchmarks

Following on from the choice of false alarm rate as the governing factor in selecting thresholds, the performance of the tests will be compared on the basis of their power to alarm a diversion. The relative performances of the tests will depend on several factors - the loss scenario (eg. large-abrupt, protracted, loss-with-replacement), the point of the campaign at which the material is removed, and, in the case of Page's Test, the choice of test parameters. These conditions should be explicitly described in any comparison.

The IAEA favour an 'accountancy verification goal', expressing the mass of material the diversion of which would be detected with 95% probability, 'with a low risk of false alarm' [1]. This would be linked to a timeliness goal, linked to the time required to convert the material into a form suitable for weapons.

Siefert [31] chose to plot the loss scenario graphically, in terms of loss against period, and thus show the detection curve in terms of alarm probability against period, with an additional 'ultimate power' chart. This fulfills the requirement of displaying all the test conditions, but each set of graphs can only show one specific mass/strategy scenario. This method also demonstrates how quickly a protracted loss is detected, important in minimizing the total loss.

The former of these is adopted in this thesis for displaying the response to a selection of possible diversion scenarios. Additionally, the power of each test will be plotted against the magnitude of the loss, to demonstrate likely detection rate for losses or measurement errors much smaller than the 95% detection level masses. This is important, as any test used in materials accountancy must present a

deterrent to removing any material at all, and so should not have a 'blind' region.

3. Plant description

3.1 Introduction

The purpose of this research is to demonstrate the adaptation of theoretical work to a practical situation. While the techniques developed are general, the specific solutions relate to a current nuclear facility - part of the Fast Reactor Fuel Reprocessing Plant at Dounreay, Caithness. An essential pre-requisite is thus an understanding of the operations of the plant and the limitations these impose on material accountancy.

3.2 Techniques and problems in nuclear material determination

The hazardous nature of nuclear materials places severe constraints on processing and measurement methods. Sensors and transducers operating in active areas must primarily be reliable and maintenance-free, which may compromise accuracy.

It is particularly difficult to quantify nuclear material in a solid form. The most common methods are passive neutron assay (counting the natural decay radiation), and 'neutron interrogation'. This involves bombarding the material with neutrons from a Cf-252 source, and counting the response in terms of delayed neutrons. Both of these rely on stochastic processes, leaving a high degree of uncertainty in the results.

Concentrations in solution can be accurately determined in the laboratory by chemical titration methods. The density of a liquor sample can also be measured in the laboratory, using an Anton-Paar

densitometer.

Bulk volumes are either calculated from hydrostatic pressures in a calibrated tank (this will be described in more detail later), or more recently by suspending the tank on load cells [47]. Errors in these mechanisms will make a significant contribution to the overall uncertainty, and are an obvious source of systematic bias.

Other measurements, such as flow metering, provide useful plant control information, but in general are not sufficiently accurate for reliable material accountancy.

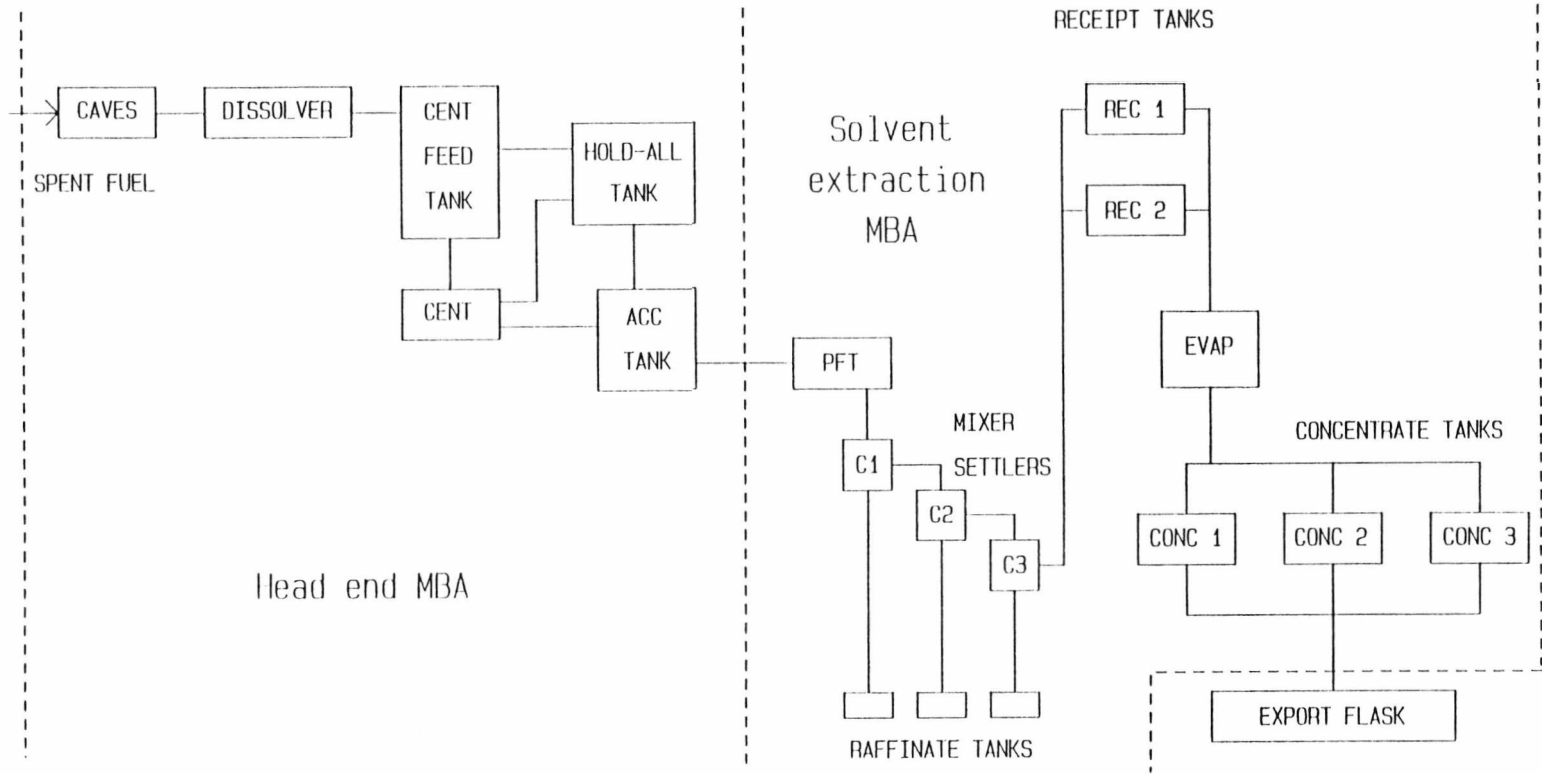
It is not practical to obtain accurate, independent measurements at every stage in the plant. The choice lies between using approximate, independent readings, or assigning a value to inaccessible inventories derived from the last accurate quantification of the batch. The former may lead to an unacceptably high standard deviation for the MUF, reducing the sensitivity of the diversion tests, while the latter introduces correlations into the MUF sequence which should be accounted for if the tests are to give reliable results.

To illustrate these problems, and to provide a basis for the simulation of realistic plant data, an analysis of part of the Dounreay reprocessing plant is described. This takes in fast reactor fuel sub-assemblies, and outputs concentrated solutions of uranium nitrate and plutonium nitrate for conversion back to fuel.

3.3 Description of the Dounreay Fast Reactor Fuel Reprocessing Plant

A schematic of the Dounreay reprocessing plant is shown in figure 3.1.

Figure 3.1 The Fast Reactor Fuel Reprocessing Plant



For the purpose of material accountancy, the plant is divided into two accountancy areas, the head-end material balance area (MBA) and the solvent extraction MBA. Used Prototype Fast Reactor (PFR) fuel sub-assemblies are brought into 'dismemberment caves' at the start of the head-end, where the fuel pins are drawn out, cropped, and divided into batches; about 2½ batches are made up from each sub-assembly. Each batch is placed in a basket, and these are passed sequentially through the dissolver, where the irradiated material is leached out of the stainless-steel hulls into solution. The dissolver will hold one basket, and the dissolution takes about 24 hours. The liquor is then centrifuged to remove any remaining insolubles, and passed into a calibrated accountancy tank. The plant incorporates a 'hold-all' tank to receive overflow from the centrifuge system. This is periodically discharged to the accountancy tank. The fuel pin hulls and centrifuge deposits are removed as waste.

The batch is transferred from the accountancy tank across the boundary to a plant feed tank in the solvent extraction and storage MBA. The output from this is a constant feed to a cascade of mixer-settlers, which separate the uranium, plutonium and fission products. The last of these are categorized as either high-active or medium/low-active, and are drawn off separately.

Each heavy metal stream passes into a receipt tank. These are used in pairs, one filling from the mixer-settlers while the other supplies an evaporator. Once the second is discharged, the valves are switched over. The evaporator concentrates the liquor by a factor of about ten, and feeds the reduced volume into one of three large concentrate tanks. Each of these will hold about thirteen batches. Here it awaits transfer to an export flask, in which the material is carried out of the MBA boundary.

As the head-end is run on a batch-mode, material balances are struck when a transfer out of the area from the accountancy tank is made. This occurs roughly every 24 hours. The solvent extraction and storage operates on a continuous-flow basis, so a period is taken as one day, and the balance struck at the same time each day.

3.4 Plant measurements in the head-end

Because of the difficulty of accurately quantifying solid nuclear material, the mass of heavy metal in the input sub-assembly is estimated by calculation, taking into account the initial make-up, position and time in the reactor core, and reactor power profile during that time - this is referred to as the 'burn-up calculation'. For the same reason, the inventory in the uncropped pins and in the batches in baskets is taken from the calculation for the source sub-assembly.

The correlation between the sub-assembly mass estimate and these inventory estimates is thus one, and the covariance between them is the product of their standard deviations.

The dissolver is designed primarily as a process tank; the instrumentation, calibration and laboratory assessments associated with it were designed only for plant control purposes. The estimates from the dissolver are not used in the conventional nuclear materials accountancy reporting system, but they did form a part of the early experiment with NRTMA. Now, however, the source sub-assembly value is used again, as it is much more precise. The analyses given in previous papers [43,48] were based on the earlier experimental system. The change has had far-reaching effects on the statistical nature of the

accountancy data, so both systems are considered and compared in this thesis.

When the dissolver is discharged, a small volume remains in the 'heel'; the mass of heavy metal in this heel is determined independently and added to the next batch in the dissolver. The hold-all tank is reassessed when there is a change in content. Waste products are assayed on the balance period in which they are created; this determination is also used when the waste is exported.

The output from the accountancy tank is determined completely independently on each balance period.

It is possible that covariance exists between sub-assembly burn-up estimates, but this lies outside the scope of this thesis.

3.5 Determination of liquor height by the pneumercator system

A 'pneumercator' system is used to determine hydrostatic pressures (and hence liquor heights) in several tanks in the Fast Reactor Fuel Reprocessing Plant. The basic system shown in figure 3.2 comprises a stainless steel 'dip-tube' immersed in the liquor, the height of the exit being accurately known, which is fed with pressurized nitrogen through a control valve. In operation, the valve is adjusted to allow slow bubbling from the dip-tube exit; the pressure in the pipe feeding the dip-tube is then recorded from a pressure gauge. Appendix I demonstrates how the liquor height is calculated from the pressure in the pipe.

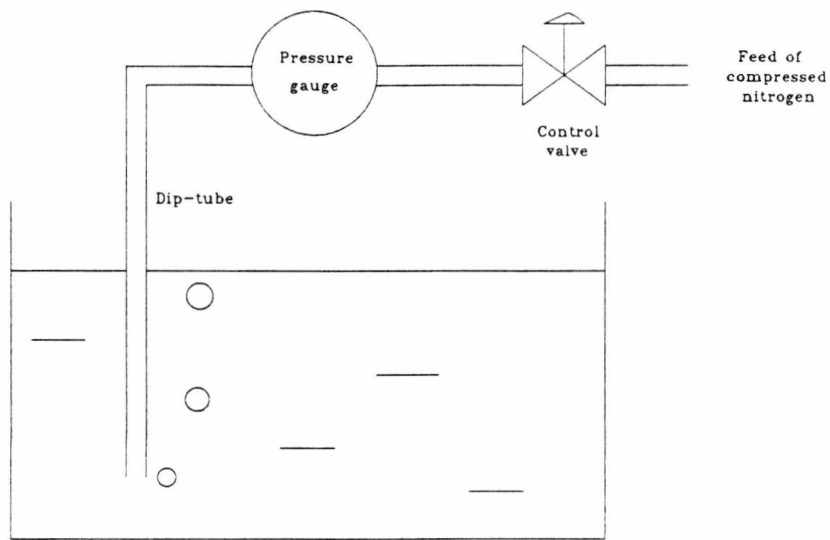


Figure 3.2 The basic pneumericator system

Two immersed dip-tubes, of known vertical separation, enable the liquor density to be calculated from the difference in pipe pressures. The bubbling does cause slight oscillation in the pressure reading - an average value is used. This method does have the overriding advantage of having no electrical or moving mechanical parts in the 'active' area.

To improve the resolution of the hydrostatic pressure to volume conversion, the accountability tank has narrowed neck and heel regions; in use, it is always filled to the neck, and emptied to the heel. The configuration of the pneumericator system is shown in figure 3.3.

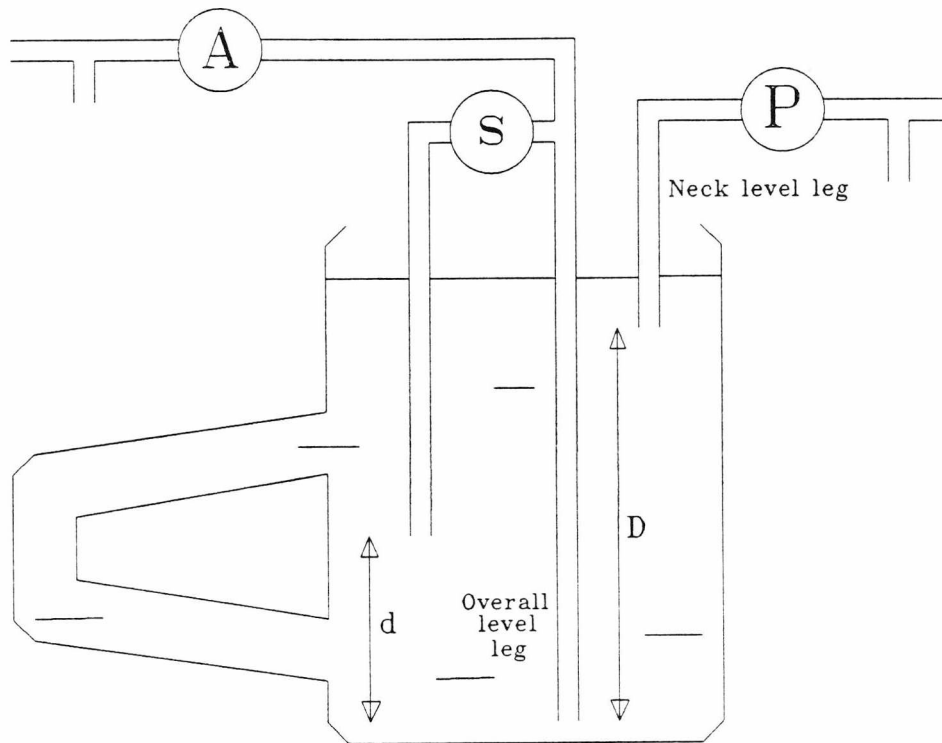


Figure 3.3 Schematic of the accountability tank

The tank is 'd' shaped for criticality reasons. 's', 'A' and 'P' are pressure gauges.

Any error in the calibration of the tank will lead to a bias in the height to volume conversion, and hence in the mass estimate. An analysis of the existing calibration data is presented in Chapter 5.

The dissolver is also fitted with a pneumericator system, but the operation of the tank does not enable accurate estimates to be made. The small volume remaining in the heel after discharge is still estimated from the dip-tube reading for accountability purposes; there is no other convenient way of determining this, and it contributes little to the overall error of the MUF.

3.6 Modelling the head-end MBA

To assess the effect of the correlations on the performance of the diversion tests, a computer model (in FORTRAN) of the head-end MBA of the Dounreay reprocessing plant was written. This generates a complete set of plant data, modelling measurement errors by Gaussian noise, creates a MUF sequence, and records all the covariances in the sequence to enable a decorrelated data set to be calculated.

To compare the performance of the different statistical tests, where an analytical approach would be impractical, the model was used for Monte-Carlo simulation to generate data equivalent to many thousands of campaigns. This technique was also used to verify some analytical results.

3.7 Summary

As described in chapter 2, correlations in the MUF sequence affect the ability of statistical tests to differentiate between random determination errors and real losses. Previous research in this area has made assumptions about the way in which material accountancy is effected in terms of plant measurements which are not realistic in a commercial and industrial environment. By analysing the operation of a plant, all the sources of correlation can be identified and quantified. It will be shown later how this information can be used to remove the correlation from the accountancy test statistics; data from a model of part of the Fast Reactor Processing Plant will be used to demonstrate the improvement in loss detection ability that this offers.

4. A minimum variance estimate of the transfer from an accountancy tank

4.1 Introduction

The material passing from the head-end MBA to the solvent extraction MBA is first held in an accountancy tank in the head-end. Approximately once a day the accountancy tank is emptied, passing its contents to the plant feed tank in the solvent extraction MBA. This accountancy tank plays an important role in determining the mass of heavy metal passing through the plant. Since the material is in the form of a nitrate solution, the mass of nuclear material transferred between the two MBAs cannot be measured directly but must be calculated from measurements of the total quantity of liquor transferred and the concentrations of plutonium and uranium in the liquor.

The error on this mass estimate is a compound function of the component determination errors. A set of four different equations to estimate the transfer, each using a different combination of measurements, has already been derived. However, only the most precise of these is currently used for material accountancy purposes.

The aim of this exercise was to show that a more reliably accurate estimate could be made by using all the data available, weighted by suitably selected coefficients.

4.2 Mass transfer measurement and instrumentation

4.2.1 The basis of mass transfer calculation

In essence, the mass of nuclear material being passed from the head-end to the solvent extraction MBA is given by:

$$\boxed{\begin{array}{c} \text{Total volume of} \\ \text{liquor transferred} \\ \text{(l)} \end{array}} \quad \times \quad \boxed{\begin{array}{c} \text{Nuclear material} \\ \text{concentration} \\ \text{(g/l)} \end{array}} \quad (4.1)$$

The most accurate analysis of the concentration yields a value in g/g, which must be combined with a density expression. The mass transfer in this case becomes:

$$\boxed{\begin{array}{c} \text{Total volume of} \\ \text{liquor transferred} \\ \text{(l)} \end{array}} \quad \times \quad \boxed{\begin{array}{c} \text{Density of} \\ \text{liquor} \\ \text{(g/l)} \end{array}} \quad \times \quad \boxed{\begin{array}{c} \text{Nuclear material} \\ \text{concentration} \\ \text{(g/g)} \end{array}}$$

└──┘
Concentration in g/l

(4.2)

ie:

$$V \times C_{w/V} \quad (4.3)$$

4.2.2 Laboratory measurements

A sample of liquor is taken from the accountancy tank at the time of transfer and sent to the chemistry laboratory. There it is analysed to determine the concentration of plutonium and uranium using methods which yield results in both grams per litre and grams per gram. The sample's density is also measured.

4.2.3 The pneumercator systems

Within the accountancy tank there are three pneumercator dip-tubes connected to three gauges (see figure 3.2). These are used to make measurements of the height of liquor in the accountancy tank before and after a transfer, and also to make estimates of the density of the liquor. The height is converted to a volume by using a height-to-volume calibration table.

Figure 3.2 shows schematically the pneumercator systems used in the accountancy tank. The gauges serve the following purposes:

Gauge 's' is connected between dip tubes the open ends of which are a distance 'd' apart. As explained in Appendix II.2, the gauge is calibrated to read Specific Gravity directly.

Gauge 'A' is used to measure the overall level and, in conjunction with gauge 'P', to provide an in-tank density estimate between the dip-tube exits distance 'D' apart. Gauge 'A' is also used to measure the heel level, immediately after a transfer.

Gauge 'P' is used to measure the neck level, and, in conjunction with 'A', to provide the in-tank density estimate.

There are several ways in which the various measurements made can be combined to form estimates of the mass transferred. Reference [49] details four methods and reference [50] presents results of a 'Monte-Carlo' analysis of the relative accuracies of the methods. For the purposes of materials accountancy (both near real time and conventional) only method one of [50] is used. This is also the method

identified in [50] as the most accurate.

The individual measurements vary in accuracy, and the method currently used for determination of the mass transferred uses many of the more accurate ones. However, a method which makes intelligent use of all measurements can produce a result which is more accurate than a method using only some of them and which will be less sensitive to instrument biases.

Section 4.3 presents a new equation for the calculation of the mass of heavy metal transferred which uses all available measurements.

4.3 Equations of Mass Transfer Calculation

Table 4.1 illustrates the various terms which go towards calculation of the mass transferred. The derivation of the individual terms is detailed in Appendix II.

The basis for the calculation is the equation

$$V \times C_{w/V} \tag{4.3}$$

However, instead of choosing a single method for calculating V and a single method for calculating $C_{w/V}$, all twelve combinations (three volume and four concentration estimates) are combined into a single Minimum Variance Unbiased Estimate.

Ideally, the weighting coefficients would be found directly by the technique described in Appendix III, inverting a 13×13 matrix Λ . However, the distribution of variance among the component terms

Volume transferred

x

liquor density

Mass = Conc x

L	Z	$\rho_{Lt} \cdot \left(\frac{1 + \alpha \cdot (20-T)}{1 + \alpha \cdot (20-t)} \right)$	$\psi \left(\frac{P \cdot (\rho_{w20} - \rho_{a20})}{\rho_{Lt} \cdot \left(\frac{1 + \alpha \cdot (20-T)}{1 + \alpha \cdot (20-t)} \right) - \rho_{aT}} \right) -$	$\psi \left(\frac{a \cdot (\rho_{w20} - \rho_{a20})}{\rho_{Lt} \cdot \left(\frac{1 + \alpha \cdot (20-T)}{1 + \alpha \cdot (20-t)} \right) - \rho_{aT}} \right)$	$1 + \delta \cdot (T-20)$
		$\frac{(\rho_{w20} - \rho_{a20}) \cdot s}{d} + \rho_{aT}$			
L	Z	$\frac{(A - P) \cdot (\rho_{w20} - \rho_{a20})}{D} + \rho_{aT}$	$\psi \left(\frac{P \cdot d}{s} \right) - \psi \left(\frac{a \cdot d}{s} \right)$	$\psi \left(\frac{P \cdot D}{(A - P)} \right) - \psi \left(\frac{a \cdot D}{(A - P)} \right)$	$1 + \delta \cdot (T-20)$
		$Y_t \cdot \left(\frac{1 + \alpha \cdot (20-T)}{1 + \alpha \cdot (20-t)} \right)$			

Table 4.1 Terms forming the accountancy tank transfer estimate

causes a problem in the numerical solution. This can best be explained by considering the physical sources of the determinations. The accountability tank has very narrow neck and heel regions; it is always filled to the neck then emptied to the heel during a transfer. A small difference in the filled volume results in a large change in the pressure reading 'P' (see figure 3.2). Thus the volume of the transfer can be calculated quite precisely. (The accuracy is dependent on the tank calibration.) The area of the neck in which gauge P operates is roughly one-tenth the area of the main body of the tank; errors in the reading 'P' are thus reduced in significance by a factor of about ten. This is illustrated clearly in the tables of sensitivity given in Appendix V. The standard deviation of 'z' ($C_{w/W}$) is proportionally similar to that of 'P', but an error on 'P' has one-tenth the effect on the resulting estimate in the methods which use it only for volume determination.

The variance in the determination of $C_{w/V}$ thus dominates the variance of the estimate. In attempting to calculate the MVUE, the parallel methods which incorporate the same $C_{w/V}$ determination have a very strong correlation, leading to an almost singular matrix Λ to be inverted for the MVUE coefficients. Even using high-precision numerical routines, the results from this are unreliable.

Three practical alternatives were investigated; an MVUE of the four existing transfer equations [1], a product of $MVUE(V)$ and $MVUE(C_{w/V})$, and a combination of three MVUEs based on the three methods of volume determination. They gave similar results in terms of variance and sensitivity to bias. The last was chosen as the closest approximation to the ideal MVUE described above.

Each of the three component equations is formed by a linear combination of the four expressions for $C_{w/v}$ multiplied by one of the volume expressions.

$$\begin{aligned}
 [L_1] &= \\
 &\left(\begin{aligned} &\gamma_1 \left\{ Z \cdot \rho_{Lt} \cdot \left(\frac{1 + \alpha \cdot (20-T)}{1 + \alpha \cdot (20-t)} \right) \right\} + \gamma_2 \left\{ Z \cdot \frac{(\rho_{w20} - \rho_{a20}) \cdot s}{d} + \rho_{aT} \right\} + \\ &\gamma_3 \left\{ Z \cdot \frac{(A - P) \cdot (\rho_{w20} - \rho_{a20})}{D} + \rho_{aT} \right\} + \gamma_4 \left\{ Y_t \cdot \left(\frac{1 + \alpha \cdot (20-T)}{1 + \alpha \cdot (20-t)} \right) \right\} \end{aligned} \right) \\
 &\quad \times \\
 &\left\{ \psi \left(\frac{P \cdot (\rho_{w20} - \rho_{a20})}{\rho_{Lt} \cdot \left(\frac{1 + \alpha \cdot (20-T)}{1 + \alpha \cdot (20-t)} \right) - \rho_{aT}} \right) - \psi \left(\frac{a \cdot (\rho_{w20} - \rho_{a20})}{\rho_{Lt} \cdot \left(\frac{1 + \alpha \cdot (20-T)}{1 + \alpha \cdot (20-t)} \right) - \rho_{aT}} \right) \cdot [1 + (T-20)\delta] \right\}
 \end{aligned} \tag{4.4}$$

$$\begin{aligned}
 [L_2] &= \\
 &\left(\begin{aligned} &\nu_1 \left\{ Z \cdot \rho_{Lt} \cdot \left(\frac{1 + \alpha \cdot (20-T)}{1 + \alpha \cdot (20-t)} \right) \right\} + \nu_2 \left\{ Z \cdot \frac{(\rho_{w20} - \rho_{a20}) \cdot s}{d} + \rho_{aT} \right\} + \\ &\nu_3 \left\{ Z \cdot \frac{(A - P) \cdot (\rho_{w20} - \rho_{a20})}{D} + \rho_{aT} \right\} + \nu_4 \left\{ Y_t \cdot \left(\frac{1 + \alpha \cdot (20-T)}{1 + \alpha \cdot (20-t)} \right) \right\} \end{aligned} \right) \\
 &\quad \times \\
 &\left\{ \psi \left(\frac{P \cdot d}{s} \right) - \psi \left(\frac{a \cdot d}{s} \right) \right\} \cdot [1 + (T-20)\delta]
 \end{aligned} \tag{4.5}$$

$$\begin{aligned}
[L_3] &= \left(\eta_1 \left\{ Z \cdot \rho_{Lt} \cdot \left(\frac{1 + \alpha \cdot (20-T)}{1 + \alpha \cdot (20-t)} \right) \right\} + \eta_2 \left\{ Z \cdot \frac{(\rho_{w20} - \rho_{a20}) \cdot s}{d} + \rho_{aT} \right\} + \right. \\
&\quad \left. \eta_3 \left\{ Z \cdot \frac{(A - P) \cdot (\rho_{w20} - \rho_{a20})}{D} + \rho_{aT} \right\} + \eta_4 \left\{ Y_t \cdot \left(\frac{1 + \alpha \cdot (20-T)}{1 + \alpha \cdot (20-t)} \right) \right\} \right) \\
&\quad \times \\
&\quad \left\{ \psi \left(\frac{P \cdot D}{A - P} \right) - \psi \left(\frac{a \cdot D}{A - P} \right) \right\} \cdot [1 + (T-20)\delta]
\end{aligned} \tag{4.6}$$

For clarity, these equations may be expressed

$$[L_1] = \gamma_1 \cdot C_1 \cdot V_1 + \gamma_2 \cdot C_2 \cdot V_1 + \gamma_3 \cdot C_3 \cdot V_1 + \gamma_4 \cdot C_4 \cdot V_1 \tag{4.7}$$

$$[L_2] = \nu_1 \cdot C_1 \cdot V_2 + \nu_2 \cdot C_2 \cdot V_2 + \nu_3 \cdot C_3 \cdot V_2 + \nu_4 \cdot C_4 \cdot V_2 \tag{4.8}$$

$$[L_3] = \eta_1 \cdot C_1 \cdot V_3 + \eta_2 \cdot C_2 \cdot V_3 + \eta_3 \cdot C_3 \cdot V_3 + \eta_4 \cdot C_4 \cdot V_3 \tag{4.9}$$

$$\text{where } C_1 = Z \cdot \rho_{Lt} \cdot \left(\frac{1 + \alpha \cdot (20-T)}{1 + \alpha \cdot (20-t)} \right) \tag{4.10}$$

$$C_2 = Z \cdot \frac{(\rho_{w20} - \rho_{a20}) \cdot s}{d} + \rho_{aT} \tag{4.11}$$

$$C_3 = Z \cdot \frac{(A - P) \cdot (\rho_{w20} - \rho_{a20})}{D} + \rho_{aT} \tag{4.12}$$

$$C_4 = Y_t \cdot \left(\frac{1 + \alpha \cdot (20-T)}{1 + \alpha \cdot (20-t)} \right) \tag{4.13}$$

$$V_1 = \left\{ \psi \left(\frac{P \cdot (\rho_{w20} - \rho_{a20})}{\rho_{Lt} \cdot \left(\frac{1 + \alpha \cdot (20-T)}{1 + \alpha \cdot (20-t)} \right)^{-\rho_{aT}}} \right) - \psi \left(\frac{a \cdot (\rho_{w20} - \rho_{a20})}{\rho_{Lt} \cdot \left(\frac{1 + \alpha \cdot (20-T)}{1 + \alpha \cdot (20-t)} \right)^{-\rho_{aT}}} \right) \right\} \times [1 + (T-20)\delta] \quad (4.14)$$

$$V_2 = \left\{ \psi \left(\frac{P \cdot d}{s} \right) - \psi \left(\frac{a \cdot d}{s} \right) \right\} \cdot [1 + (T-20)\delta] \quad (4.15)$$

$$V_3 = \left\{ \psi \left(\frac{P \cdot D}{A - P} \right) - \psi \left(\frac{a \cdot D}{A - P} \right) \right\} \cdot [1 + (T-20)\delta] \quad (4.16)$$

A general method for calculating the values of coefficients necessary to form a Minimum Variance Unbiased (Linear) Estimator is derived in Appendix III. The general result shows that $\gamma_1, \gamma_2, \gamma_3$ and γ_4 can be calculated in terms of Σ_γ^{-1} where Σ_γ is the covariance matrix of results from the four methods of calculating the transfer using V ; similarly, the coefficients v_{1-4} and η_{1-4} can be found in terms of Σ_v^{-1} and Σ_η^{-1} where Σ_v and Σ_η are the covariance matrices from V_2 and V_3 respectively.

Appendix IV details the calculation of the covariance matrices and the coefficients γ_{1-4}, v_{1-4} and η_{1-4} . The results of the calculations were confirmed by Monte-Carlo simulation.

Looking at the volume and concentration expressions, it can be seen that there is a correlation between $V_1, V_2,$ and V_3 (due to 'P' and 'a'), between C_1 and V_1 (' ρ '), between C_2 and V_2 ('s'), and between C_3 and V_3 ('A' and 'P').

This, combined with the common occurrence of $C_1, C_2, C_3,$ and $C_4,$

results in the three minimum variance estimates having a very high correlation - greater than 0.999999 for any pair. Thus, for practical purposes, the Minimum Variance Unbiased Linear Estimator can be taken as an equally weighted combination of these three estimators.

$$\begin{aligned}
 [L] &= (\omega_1 \cdot C_1 + \omega_2 \cdot C_2 + \omega_3 \cdot C_3 + \omega_4 \cdot C_4) \cdot V_1 \\
 &+ (\omega_5 \cdot C_1 + \omega_6 \cdot C_2 + \omega_7 \cdot C_3 + \omega_8 \cdot C_4) \cdot V_2 \\
 &+ (\omega_9 \cdot C_1 + \omega_{10} \cdot C_2 + \omega_{11} \cdot C_3 + \omega_{12} \cdot C_4) \cdot V_3
 \end{aligned}$$

(4.17)

where

$\omega_1 = \frac{\gamma_1}{3}$	$\omega_2 = \frac{\gamma_2}{3}$	$\omega_3 = \frac{\gamma_3}{3}$	$\omega_4 = \frac{\gamma_4}{3}$
$\omega_5 = \frac{\nu_1}{3}$	$\omega_6 = \frac{\nu_2}{3}$	$\omega_7 = \frac{\nu_3}{3}$	$\omega_8 = \frac{\nu_4}{3}$
$\omega_9 = \frac{\eta_1}{3}$	$\omega_{10} = \frac{\eta_2}{3}$	$\omega_{11} = \frac{\eta_3}{3}$	$\omega_{12} = \frac{\eta_4}{3}$

From Appendix IV, the MVUE coefficients for the sample data are thus

ω_1	=	0.1916
ω_2	=	0.0672
ω_3	=	0.0729
ω_4	=	0.0016
ω_5	=	0.1578
ω_6	=	0.1014
ω_7	=	0.0735
ω_8	=	0.0016
ω_9	=	0.1577
ω_{10}	=	0.0668
ω_{11}	=	0.1073
ω_{12}	=	0.0016

4.4 Sensitivity of the weighting coefficients

The weighting coefficients have been calculated for a 'typical' set of transfer data. They are, however, fairly insensitive to changes in the transfer data.

The coefficients are functions of the variance for each combination of concentration x volume. The two most important components of these variances are the variance of the mass of heavy metal in the tank 'body' (up to the neck), and the covariance between the mass in the body and the mass in the neck (due to the common concentration term). The latter

represents about 13% of the former when a common density determination is used, and about 23% when different density estimates are employed. Other contributions, such as the variance of the neck and heel masses, are at least an order of magnitude smaller than this covariance.

Large changes in 'a', 'T', and 't' will have very small effect on the variances, and hence on the weighting coefficients.

A washout batch will have a very low concentration of heavy metal. As the contribution of the volume error only operates on about 10% of the total volume, for a normal batch the variance of the transfer estimate is dominated by the concentration variance. The lower variance of the concentration estimate for a washout batch reduces this dominance slightly, but not significantly for even a hundredfold reduction. The ratio of variances between the different estimates, and hence the weighting coefficients, change little.

The liquor density may vary over the range 1100 to 1450 g/l. The density determination contributes to the variance of the mass in the body of the tank; over this limited range a change in density affects the variance of all estimates almost linearly, with little effect on the coefficients.

The reading on the neck level pressure gauge 'P' may lie between 0 and 2000mm H²O for a typical batch. This affects the covariance term described above by different amounts for each estimate: as the liquor level in the neck rises, the variance of methods employing two density estimates increases more than those using a single density determination. Thus with the neck filled, the variances of C1.V1, C2.V2, and C3.V3 are proportionally lower than the other methods, compared to the situation with the neck empty.

This effect causes the weighting coefficients to favour the single-density methods listed above, as the volume of the batch increases.

The instrument error ranges quoted by Miller attribute additive and multiplicative elements to the uncertainty on the pressure gauge readings. The multiplicative element causes the standard deviations of the in-tank density estimates to decrease as the liquor level decreases. This effect is amplified in C3 and V3, which uses two pressure readings to calculate the density. The effect on C3 is dominant; the standard deviations of estimates using C3 drop substantially as 'P' decreases, resulting in a significant change in the MVUE weighting coefficients towards C3 based methods.

An algorithm has been written to calculate the coefficients accurately for any set of plant data.

4.5 Analysis of the sensitivity of the transfer estimate to systematic errors

Knowledge of bias is, by its nature, very restricted, even in a statistical sense. However, where a measurement technique M is compared against a more accurate reference technique R, it can generally be concluded that the bias in M is small compared with the variance. If the mean of M values differed substantially from the R values a correction would be applied to M, removing the known bias. Thus in estimating the effect on bias of the MVUE, it is reasonable to give most attention to the scenario where biases are proportional to variance. Other bias scenarios cannot, however, be ruled out, and simply by

looking at limiting cases it can be seen that the bias on an MVUE may be higher than that on some of the component methods.

An analysis of the sensitivities of the existing four transfer estimates has been carried out by Miller [51], demonstrating the percentage change in the estimates given a $\pm 3\sigma$ bias on each of the measurements. This criterion has been applied to the MVUE, and the results are presented together in Table V.1, Appendix V, for comparison.

Table V.2, Appendix V, shows the error percentages resulting from a bias of 1% of the measurement magnitude. These correspond to Miller's 'coefficients of sensitivity'.

The random measurement errors have all been assumed normally distributed, with standard deviation equal to half the quoted uncertainty (± 1 corresponds to a standard deviation of $\frac{1}{2}$). The MVUE minimizes the likely combined effect of these errors; if the systematic errors have a similar structure to this, with the standard deviations of all the determination biases a fixed proportion of the random error standard deviations, the MVUE will give a minimum sensitivity to the likely error resulting from this. However, if a different bias structure is suspected, coefficients for a 'best estimate' can be calculated by a similar method to the one described, substituting the proposed error model.

It must be emphasized that this is not a technique for handling known systematic errors; it is merely a means of obtaining a best estimate against a proposed statistical model of unknown errors.

The MVUE is an optimal estimator for 'no systematic errors' and the scenario described above.

A possible source of systematic error lies in the conversion of the liquor height in the tank to a volume, which is effected by interpolating from a calibration table. The calibration plays a key role in the overall quality of quantifiable safeguards, and no statistical techniques can be applied to the transformed data to ameliorate the effect of this bias. The calibration techniques are described by Hamilton [52]. The methods used in the Tokai reprocessing plant are detailed by Shimojima [53]; a comprehensive appraisal of the sources and magnitudes of accountancy tank determination errors, many of which apply to calibration, are presented by Davis et al [54] and Foggi et al [55].

4.6 Results

The following table summarizes the results

Method	Current methods				New method
	Number 1	Number 2	Number 3	Number 4	
Mean (g)	4795.6	4796.1	4795.6	4795.6	4795.6
Standard dev. (g)	12.25	169.93	13.81	13.90	11.57

As can be seen from the above table, the effect of using the MVUE calculation is indeed to reduce the standard deviation of the mass transferred. The reduction compared with Method 1 is significant albeit quite small.

As it uses all the measurements, the MVUE is affected to some extent by a bias on any of them, whereas each of the other methods only takes a subset of the available data and is thus immune to errors outside the

subset. As the weight-aliquoting method of concentration determination is much more accurate than the parallel volume-aliquoting method, the MVUE offers little improvement in sensitivity to bias in the former. The effect of the measurement uncertainty of the volume-aliquoting technique is clearly illustrated in the high standard deviation of Method 2.

Currently, only Method 1 is used in the material accountancy calculations. Compared with this, the MVUE introduces a slight sensitivity to the volume-aliquoting concentration determination, and more significant sensitivities to the 'overall' pneumatic reading 'A' and the in-tank density determination 's'. However, it substantially reduces the error caused by bias on the laboratory determination of density.

From the analysis given in section 4.5, if there is no reason to suspect that the systematic errors are not proportional to the determination errors, the MVUE also minimizes the probable sensitivity to unknown biases.

4.7 Summary

The mass estimate from the accountancy tank is an important measure in materials accountancy. This chapter demonstrates a means of minimizing the error on an existing tank, where redundant determinations are available. It also illustrates the benefits to be gained by incorporating diverse instrumentation in the design of a new tank, even where the diverse measurements are less accurate than the principal determinations. If the diversity extends to at least three quantifications of a key parameter, this can be used to even greater

advantage to identify biases and transcription errors [56]. More generally, the methods and conclusions pertain to any application in which the required precision cannot quite be practically or economically met by any single set of instrumentation.

5. Analysis of correlations in the MUF sequence

5.1 Introduction

Most quantitative techniques for nuclear materials accountancy require the distillation of the data collected on each balance period down to two figures, a 'test statistic' and an associated error estimate. It is generally agreed that the ideal test sequence will contain no serial correlation; the basic MUF sequence has an inherent covariance between successive values due to the appearance of Inv_{k-1} in both MUF_k and MUF_{k-1} of

$$\text{Cov}(MUF_{k-1}, MUF_k) = -\sigma^2(Inv_{k-1}) \quad (5.1)$$

If all inventories, inputs and outputs were determined independently on each balance period, this would be the only source of correlation. This is the situation that most authors have considered, although Pike & Woods [28] have introduced an allowance for bias caused by instrument calibration.

However, this regime is often not economically practical; other correlations arise from the operation of the plant measurement systems. This chapter describes a method for producing an optimal statistic from 'real plant' conditions, by matrix transformation techniques. This entails the development of an accurate MUF covariance matrix, from a detailed knowledge of the plant data-acquisition techniques and movement history of the material within the accountancy area. An independent set of filtered 'MUF-residuals' can then be calculated.

5.2 Derivation of the covariance between successive MUF values

For balance period k,

$$MUF_k = Inv_{k-1} + IP_k - OP_k - Inv_k \quad (5.2)$$

where Inv_k is the measured inventory of the plant at the end of balance period k, IP_k is the input to the plant during balance period k and OP_k is the output from the plant during balance period k.

The variance of MUF_k is the sum of the variances of the above elements, modified by the covariances between them:

$$\begin{aligned} \sigma^2(MUF_k) &= \sigma^2(Inv_{k-1}) + \sigma^2(IP_k) + \sigma^2(OP_k) + \sigma^2(Inv_k) \\ &+ 2.Cov(Inv_{k-1}, IP_k) - 2.Cov(Inv_{k-1}, OP_k) - 2.Cov(Inv_{k-1}, Inv_k) \\ &- 2.Cov(IP_k, OP_k) - 2.Cov(IP_k, Inv_k) + 2.Cov(OP_k, Inv_k) \end{aligned} \quad (5.3)$$

where $\sigma^2(x)$ is the variance of x, and $Cov(x,y)$ is the covariance between x and y.

To find the covariance between MUF_k and MUF_{k-1} , an expression for the variance of $(MUF_k + MUF_{k-1})$ is needed.

$$\text{MUF}_k + \text{MUF}_{k-1} = \text{Inv}_{k-2} + \text{IP}_{k-1} - \text{OP}_{k-1} + \text{IP}_k - \text{OP}_k - \text{Inv}_k \quad (5.4)$$

$$\begin{aligned} \sigma^2(\text{MUF}_k + \text{MUF}_{k-1}) &= \sigma^2(\text{Inv}_{k-2}) + \sigma^2(\text{IP}_{k-1}) + \sigma^2(\text{OP}_{k-1}) + \sigma^2(\text{IP}_k) \\ &+ \sigma^2(\text{OP}_k) + \sigma^2(\text{Inv}_k) + 2.\text{Cov}(\text{Inv}_{k-2}, \text{IP}_{k-1}) - 2.\text{Cov}(\text{Inv}_{k-2}, \text{OP}_{k-1}) \\ &+ 2.\text{Cov}(\text{Inv}_{k-2}, \text{IP}_k) - 2.\text{Cov}(\text{Inv}_{k-2}, \text{OP}_k) - 2.\text{Cov}(\text{Inv}_{k-2}, \text{Inv}_k) \\ &- 2.\text{Cov}(\text{IP}_{k-1}, \text{OP}_{k-1}) + 2.\text{Cov}(\text{IP}_{k-1}, \text{IP}_k) - 2.\text{Cov}(\text{IP}_{k-1}, \text{OP}_k) \\ &- 2.\text{Cov}(\text{IP}_{k-1}, \text{Inv}_k) - 2.\text{Cov}(\text{OP}_{k-1}, \text{IP}_k) + 2.\text{Cov}(\text{OP}_{k-1}, \text{OP}_k) \\ &+ 2.\text{Cov}(\text{OP}_{k-1}, \text{Inv}_k) - 2.\text{Cov}(\text{IP}_k, \text{OP}_k) - 2.\text{Cov}(\text{IP}_k, \text{Inv}_k) \\ &+ 2.\text{Cov}(\text{OP}_k, \text{Inv}_k) \end{aligned} \quad (5.5)$$

Using the formula

$$\begin{aligned} \sigma^2(\text{MUF}_k + \text{MUF}_{k-1}) &= \sigma^2(\text{MUF}_k) + \sigma^2(\text{MUF}_{k-1}) + 2.\text{Cov}(\text{MUF}_k, \text{MUF}_{k-1}) \\ &= \sigma^2(\text{Inv}_{k-1}) + \sigma^2(\text{IP}_k) + \sigma^2(\text{OP}_k) + \sigma^2(\text{Inv}_k) \\ &+ 2.\text{Cov}(\text{Inv}_{k-1}, \text{IP}_k) - 2.\text{Cov}(\text{Inv}_{k-1}, \text{OP}_k) - 2.\text{Cov}(\text{Inv}_{k-1}, \text{Inv}_k) \\ &- 2.\text{Cov}(\text{IP}_k, \text{OP}_k) - 2.\text{Cov}(\text{IP}_k, \text{Inv}_k) + 2.\text{Cov}(\text{OP}_k, \text{Inv}_k) \\ &+ \sigma^2(\text{Inv}_{k-2}) + \sigma^2(\text{IP}_{k-1}) + \sigma^2(\text{OP}_{k-1}) + \sigma^2(\text{Inv}_{k-1}) \\ &+ 2.\text{Cov}(\text{Inv}_{k-2}, \text{IP}_{k-1}) - 2.\text{Cov}(\text{Inv}_{k-2}, \text{OP}_{k-1}) \\ &- 2.\text{Cov}(\text{Inv}_{k-2}, \text{Inv}_{k-1}) - 2.\text{Cov}(\text{IP}_{k-1}, \text{OP}_{k-1}) \\ &- 2.\text{Cov}(\text{IP}_{k-1}, \text{Inv}_{k-1}) + 2.\text{Cov}(\text{OP}_{k-1}, \text{Inv}_{k-1}) \\ &+ 2.\text{Cov}(\text{MUF}_k, \text{MUF}_{k-1}) \end{aligned} \quad (5.6)$$

the covariance between the balance periods can be isolated as

$$\begin{aligned}
\text{Cov}(\text{MUF}_k, \text{MUF}_{k-1}) &= \text{Cov}(\text{Inv}_{k-2}, \text{IP}_k) - \text{Cov}(\text{Inv}_{k-2}, \text{OP}_k) \\
&- \text{Cov}(\text{Inv}_{k-2}, \text{Inv}_k) + \text{Cov}(\text{IP}_{k-1}, \text{IP}_k) - \text{Cov}(\text{IP}_{k-1}, \text{OP}_k) \\
&- \text{Cov}(\text{IP}_{k-1}, \text{Inv}_k) - \text{Cov}(\text{OP}_{k-1}, \text{IP}_k) + \text{Cov}(\text{OP}_{k-1}, \text{OP}_k) \\
&+ \text{Cov}(\text{OP}_{k-1}, \text{Inv}_k) - \text{Cov}(\text{Inv}_{k-1}, \text{IP}_k) + \text{Cov}(\text{Inv}_{k-1}, \text{OP}_k) \\
&+ \text{Cov}(\text{Inv}_{k-1}, \text{Inv}_k) + \text{Cov}(\text{Inv}_{k-2}, \text{Inv}_{k-1}) + \text{Cov}(\text{IP}_{k-1}, \text{Inv}_{k-1}) \\
&- \text{Cov}(\text{OP}_{k-1}, \text{Inv}_{k-1}) - \sigma^2(\text{Inv}_{k-1}) \tag{5.7}
\end{aligned}$$

The correlation between successive MUF values is found from:

$$\text{Cor}(\text{MUF}_k, \text{MUF}_{k-1}) = \frac{\text{Cov}(\text{MUF}_k, \text{MUF}_{k-1})}{\sqrt{\sigma^2(\text{MUF}_k) \cdot \sigma^2(\text{MUF}_{k-1})}} \tag{5.8}$$

5.3 Correlations over more than one interval

The MUF values for balance periods that are not in juxtaposition may still exhibit correlation. The analysis is similar to that given above, but there is no common inventory between the two MUF figures. The covariance between two MUF values of separation n balance periods, where $n > 1$, is given below.

$$\begin{aligned}
\text{Cov}(\text{MUF}_k, \text{MUF}_{k-n}) &= \text{Cov}(\text{Inv}_{k-n-1}, \text{IP}_k) - \text{Cov}(\text{Inv}_{k-n-1}, \text{OP}_k) \\
&- \text{Cov}(\text{Inv}_{k-n-1}, \text{Inv}_k) + \text{Cov}(\text{IP}_{k-n}, \text{IP}_k) - \text{Cov}(\text{IP}_{k-n}, \text{OP}_k) \\
&- \text{Cov}(\text{IP}_{k-n}, \text{Inv}_k) - \text{Cov}(\text{OP}_{k-n}, \text{IP}_k) + \text{Cov}(\text{OP}_{k-n}, \text{OP}_k) \\
&+ \text{Cov}(\text{OP}_{k-n}, \text{Inv}_k) - \text{Cov}(\text{Inv}_{k-n}, \text{IP}_k) + \text{Cov}(\text{Inv}_{k-n}, \text{OP}_k) \\
&+ \text{Cov}(\text{Inv}_{k-n}, \text{Inv}_k) + \text{Cov}(\text{Inv}_{k-n-1}, \text{Inv}_{k-1}) + \text{Cov}(\text{IP}_{k-n}, \text{Inv}_{k-1}) \\
&- \text{Cov}(\text{OP}_{k-n}, \text{Inv}_{k-1}) - \text{Cov}(\text{Inv}_{k-n}, \text{Inv}_{k-1}) \tag{5.9}
\end{aligned}$$

As $\sigma^2(\text{Inv}_{k-1})$ is the same as $\text{Cov}(\text{Inv}_{k-1}, \text{Inv}_{k-1})$, it can be seen that this expression also applies for $n=1$, and is thus completely general for any covariance in any accountancy area.

5.4 Application to the Fast Reactor Fuel Reprocessing Plant

5.4.1 Plant measurements in the head-end MBA

The mass of heavy metal in the uncropped pins and the batches in baskets is taken from the burn-up calculation for the source sub-assembly. Currently, the dissolver estimate is also taken from this. The correlation between the sub-assembly mass estimate and these inventory estimates is thus one, and the covariance between them is the product of their standard deviations. The dissolver heel is determined independently on each balance period, and the hold-all tank is reassessed when there is a change in content. Waste products are assayed on the balance period in which they are created; this determination is also used when the waste is exported, introducing a correlation between the output and past inventories.

The output from the accountancy tank is determined completely independently on each balance period, and so makes no contribution to the random error. However, as discussed in chapter 5, it is a possible source of systematic errors; this will be investigated further in chapter 7.

Covariance may exist between sub-assembly burn-up estimates, but this lies outside the scope of this thesis; they are assumed to be independent, so there will be no correlation between inputs, or between the inventory at the end of period $k-x$ ($x>0$) and the input during period k . The covariance expression thus reduces to:

$$\begin{aligned}
 \text{Cov}(\text{MUF}_k, \text{MUF}_{k-n}) &= \text{Cov}(\text{IP}_{k-n}, \text{Inv}_{k-1}) + \text{Cov}(\text{Inv}_{k-n}, \text{Inv}_k) \\
 &+ \text{Cov}(\text{Inv}_{k-n-1}, \text{Inv}_{k-1}) - \text{Cov}(\text{IP}_{k-n}, \text{Inv}_k) \\
 &- \text{Cov}(\text{Inv}_{k-n-1}, \text{Inv}_k) - \text{Cov}(\text{Inv}_{k-n}, \text{Inv}_{k-1}) \\
 &- \text{Cov}(\text{Inv}_{k-n-1}, \text{OP}_k) + \text{Cov}(\text{Inv}_{k-n}, \text{OP}_k) \quad (5.10)
 \end{aligned}$$

The terms remaining refer to the covariances arising from common inventories, caused by material remaining within the accountancy area over two or more balance periods without reassessment, the covariances between inventory estimates and the source sub-assembly estimates, and the covariances between output waste and their inventory determinations.

In applying these formulae, it should be noted that where there are two or more terms in a balance period inventory whose heavy metal content is assumed from a common sub-assembly, the correlations between these elements will increase the inventory variance (by twice the covariance

for each combination).

It should be noted that the earlier NRTMA plant measurement regime used an independent assessment of the dissolver inventory, taken from its internal dip-tube system. This resulted in a much higher MUF standard deviation, and a very different covariance matrix; this inaccurate inventory measurement introduced a dominant negative correlation between successive MUF figures, which has now been replaced by a positive correlation from the covariance between the inputs and the inventories. The results cited in [43] and [48] refer to the earlier accountancy system, and are included here for comparison.

5.4.2 Plant measurements in the solvent extraction MBA

If there is no input to or output from any of the concentrate tanks between balance periods, the content is assumed from the measurement made after the last material transfer. When tank 1 is filled, it is not discharged or re-evaluated until another tank is filled. This can give rise to large covariances between inventories. All other determinations are made independently on each balance period. The covariance expression for this area is thus simplified to:

$$\begin{aligned} \text{Cov}(\text{MUF}_k, \text{MUF}_{k-n}) &= \text{Cov}(\text{Inv}_{k-n}, \text{Inv}_k) + \text{Cov}(\text{Inv}_{k-n-1}, \text{Inv}_{k-1}) \\ &\quad - \text{Cov}(\text{Inv}_{k-n-1}, \text{Inv}_k) - \text{Cov}(\text{Inv}_{k-n}, \text{Inv}_{k-1}) \end{aligned} \tag{5.11}$$

5.5 Application of the MUF-residuals transformation

The two models of the head-end were used to generate simulated MUF data and the associated inter-MUF correlations. For comparison, the MUF-residual sequence was created from these calculated correlations, and the ITMUF sequence was formed using a uniform tri-diagonal correlation matrix, with the off-diagonal terms equal to the average correlation between successive MUF figures of -0.4.

Alarm thresholds to give a constant false alarm for the MUF, MUFR and ITMUF sequences were found by iteration; they are listed in Appendix VI. These thresholds were then applied to simulated data with various diversion scenarios. Example results for both the old and new accountancy systems are illustrated graphically in the next section.

A more powerful tool for diversion detection is offered by applying Page's cumulative sum test to the data. As described in chapter 2, this can be expressed

$$\text{alarm if } \max_{1 \leq r \leq n} \left[\begin{array}{c} n \\ \sigma \\ i=r \end{array} \left\{ \frac{x_i}{\sigma_i} - K \right\} \right] \geq H \quad (5.12)$$

where x is the test statistic. The parameters 'H' and 'K' can be 'tuned' to be optimal for a large single diversion or a protracted loss; several papers have been written about the choice of these parameters and the performance of the test eg. [17],[45]. Reference [57] describes a method for calculating the parameters for the SITMUF (Standardised ITMUF) sequence, assuming each value is independent. For the plant under investigation the usual ITMUF transformation does not yield a set of independent elements, so to compare the MUF-residuals sequence with MUF and ITMUF all three were tested by simulation, applying each to the

same plant data.

For the purpose of the comparison, a value of 'K' was chosen, and 'H' for each of the test statistics was selected by simulation to give a false alarm rate of 5% (1 campaign in 20 alarming under no loss, 40 balance periods per campaign). The test was then applied with these values to data containing different diversions. The percentage of campaigns ending in an alarm indicates the power of the test to detect that diversion.

Appendix VII describes a useful algorithm to calculate MUF-residuals (or ITMUF) for the application of Page's Test, in which the test is reset after an alarm is signalled.

5.6 Results

The use of an accurate covariance matrix to transform the MUF data to MUF-residuals (MUFR) gives a sequence with significantly better performance as a test statistic than MUF or ITMUF.

For the old accountancy system, where ITMUF represents a simple model of the MUF covariances, a plot of the statistics for a simulated campaign (fig. 5.1) shows that both MUFR and ITMUF in general suppress the swings of MUF.

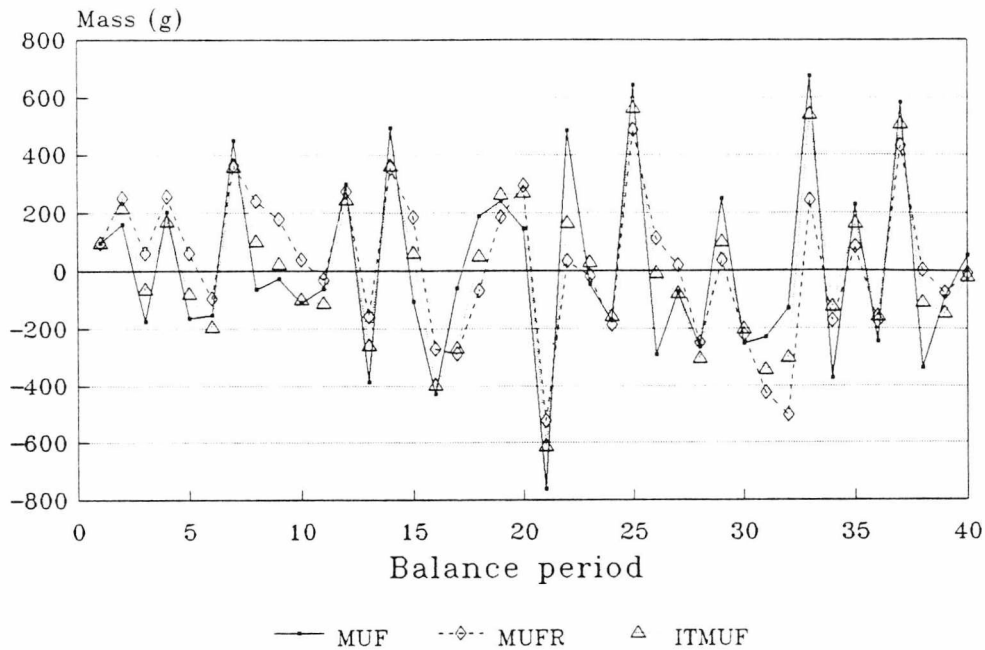


Figure 5.1 Sample data, old accountancy system (independent dissolver assessment)

It is not obvious from this which is the 'better' statistic. Turning to the performance of the tests in terms of identifying a loss with a threshold test, MUFR shows a clear superiority. For an abrupt loss on period 30, the 95%-alarm-probability mass is less than 1200g for MUFR, around 1400g for ITMUF, and about 1600g for MUF (fig. 5.2). It is interesting to note that MUF, if it alarms, alarms instantaneously, while MUFR in particular shows a degree of 'delayed detection'. The loss may be concealed by random error on the period in which it occurs, but the MUFR expectation of the MUF mean on the immediately-following periods is distorted. The diversion on period 30 may thus put the residual on period 31 or even 32 'out of bounds'. While the cause of this delayed alarm may be more difficult to trace, this knock-on effect does enhance the overall power of the decorrelating techniques.

The performance of Page's Test is dependent on the choice of the H-K pair; a large 'K' is most suitable for detecting abrupt losses, while a

small 'K' offers a greater sensitivity to protracted diversions. A compromise of $K=0.2$, 'tuned' for losses of 0.4σ , or around 120g, is demonstrated here.

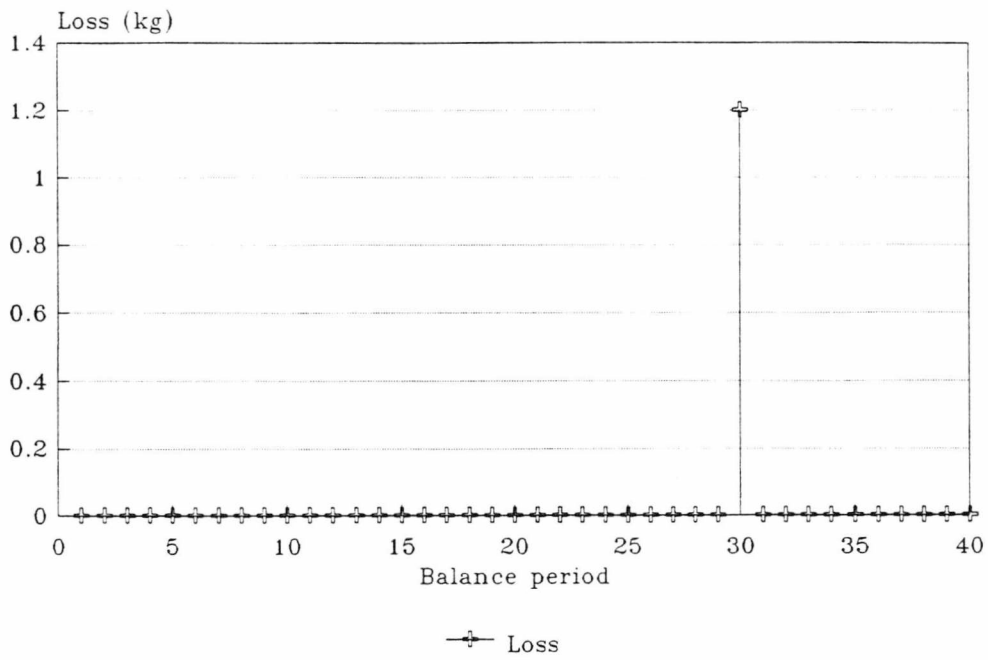
The use of Page's Test increases the sensitivity of the tests, and reduces the benefits of the accurate modelling; these masses are now 800g for MUFR and ITMUF, and 1200g for MUF (fig. 5.3). It can be seen from fig. 5.1 that the MUFR and ITMUF plots do still demonstrate a tendency to echo the MUF zig-zag over the zero point. The CUSUM technique will smooth this and help identify any underlying anomaly. ITMUF, using a correct average value for the correlation, benefits particularly from this.

For campaign-long diversions or instrument errors, the improvement offered by MUFR in the threshold test is even more pronounced, almost 100% of campaigns concealing a diversion of 100g/period giving rise to MUFR alarms, compared with 25% for ITMUF and 9% for MUF (fig. 5.4). MUFR also displays a steep detection probability curve - there is a 90% chance that it would alarm this scenario in less than 20 periods, minimizing the total loss. Again, better results are obtained from Page's Test, the 95% alarm rate falling at less than 50g/period for MUFR, 50g/period for ITMUF, and just under 100g/period for MUF (fig. 5.5). While ITMUF has almost the same absolute power, MUFR is again likely to detect the loss much sooner.

Similar results are obtained in loss scenarios involving loss over several periods (figs. 5.6, 5.7), or loss with fractional replacement (figs. 5.8, 5.9). In general, MUFR is much more powerful than ITMUF or MUF when used in a threshold test, and slightly more powerful than ITMUF in Page's Test.

Graphs illustrating the absolute power of the tests against the magnitude of an abrupt loss on period 30 are shown in figures 5.10 & 5.11, and against a campaign-long protracted loss in figures 5.12 & 5.13. Page's Test somewhat ameliorates the effects of modelling errors, but the highest detection probabilities are given by MUFR with Page's Test in all cases.

Loss scenario



Cumulative alarm probabilities Independent dissolver estimate

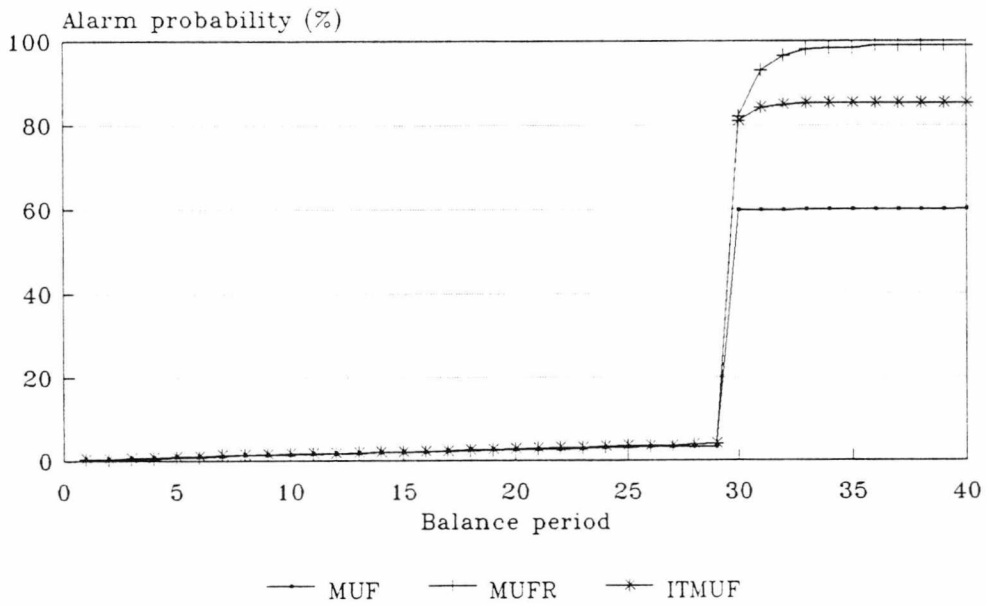
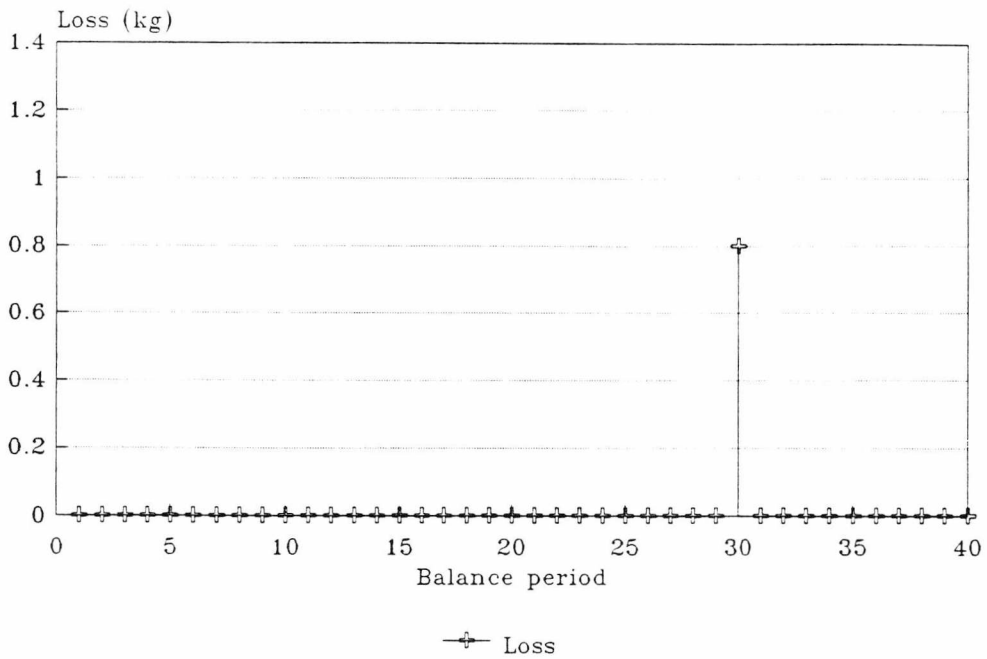


Fig 5.2 Cumulative alarm probabilities for abrupt loss, old system
Threshold test with MUF, MUFR, ITMUF

Loss scenario



Cumulative alarm probabilities Independent dissolver estimate

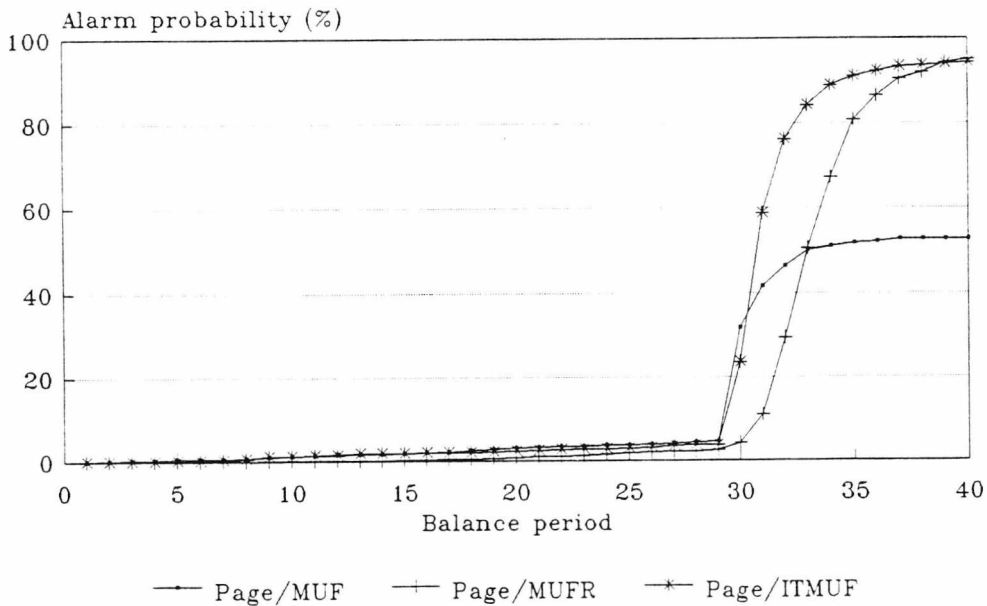
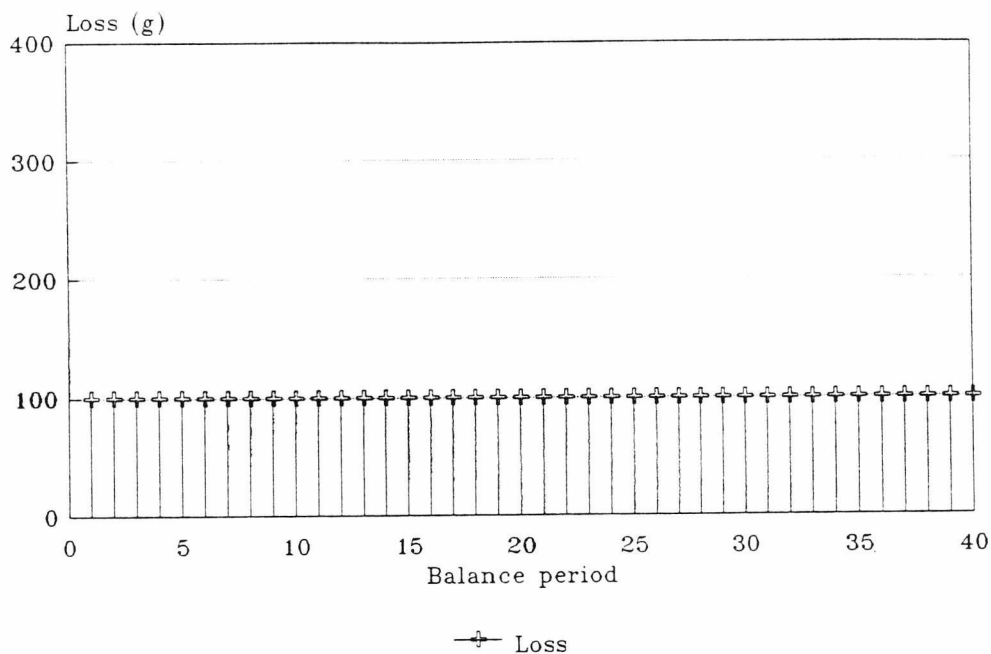


Fig 5.3 Cumulative alarm probabilities for abrupt loss, old system
Page's Test with MUF, MUFR, ITMUF

Loss scenario



Cumulative alarm probabilities Independent dissolver estimate

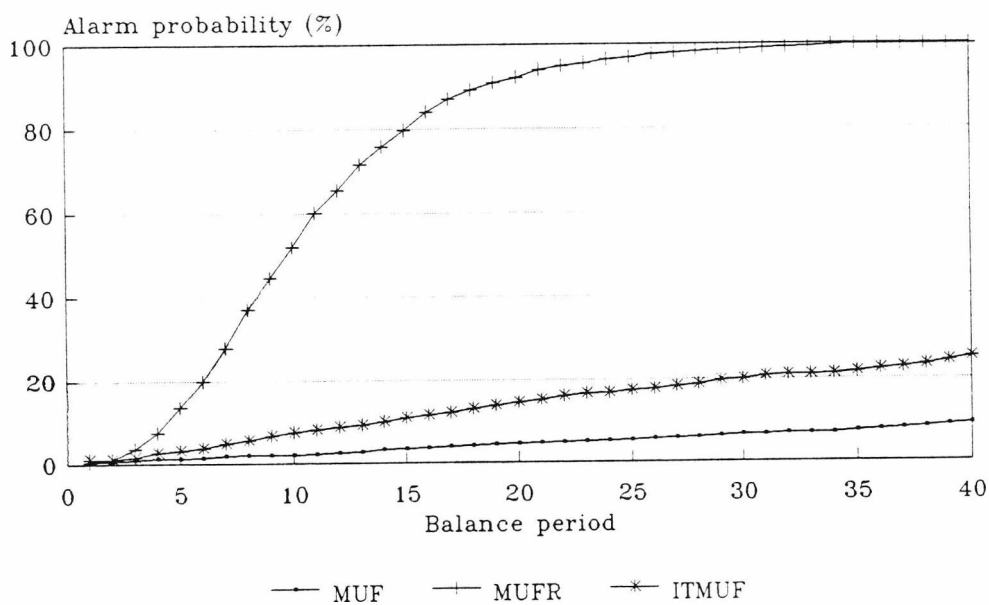
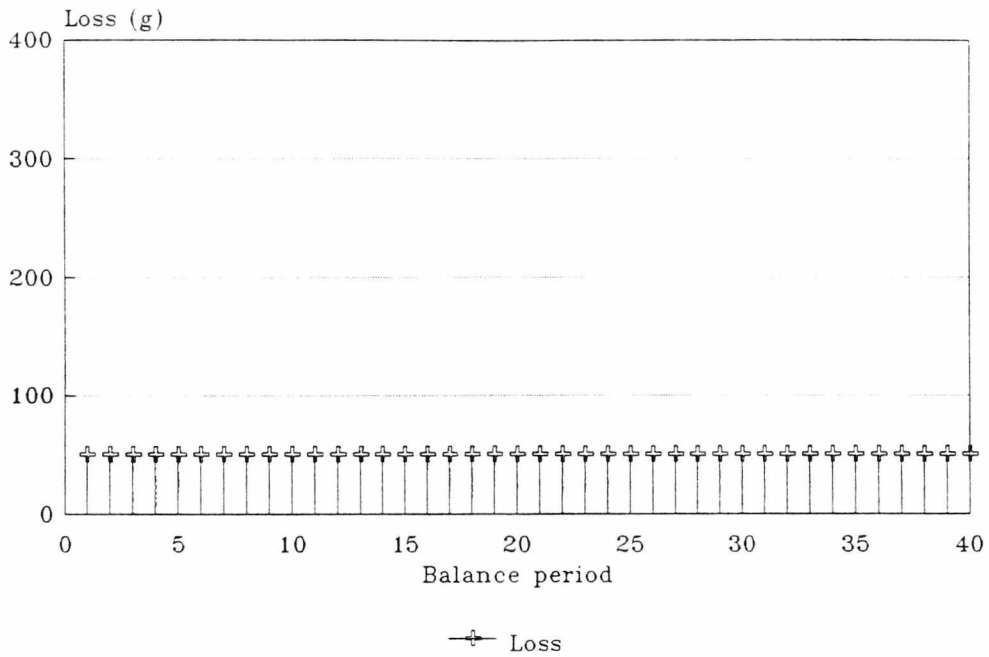


Fig 5.4 Cumulative alarm probs. for protracted loss, old system
Threshold test with MUF, MUFR, ITMUF

Loss scenario



Cumulative alarm probability Independent dissolver estimate

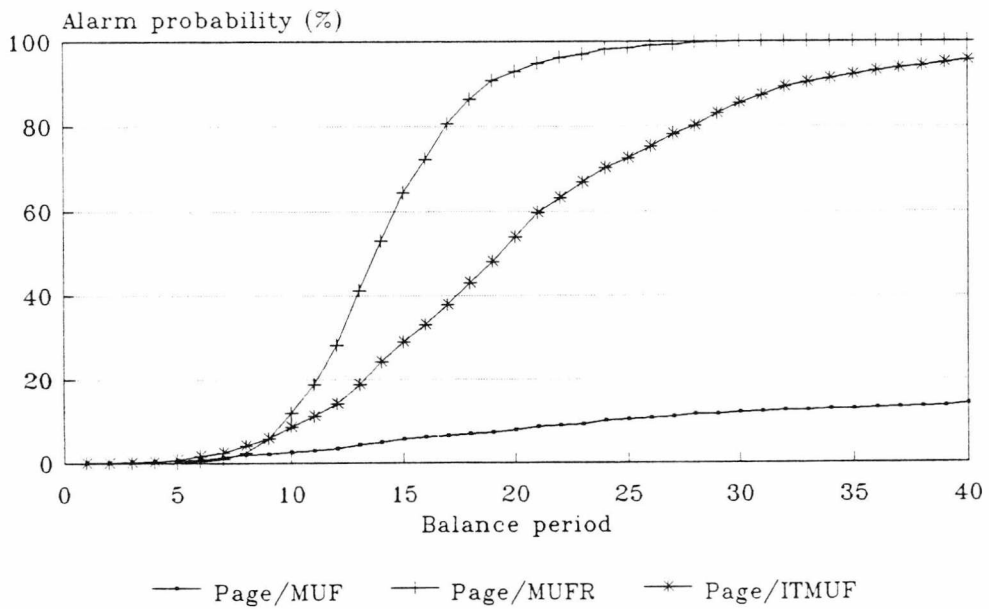
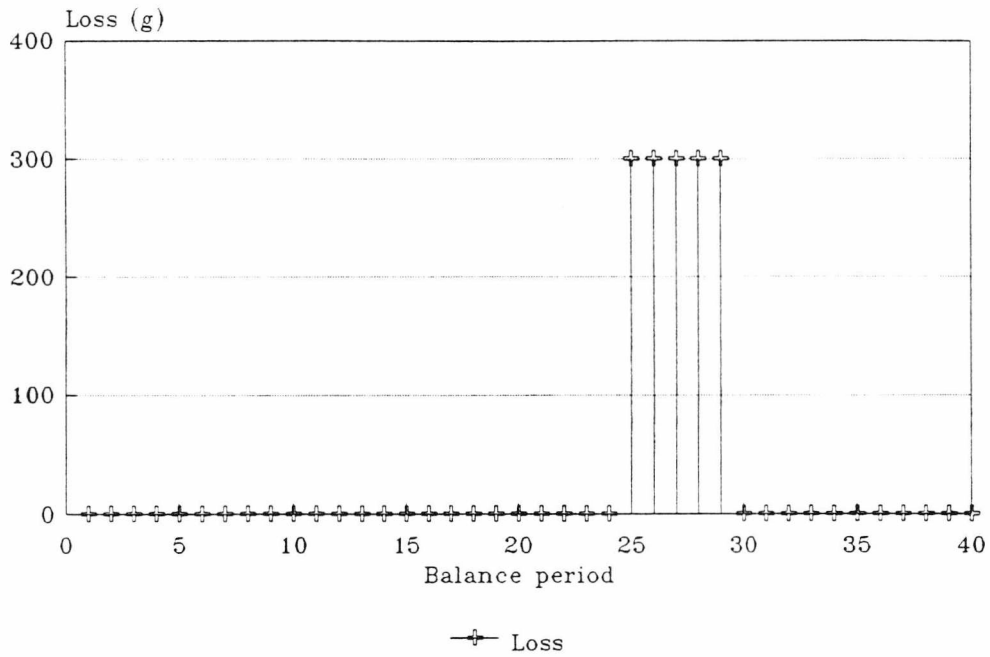


Fig 5.5 Cumulative alarm probs. for protracted loss, old system
Page's Test with MUF, MUFR, ITMUF

Loss scenario



Cumulative alarm probabilities Independent dissolver estimate

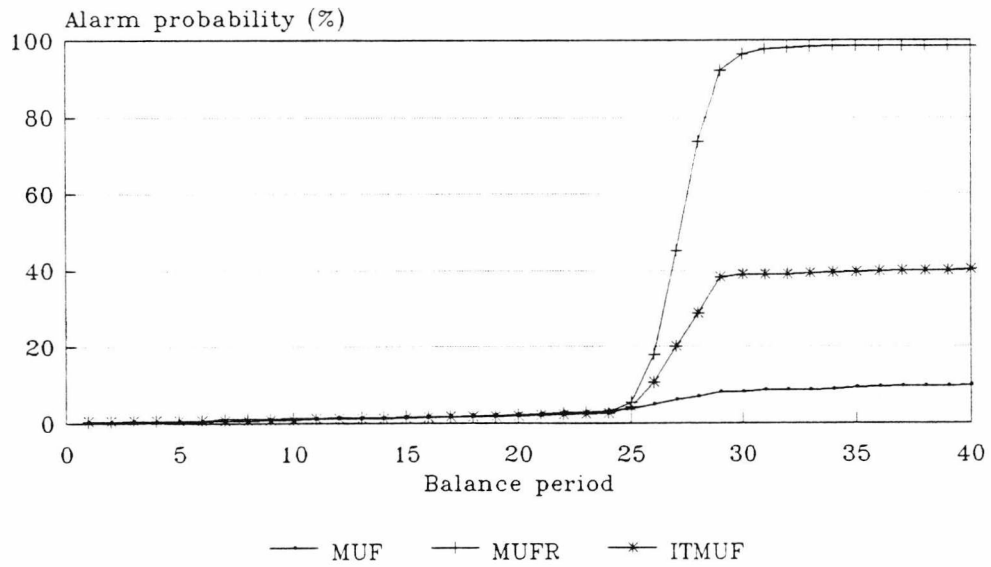
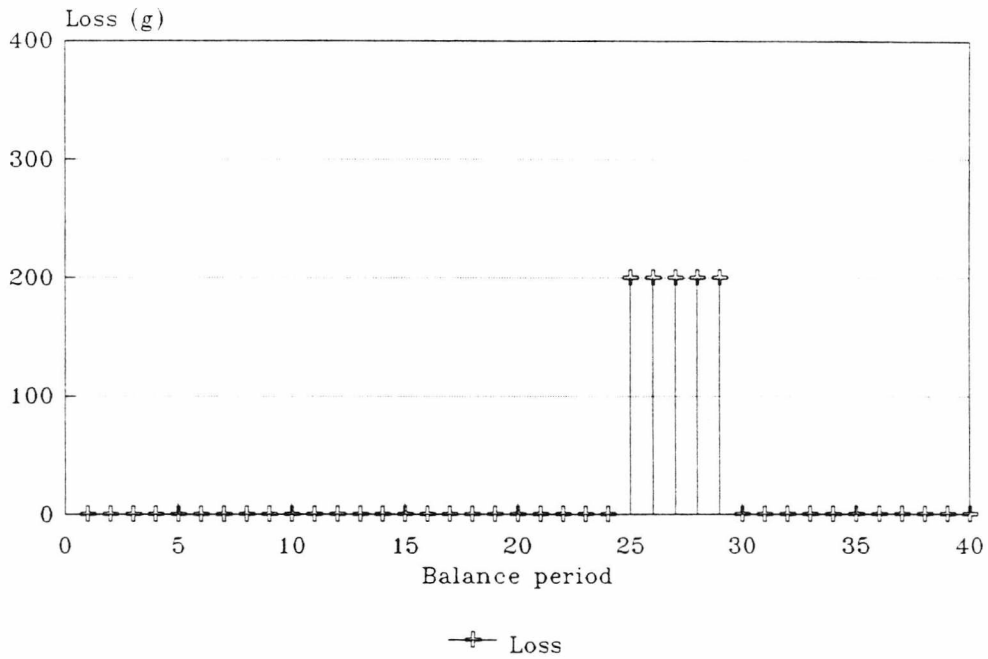


Fig 5.6 Cumulative alarm probs. for loss over 5 periods, old system
Threshold test with MUF, MUFR, ITMUF

Loss scenario



Cumulative alarm probabilities Independent dissolver estimate

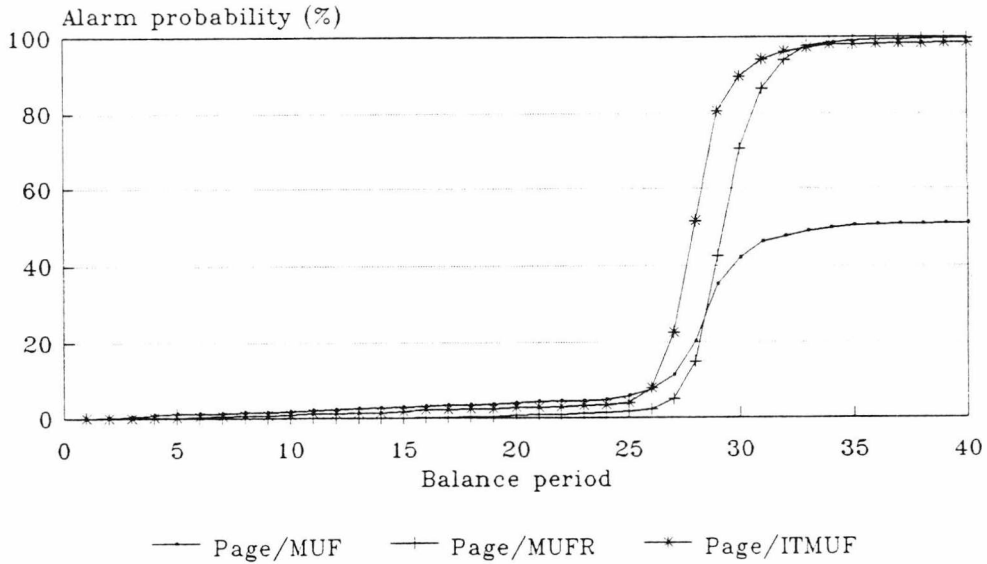
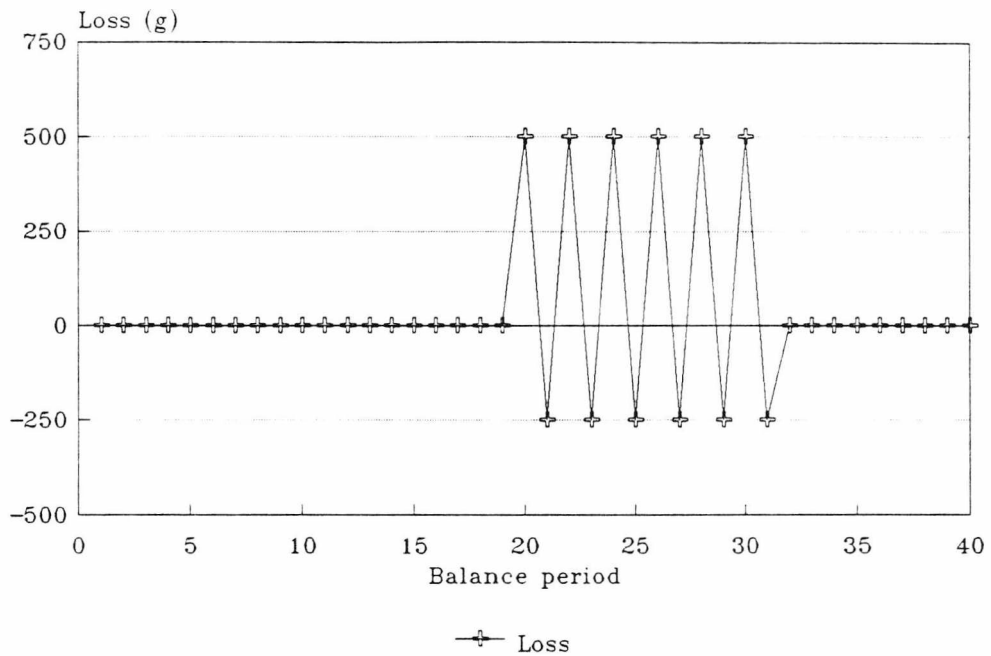


Fig 5.7 Cumulative alarm probs. for loss over 5 periods, old system
Page's Test with MUF, MUFR, ITMUF

Loss scenario



Cumulative alarm probabilities Independent dissolver estimate

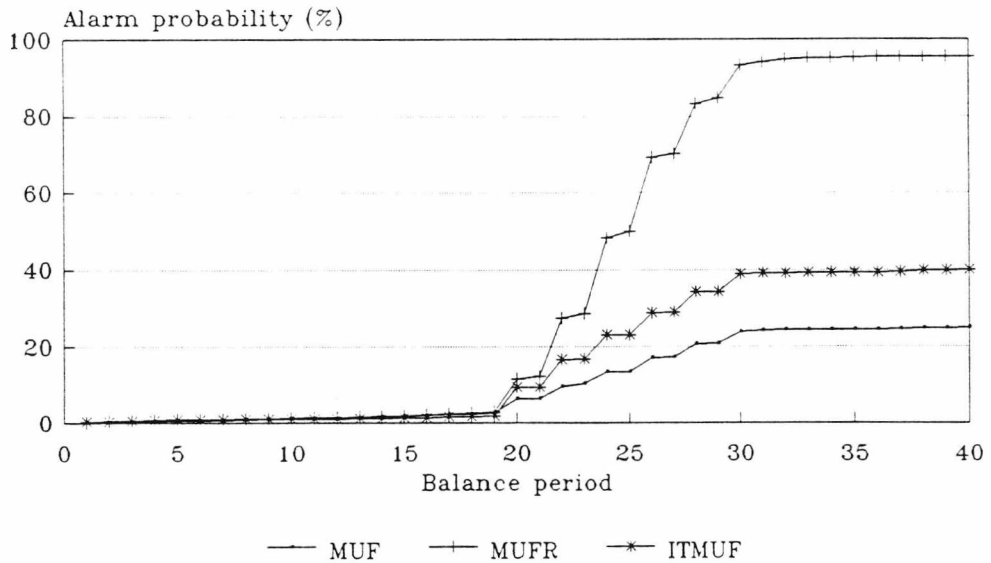
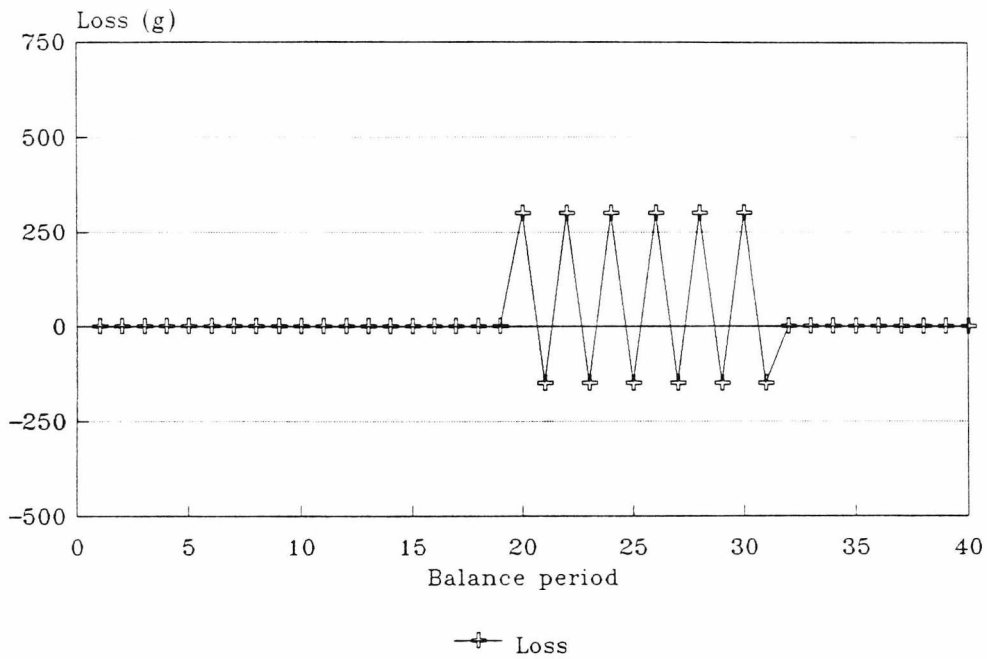


Fig 5.8 Cumulative alarm probabilities for alternate loss with fractional replacement, old system
Threshold test with MUF, MUFR, ITMUF

Loss scenario



Cumulative alarm probabilities Independent dissolver estimate

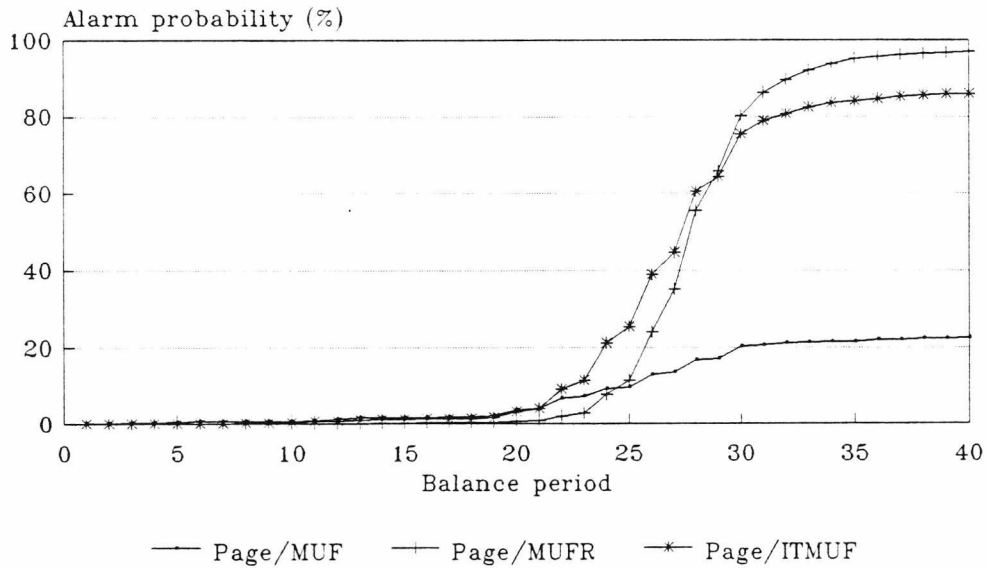


Fig 5.9 Cumulative alarm probabilities for alternate loss with fractional replacement, old system
Threshold test with MUF, MUFR, ITMUF

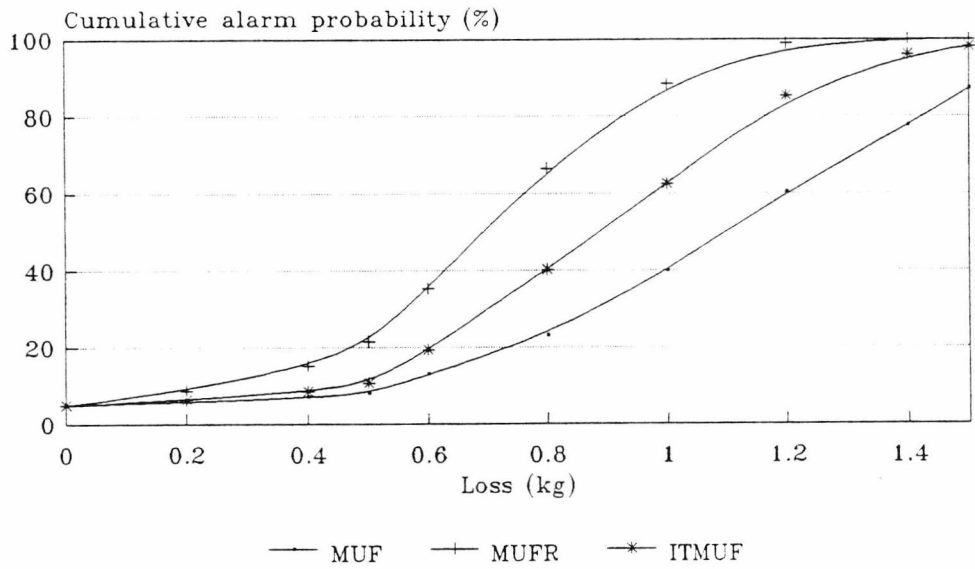


Fig 5.10 Absolute power for abrupt loss on period 30, old system
Threshold test with MUF, MUFR, ITMUF

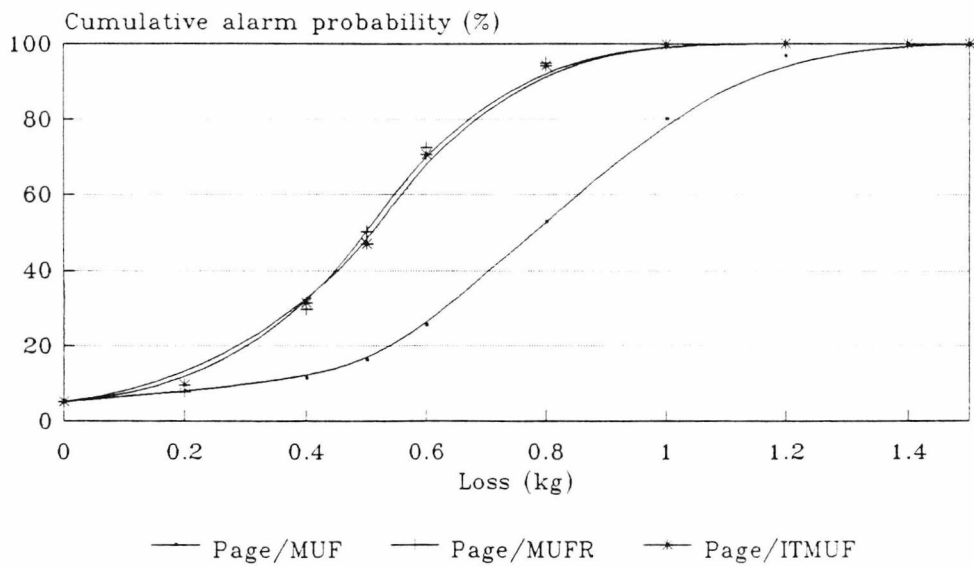


Fig 5.11 Absolute power for abrupt loss on period 30, old system
Page's Test with MUF, MUFR, ITMUF

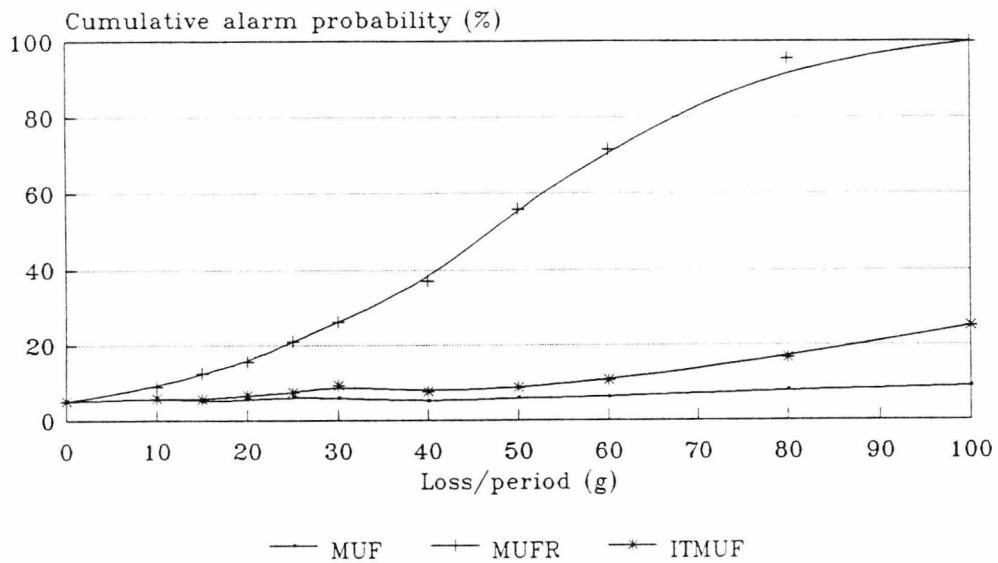


Fig 5.12 Absolute power for protracted loss, old system
 Threshold test with MUF, MUFR, ITMUF

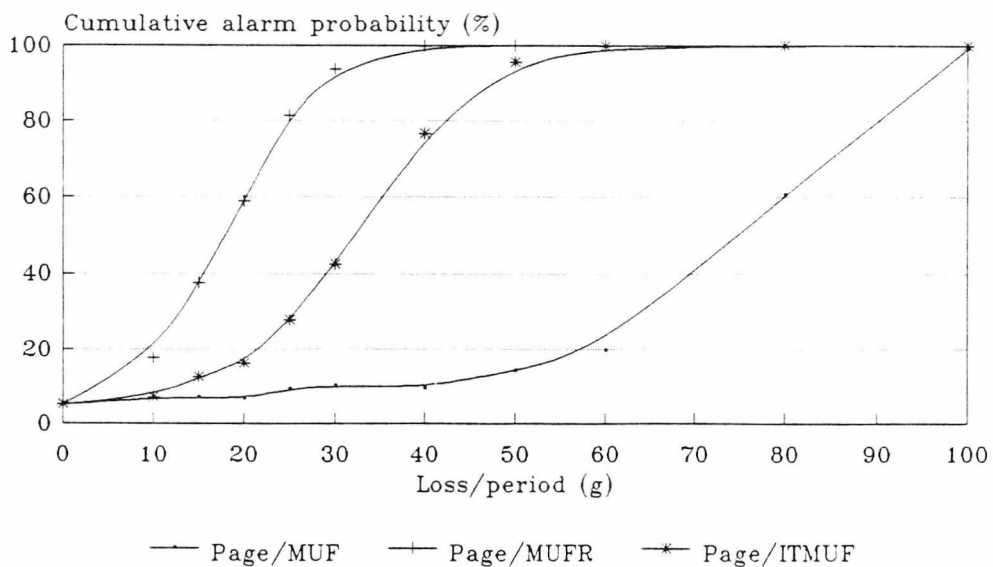


Fig 5.13 Absolute power for protracted loss, old system
 Page's Test with MUF, MUFR, ITMUF

The improvement over the simple-model ITMUF statistic is, not surprisingly, much more pronounced in the new accountancy system, where the ITMUF assumptions are wrong rather than just inaccurate. The effect of this modelling error, and the performance of the MUF statistic, is illustrated in the simulated campaign data in figure 5.14.

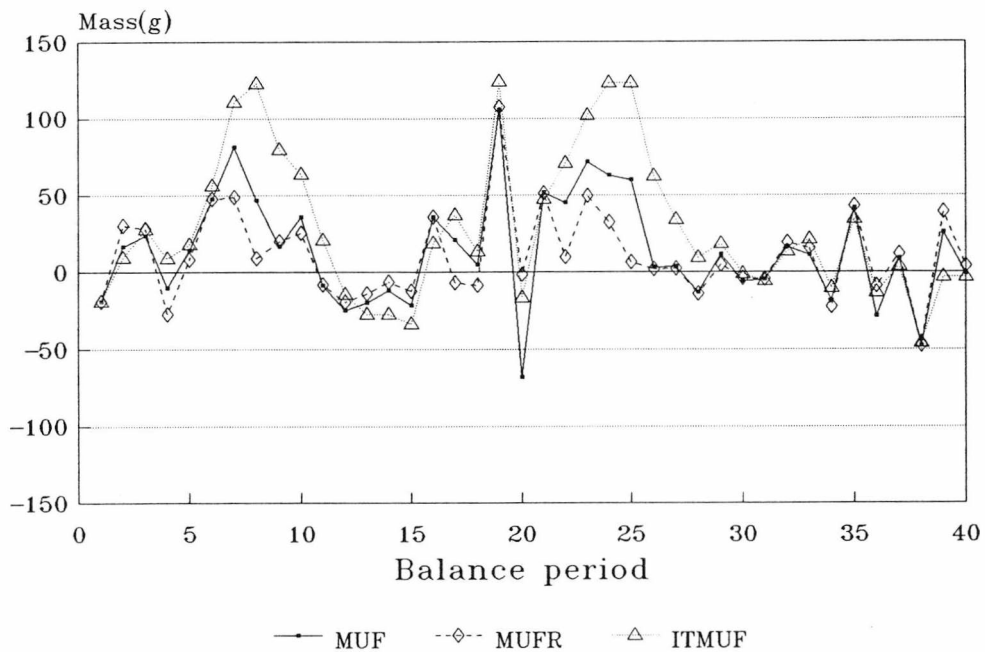


Figure 5.14 Sample data, new accountancy system (dissolver assumed from fuel sub-assembly burn-up calculation)

The MUF in general suppresses the swings of the MUF data, while ITMUF, expecting a negative correlation when it is in fact positive, overshoots. In terms of diversion detection, this means that the false alarm thresholds for the ITMUF must be set very high.

It is immediately evident in data simulating the new operating practice that removing the inaccurate inventory estimate greatly reduces the MUF

standard deviation, now down to an average of around 40g. This is reflected in the 95% detection probability mass for an abrupt diversion, of interest to the IAEA as an accountancy goal; it is down to 200g with MUF_R (fig. 5.15). The new covariance matrix structure means that the benefits over MUF are less pronounced - MUF will detect the 200g abrupt loss with a 92% probability. The overall link between successive MUF figures is weaker, because the positive correlation from the input-inventory estimate connections is partly offset by the expected negative inventory correlation.

In this scenario, the use of Page's Test with MUF has a reverse effect to the above examples - it actually reduces the sensitivity. The positive correlation between the MUF values means that any summation technique will require high thresholds; in this case, a better performance can be obtained from the 'raw' statistic. Accounting for the obvious negative correlation but ignoring the others creates a statistic in which this effect is even more pronounced. The ITMUF sequence contains a very strong positive correlation, and demands very high thresholds to limit the false alarm rate. Fig. 5.16 shows the alarm plot for a 250g diversion on period 30, which corresponds to the 95% detection level for MUF_R.

An additional problem in this application is the limited 'bandwidth' of Page's Test centered around the choice of K . In selecting a $H-K$ pair to compromise between large and small loss detection, the performance at both extremes suffers. The choice of $K=0.5$ gives the CUSUM test with MUF_R a slightly poorer performance against abrupt losses than the threshold test. This problem is largely overcome by the use of a twin test, one with a small ' K ' for optimal performance against small losses, and one with a large ' K ' to identify abrupt diversions. However, the thresholds would have to be increased to maintain the false alarm rate.

The use of twin tests, and the performance benefits to be gained, are discussed further in chapter 7.

An interesting situation arises in the analysis of the test performances against protracted diversions, shown in figures 5.17 & 5.18 for the Threshold and Page's Test respectively. Firstly, the detectable loss is not reduced as significantly as might be expected from the decrease in the MUF standard deviation. Secondly, the MUFR statistic offers a poorer chance of detection than the MUF, and the best performance is given by ITMUF.

It appears that the assumption of negative correlation, when in fact the sequence is predominantly positively correlated, does actually increase the power to detect a protracted diversion. The reason for this is illustrated in figure 5.19. The two MUF values conceal a positive diversion of μ . While MUFR attributes much of the anomaly on period 2 to the positive correlation, ITMUF is expecting a negative MUF to offset the first positive MUF. Thus, the diversion lies much closer to the ITMUF threshold (even though it is higher than the MUFR threshold). This pattern will be repeated while the loss continues; a small positive random element on one of the MUF estimates is now very likely to cause an ITMUF alarm.

Inaccurate modelling techniques are not the most effective means of identifying a protracted anomaly, however; CUMUF and state-estimation techniques using accurate representations are both more powerful, as will be demonstrated in chapter 7.

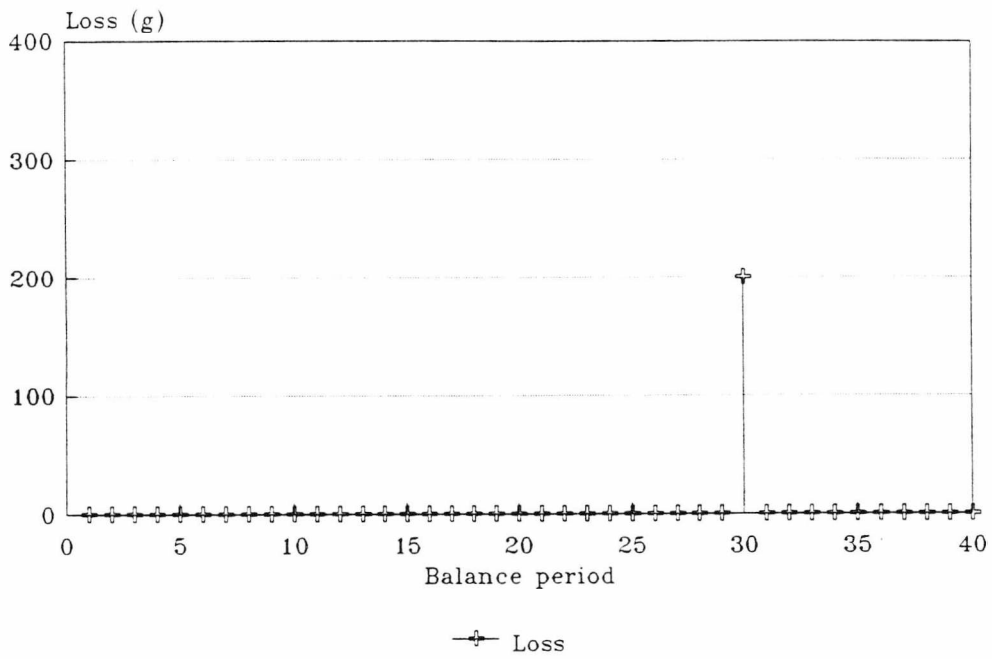
MUFR again offers considerably more power against the more sophisticated diversion-with-fractional-replacement strategy, shown in figures 5.20 & 5.21.

The inaccurate modelling thus leads to an unreliable test with poor robustness.

The replacement of the pronounced oscillatory nature of the sequence with a much smoother data set also reduces the power of Page's Test with MUFR if a fraction of the diverted material is returned on the following period. In the 'old' accountancy system, MUFR 'expects' a negative MUF to offset the positive MUF caused by the diversion. The replacement of material thus does not tend to reduce the MUFR CUSUM significantly. However, here it expects another positive MUF to compliment the relatively high positive MUF of the diversion. The effect of the negative MUF is thus amplified in the MUFR statistic, reducing the MUFR CUSUM and decreasing the probability of alarming on the next positive diversion.

The absolute power against loss magnitude plots for the Threshold test/abrupt loss, Page's Test/abrupt loss, Threshold test/protracted loss and Page's test/protracted loss are shown in figures 5.22-5.25. These illustrate again the superiority of MUFR and the drawback of the single Page's Test for an abrupt diversion, and the anomalous advantage of ITMUF against a protracted loss.

Loss scenario



Cumulative alarm probabilities Dissolver estimated from burn-up calculn

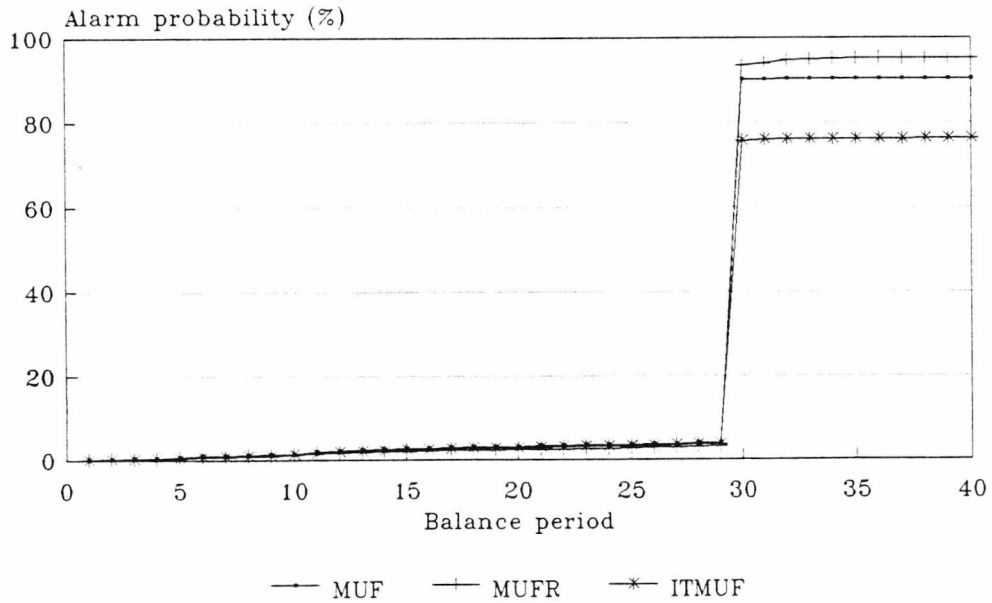
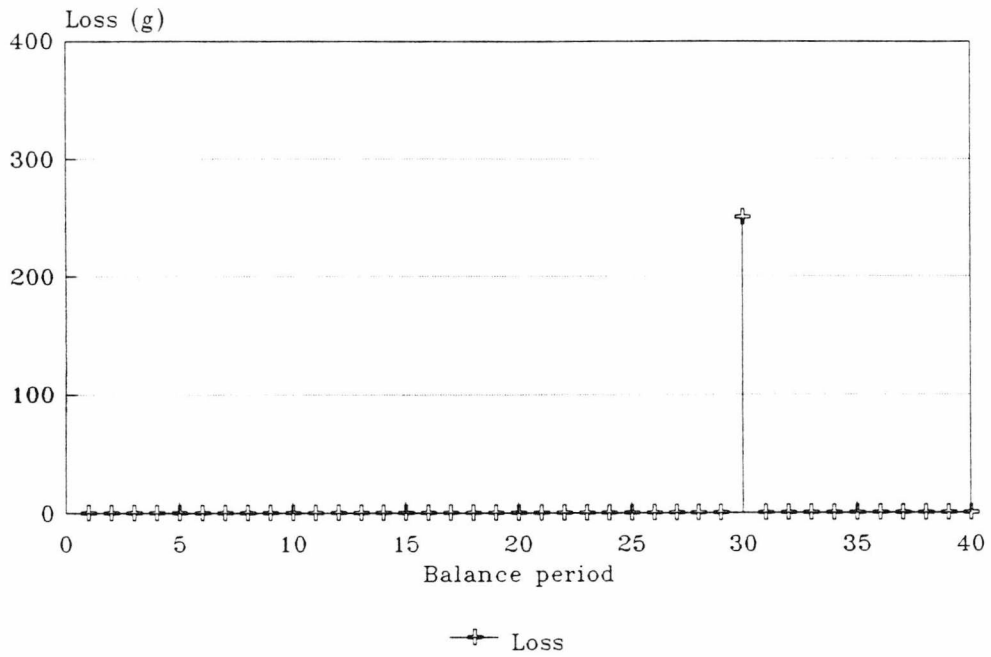


Fig 5.15 Cumulative alarm probabilities for abrupt loss, new system
Threshold test with MUF, MUFR, ITMUF

Loss scenario



Cumulative alarm probabilities Dissolver estimated from burn-up calculn

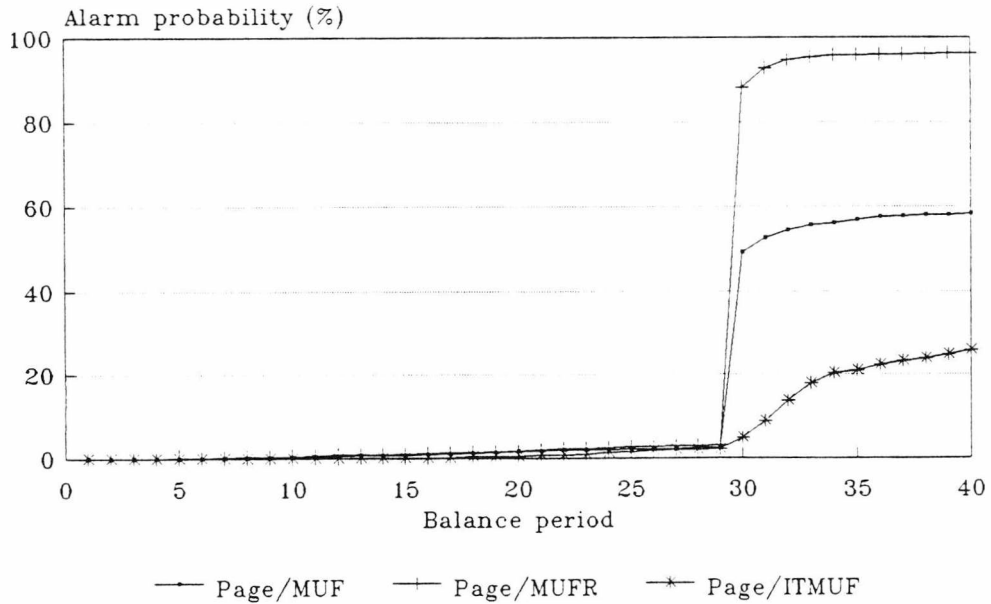
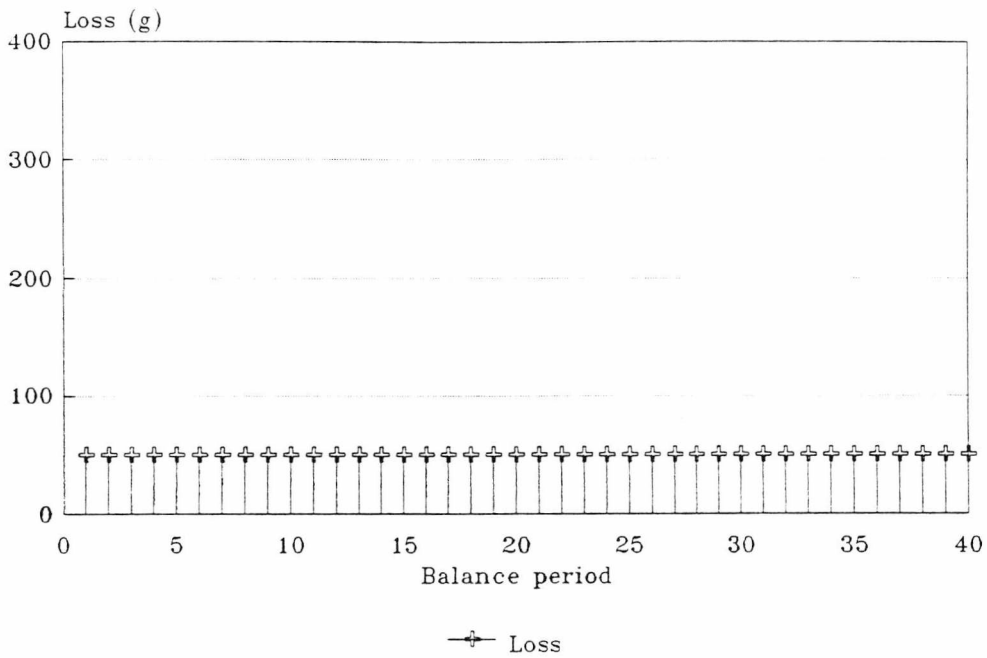


Fig 5.16 Cumulative alarm probabilities for abrupt loss, new system
Page's Test with MUF, MUFR, ITMUF

Loss scenario



Cumulative alarm probabilities Dissolver estimated from burn-up calculn

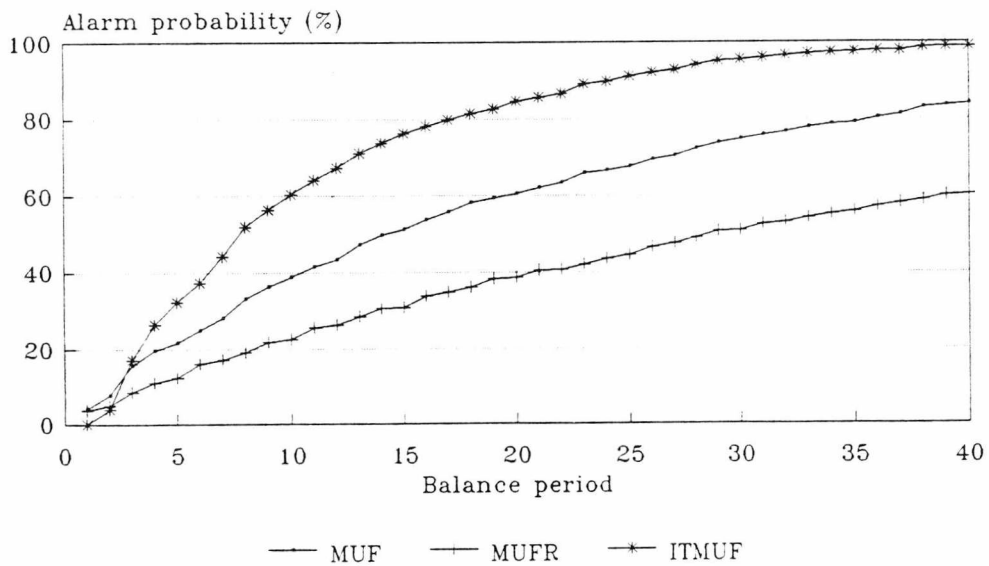
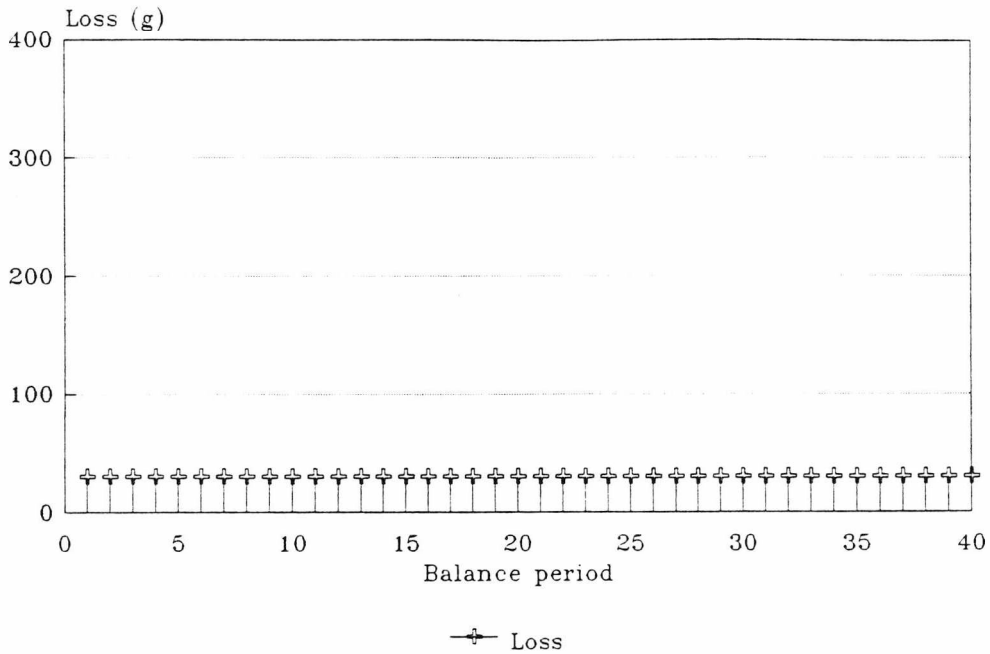
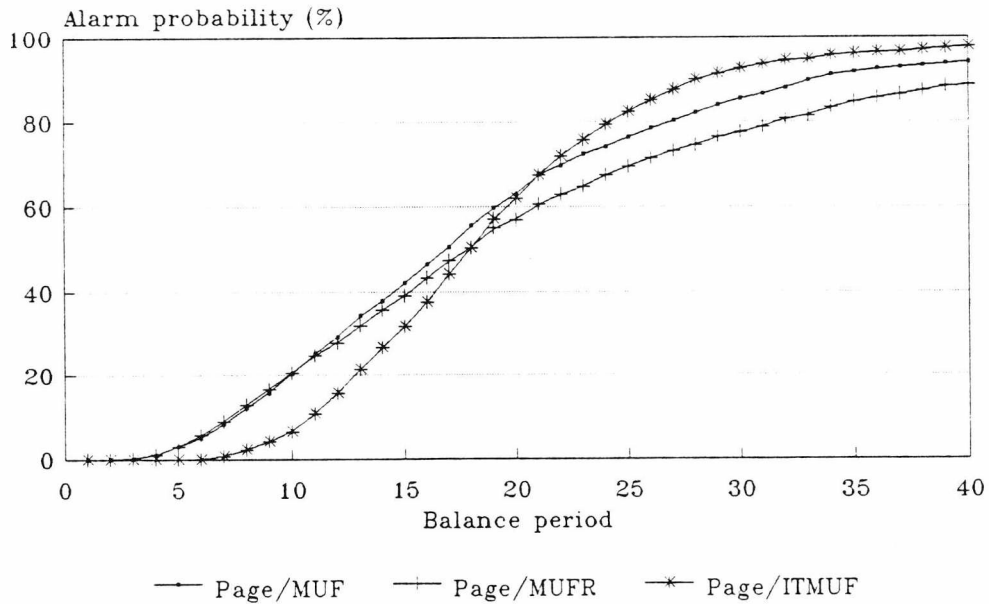


Fig 5.17 Cumulative alarm probs. for protracted loss, new system
Threshold test with MUF, MUFR, ITMUF

Loss scenario

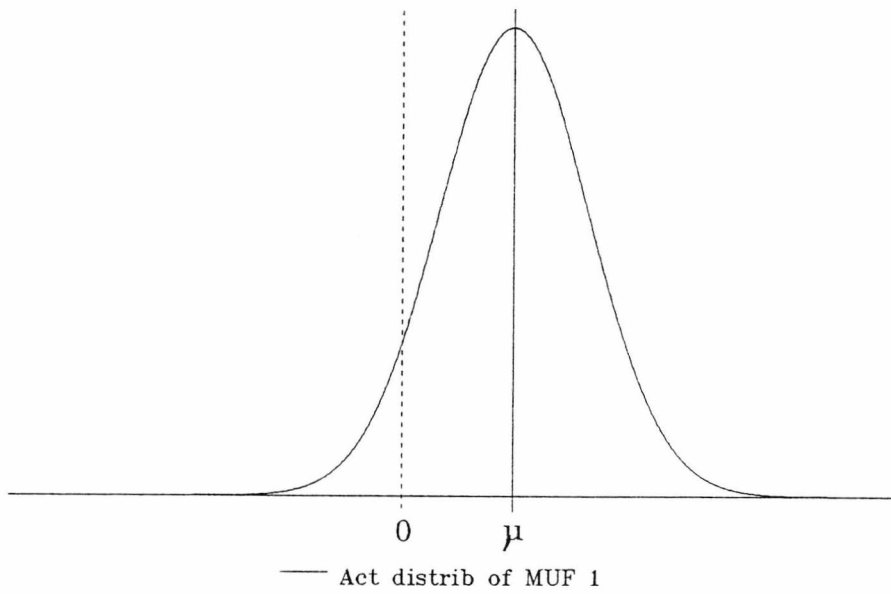


Cumulative alarm probabilities Dissolver estimated from burn-up calculn



**Fig 5.18 Cumulative alarm probs. for protracted loss, new system
Page's Test with MUF, MUFR, ITMUF**

Period 1



Period 2

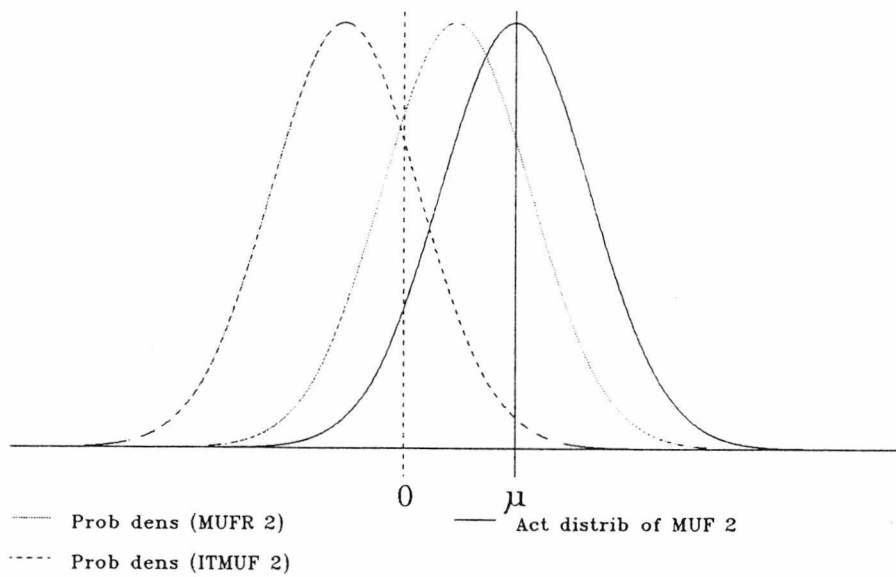
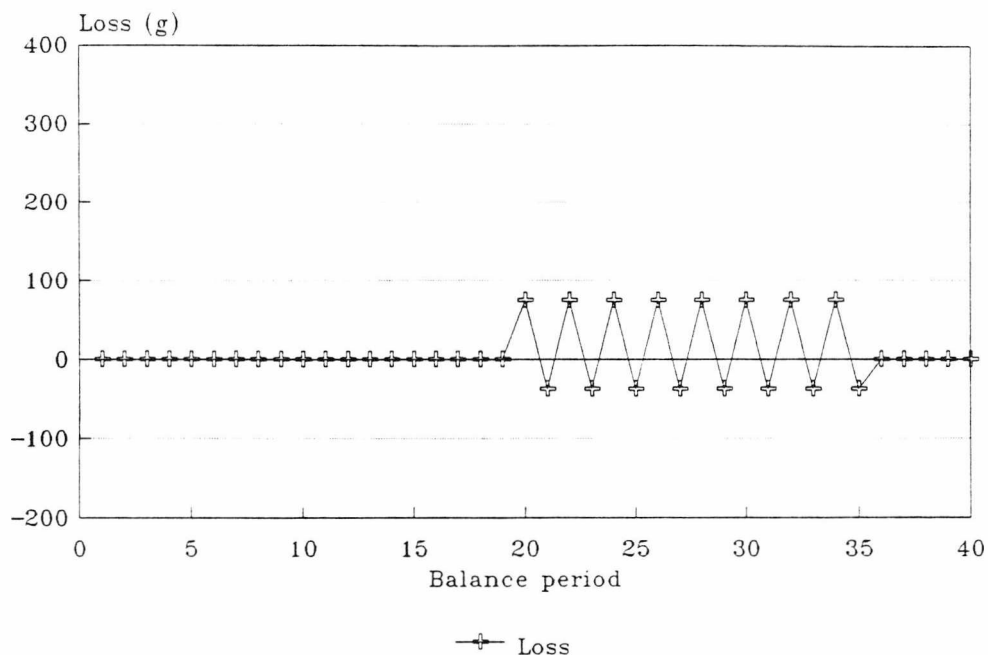


Fig 5.19 Increase in power due to the incorrect assumption of negative correlation

Loss scenario



Cumulative alarm probabilities Dissolver assumed from burn-up calculn

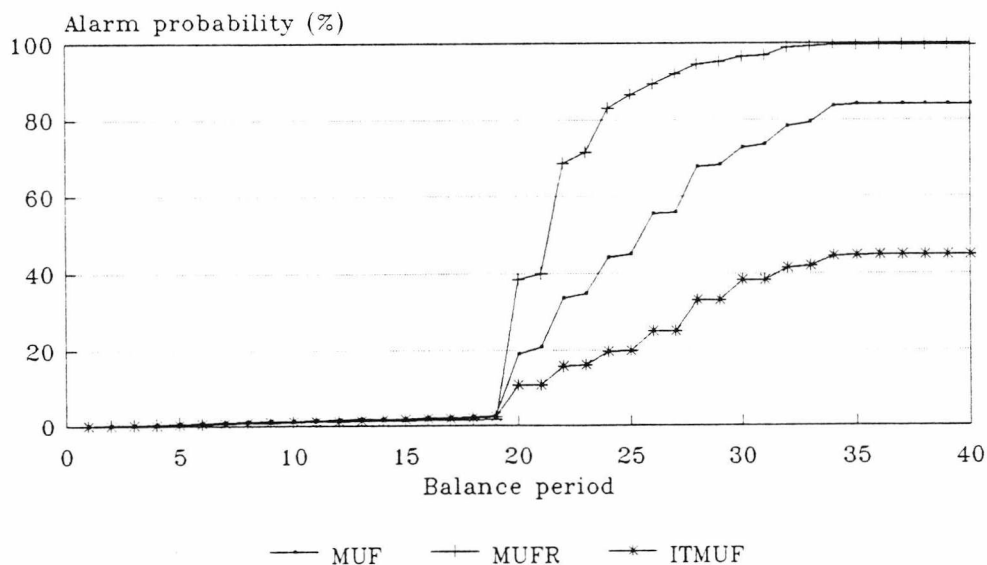
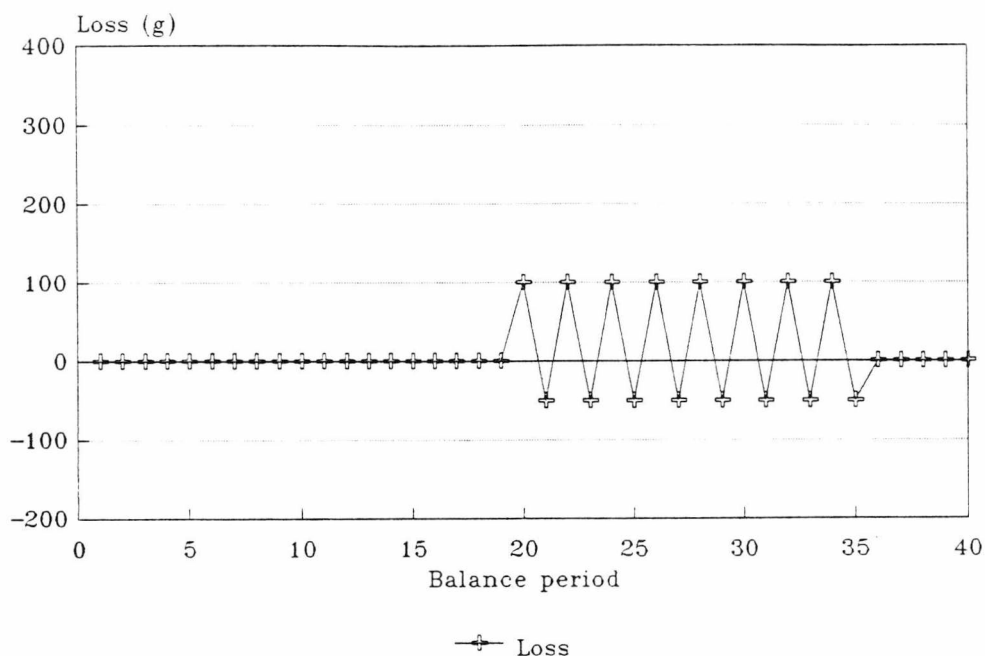


Fig 5.20 Cumulative alarm probabilities for alternate loss with fractional replacement, new system
Threshold test with MUF, MUFR, ITMUF

Loss scenario



Cumulative alarm probabilities Dissolver estimated from burn-up calculn

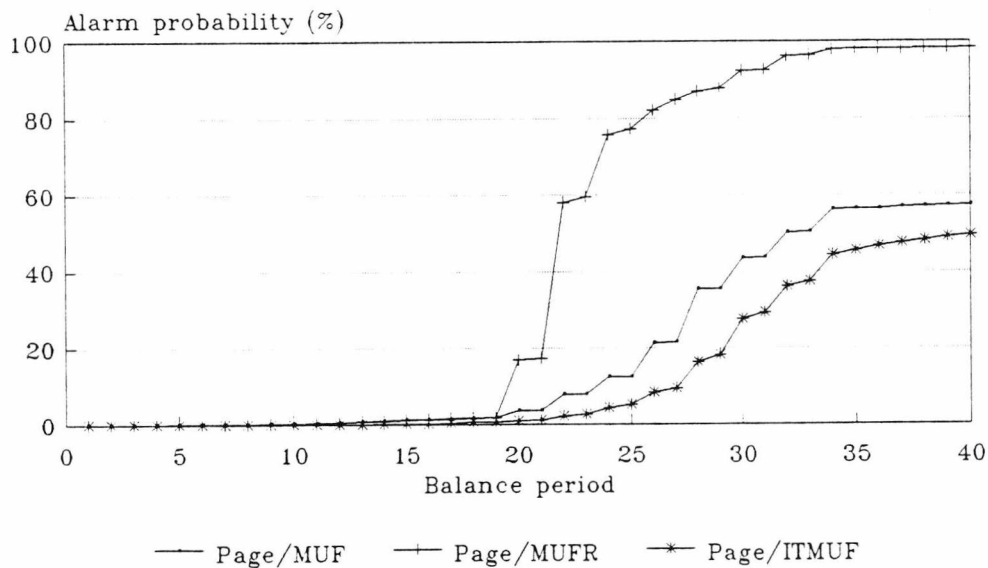


Fig 5.21 Cumulative alarm probabilities for alternate loss with fractional replacement, new system
Page's Test with MUF, MUFR, ITMUF

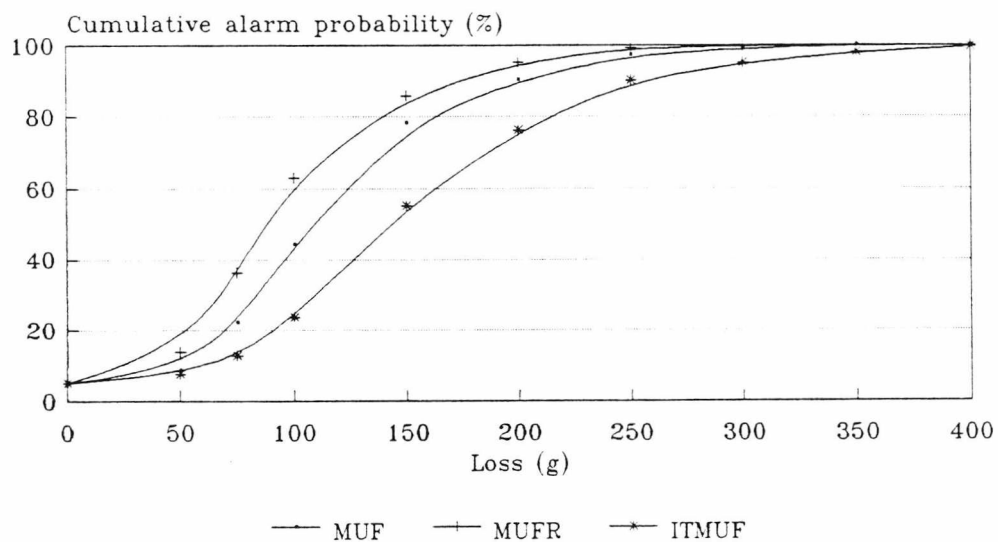


Fig 5.22 Absolute power for abrupt loss on period 30, new system
Threshold test with MUF, MUFR, ITMUF

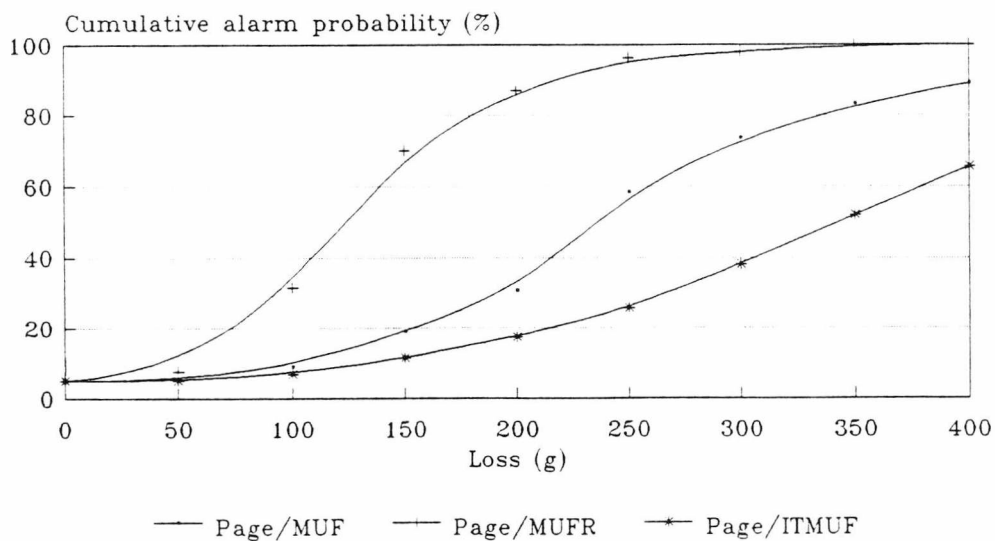


Fig 5.23 Absolute power for abrupt loss on period 30, new system
Page's Test with MUF, MUFR, ITMUF

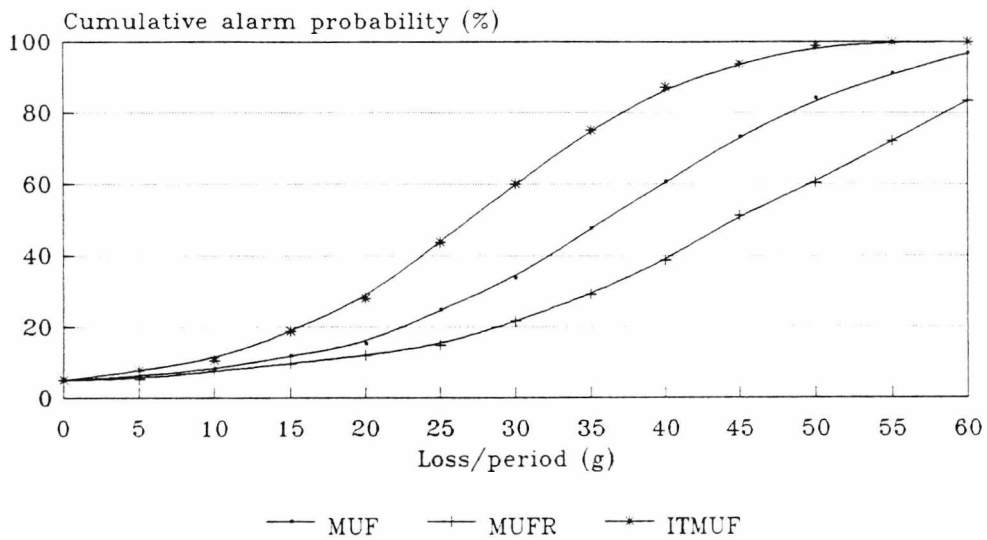


Fig 5.24 Absolute power for protracted loss, new system
Threshold test with MUF, MUFR, ITMUF

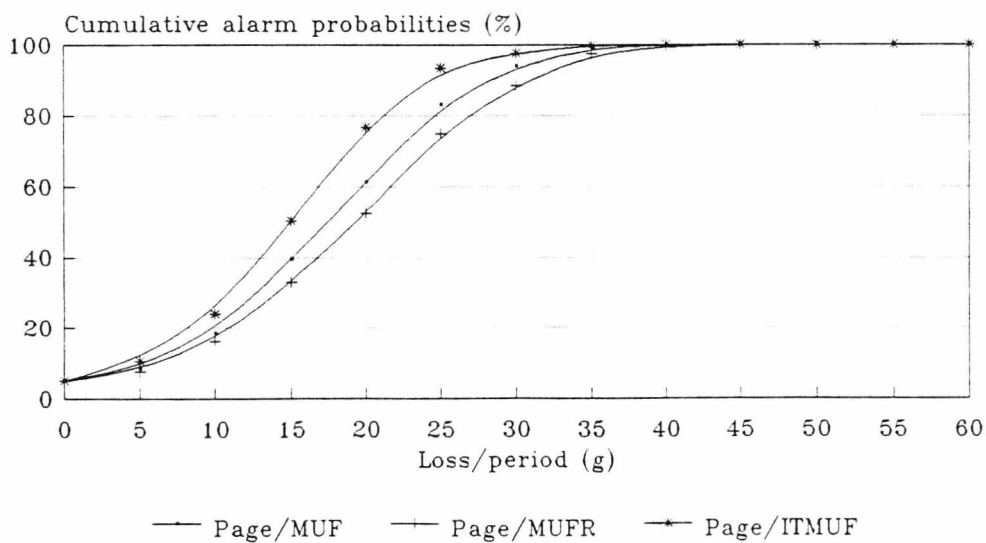


Fig 5.25 Absolute power for protracted loss, new system
Page's Test with MUF, MUFR, ITMUF

5.7 Summary

Accurate plant modelling allows the MUF sequence to be accurately filtered; the knowledge of the uncertainties on the filtered estimates, and the performance of the filtered sequence as the basis for loss detection, are improved. This chapter explains how this is implemented in terms of the MUF covariance matrix, and illustrates the benefits in simulated diversion detection comparisons. The resulting statistic is particularly effective against abrupt loss, and diversion/replacement strategies. It is not an efficient means of identifying small, protracted diversions, however.

This problem will be addressed in the next chapter, where it is demonstrated that the modelling can also be effected in terms of state-estimation techniques. A Kalman Filter is used to solve a set of simultaneous matrix equations describing the system, producing an optimal filtered estimate. This can be configured to produce MUF-residuals, but it offers greater versatility in adapting to the loss scenario.

6. Application of a Kalman Filter to materials accountancy

6.1 Introduction

The Kalman Filter uses recursive state estimation techniques to simultaneously evaluate a set of plant parameters. It uses a progression model of the plant, taking information at period (k) to produce an estimate of the state at (k+1), and a measurement model, describing the plant determinations; each has an associated error covariance matrix. The Filter produces an optimal, linear estimate of the plant parameters by suitable weighting of the prediction and measurements. This approach offers several benefits for materials accountancy; it monitors several variables, aiding anomaly investigation, it adapts to be optimal for a diversion scenario fitting its loss model, and, in general, it requires the storage of less information than the transformation techniques. The Kalman Filter has been described as a means of generating approximate MUF-residuals [32]; it can in fact be configured to produce exact MUF-residuals, which could provide a useful diverse verification of the accountancy software.

6.2 The basic Kalman Filter

A derivation of the Kalman Filter is presented in Appendix VIII. The basic equations of the Filter used in this application are set out below. This assumes that the noise vectors have zero-mean, and there is no covariance between the progression model noise and the measurement noise.

Progression model

The state variables are written as a set of recursive equations, relating the values at (k+1) to those at (k). This relationship is summarized in a progression matrix. Uncertainty in the progression and any input is described by a random noise vector.

$$\underline{x}_{k+1} = A_k \cdot \underline{x}_k + \underline{u}_k + \underline{\omega}_k \quad (6.1)$$

where \underline{x} = State vector, comprising the state variables
A = Progression matrix
 \underline{u} = Input vector
 $\underline{\omega}$ = Zero-mean random noise vector representing uncertainty in A and \underline{u}

Measurement model

The state vector may or may not represent a set of plant measurements. A measurement model is used to express the relationship between the two.

$$\underline{z}_k = H_k \cdot \underline{x}_k + \underline{v}_k \quad (6.2)$$

where \underline{z} = Measurement vector, comprising the relevant plant data
H = Observation matrix, linking the measurements to the state vector
 \underline{v} = Zero-mean random measurement noise vector

It is assumed that the variances and covariances between the elements of the noise vectors $\underline{\omega}$ and \underline{v} are known. The covariance

matrices are termed Q and R respectively:

$$Q_{ij} = \text{Cov}(\omega_i, \omega_j) \quad (6.3)$$

$$R_{ij} = \text{Cov}(v_i, v_j) \quad (6.4)$$

The Kalman Filter first predicts the value of the new state, from the progression model. The measurement model is then used to correct the prediction, according to the relative accuracies, to give the final estimate. The following notation will be used to describe the two stages:

$\tilde{\underline{x}}$ = Predicted state vector, from progression

P = Covariance matrix of predicted state

$\hat{\underline{x}}$ = Estimated state vector, using prediction and measurements

G = Covariance matrix of estimated state

K = Kalman gain, the multiplying factor to optimize the estimate

The Filter is initialized by selecting $\hat{\underline{x}}_0$, an unbiased estimator of \underline{x}_0 , and G_0 , its associated covariance matrix. At each period, the following algorithm is implemented to effect the Kalman Filter:

1. State prediction

$$\tilde{\underline{x}}_{k+1} = A_k \cdot \hat{\underline{x}}_k + u_k \quad (6.5)$$

2. Calculate error covariance matrix for the predicted state

$$P_{k+1} = A_k \cdot G_k \cdot A_k^T + Q_k \quad (6.6)$$

3. Calculate Kalman gain

$$K_{k+1} = P_{k+1} \cdot H_{k+1}^T \cdot [H_{k+1} \cdot P_{k+1} \cdot H_{k+1}^T + R_{k+1}]^{-1} \quad (6.7)$$

4. Correct state prediction to give state estimate

$$\hat{x}_{k+1} = \tilde{x}_{k+1} + K_{k+1} \cdot [z_{k+1} - H_{k+1} \cdot \tilde{x}_{k+1}] \quad (6.8)$$

5. Calculate error covariance matrix for the state estimate

$$G_{k+1} = [I - K_{k+1} \cdot H_{k+1}] \cdot P_{k+1} \quad (6.9)$$

This Filter, similar to those described in references [35,58,59,60] covers the application to materials accountancy detailed below. A more general form is given by Sage & Melsa [61].

6.3 Application of the Kalman Filter to the Fast Reactor Reprocessing Plant

6.3.1 Introduction

The materials accountancy measurement system employed in the head-end of the Fast Reactor Reprocessing Plant poses particular problems in the implementation of a Kalman Filter. The principal inventories, excluding the dissolver in the old accountancy system, are calculated from the value assigned to the source sub-assembly by the fuel burn-up calculations. The Kalman Filter proposed by Pike et al [35], with the inventory estimate as the key element of the state vector, would thus be unsuitable as there is no accurate observation to balance against the

prediction. The MUF is generally accepted as the principal parameter in materials accountancy. It thus makes sense to choose this as the primary variable in the Kalman Filter; indeed, this is the route developed by Shipley [36], and adopted by Sellinschegg [32] and Russell [19].

In the original form, Shipley made allowance for systematic errors in the inventory and transfer estimates. The Filter demands variance and covariance information about the modelled errors; there is currently no information available about the size of systematic errors in determinations at the Dounreay facility. If any were discovered, they would be corrected. It would be possible to include them in the Filter, and assign arbitrarily large values to them. However, this would increase the variance of the filtered estimate.

Systematic discrepancies between the input/inventory and the output will appear in the MUF; it will be demonstrated that, without allowing specifically for transfer biases, they can be detected in the MUF estimate.

A systematic error in an inventory estimate, caused perhaps by miscalibration of an instrument or an unidentified hold-up of material, can only be detected as spikes in the MUF sequence at plant start-up (or when the bias first occurs) and washout. This may well be swamped by the random errors of the balance. The Filter distributes the measured MUF among the possible sources according to their relative variances. As the bias is likely to be small in relation to the inventory standard deviation, it is unlikely that an inventory bias term in the Filter will be able to detect it.

For these reasons, the systematic error terms will not be included in

the Kalman Filter. Should this facility be required, it is a relatively simple task to augment the state vector [62] for their inclusion.

6.3.2 Modelling the 'ideal' plant

The MUF equation (2.1) can be rewritten:

$$\text{MUF}_k = e_k^{\text{inv}} + e_k^{\text{ip}} - e_k^{\text{op}} - e_{k-1}^{\text{inv}} + \text{MUF}_k^{\circ} \quad (6.10)$$

where

- e = error
- ip = input
- op = output
- inv = inventory
- MUF[°] = actual loss of material

MUF is the 'observed' quantity; an estimate of MUF[°] would obviously be desirable for materials accountancy purposes, and this forms the key element of the Kalman Filter state vector. To obtain this estimate, which will be called Kalman-MUF or KALMUF, a progression model of MUF[°] must be pre-supposed, expressing KALMUF_{k+1} in terms of KALMUF_k, with a modelling 'uncertainty' term.

$$\text{KALMUF}_{k+1} = \alpha_k^{\text{KALMUF}} \cdot \text{KALMUF}_k + \omega_k^{\text{KALMUF}} \quad (6.11)$$

Setting $\alpha_k^{\text{KALMUF}} = 0$ implies no relationship between successive losses. In view of the lack of knowledge of MUF[°], this appears to be a sensible model. However, as will be demonstrated later, the use of KALMUF is much more suited to the detection of protracted losses or transfer biases than abrupt losses. The model that will be used is

$$\text{KALMUF}_{k+1} = \text{KALMUF}_k \quad (6.12)$$

setting $\alpha_k^{\text{KALMUF}} = 1$ for all k . ω_k^{KALMUF} is chosen as zero to optimize the model for the constant loss/constant bias scenario; any true loss scenario is obviously unknown, and the flexibility of the model can only be increased at the expense of the variance of KALMUF.

The observation of MUF_k must be expressed in terms of its components at time k . This is effected by introducing a variable $\eta_k = e_{k-1}^{\text{inv}}$.

The state vector is augmented with this term. The basic models for the Filter can now be written [19]:

Progression

$$\begin{pmatrix} \text{KALMUF} \\ \eta \end{pmatrix}_{k+1} = \begin{pmatrix} 1 & 0 \\ 0 & 0 \end{pmatrix} \cdot \begin{pmatrix} \text{KALMUF} \\ \eta \end{pmatrix}_k + \begin{pmatrix} 0 \\ e_k^{\text{inv}} \end{pmatrix} \quad (6.13)$$

Observation

$$\text{MUF}_k = (1 \quad 1) \cdot \begin{pmatrix} \text{KALMUF} \\ \eta \end{pmatrix}_k + e_k^{\text{ip}} - e_k^{\text{op}} - e_k^{\text{inv}} \quad (6.14)$$

where η_{k+1} = inventory error on period k
 e = error contribution

6.3.3 Augmentation of the state vector to describe plant conditions

The equations above fully describe a system in which all inputs, outputs and inventories are determined independently on each balance period -

the 'ideal plant'. However, in the plant under consideration many of the inventories are linked to inputs, and one of the outputs is correlated with old inventories. To model these correlations, the state vector must be augmented to include recursive equations expressing the correlated variables. As the contents of the uncropped pins and batches in baskets (and the dissolver for the new accountancy system) are taken from the source sub-assembly, correlation exists between elements of the same sub-assembly, but not between inventories sourced from different sub-assemblies. The models must thus divide these according to their parentage; this version allows for components from a total of five sub-assemblies within the balance area. It was thought that this would cover all usual plant operation; the Filter would need to be reconfigured if this parameter was exceeded.

It is assumed that all sub-assemblies entering the dismemberment cave will be processed sequentially; any pins left over from the last sub-assembly will form part of the first batch with pins from the new sub-assembly.

The correlations are accommodated in the progression model by expressing the error terms recursively. Firstly, e_k^{inv} will now be included in the state vector. To achieve this, it must first be expressed in terms of its components:

$$e_k^{inv} = e_k^{p\&b\&d} + e_k^{dissh} + e_k^{HAT} + e_k^{wst} \quad (6.15)$$

where p&b&d = pins, batches and dissolver
dissh = dissolver heel
HAT = hold-all-tank
wst = waste in crates

Each term on the right hand side, apart from the error in the dissolver heel estimate (and the dissolver itself for the old accountancy system) may contain correlation with the previous balance period: the hold-all-tank is only reassessed if there is an overflow of liquor into it, and waste is only assayed on the balance period in which it is created. As it is quite simple to include uncorrelated terms in the state vector - the progression multiplier is just zero - the inventory terms will all be included.

The uncropped pins, batches in baskets, and dissolver for the new accountancy system, may contain components of more than one sub-assembly. These must thus be sub-divided further, as the errors are traceable to the source sub-assembly.

$$e_k^{p\&b\&d} = e_{1k}^{p\&b\&d} + e_{2k}^{p\&b\&d} + e_{3k}^{p\&b\&d} + e_{4k}^{p\&b\&d} + e_{5k}^{p\&b\&d} \quad (6.16)$$

where the numerical subscript '1' refers to the error due to the 'newest' sub-assembly component in the inventory. This allows for parts of five sub-assemblies in uncropped pins, batches in baskets (there may be several batches awaiting dissolution), and the dissolver (this holds only one batch).

Two other terms should be included in the state vector; firstly, waste is not reassessed when it is exported, leading to a correlation with the waste inventory on the previous balance period. Thus, an output waste term is required. Secondly, the inclusion of the sub-assembly input error will avoid problems due to correlation between the progression noise vector and the measurement noise vector.

The state vector thus becomes

(KALMUF)

η
 $e_1^{p\&b\&d}$
 $e_2^{p\&b\&d}$
 $e_3^{p\&b\&d}$
 $e_4^{p\&b\&d}$
 $e_5^{p\&b\&d}$
 e_{dissh}
 e_{HAT}
 e_{wst}
 e_{opwst}
 e_{ip}

6.3.4 Calculation of the progression matrix and progression noise vector

The progression matrix for the above state vector will contain 12x12 elements. The models for the first two terms are described in the above section; these will have no additional noise terms.

In calculating the progressions for the pins & batches and dissolver error terms, it should be noted that the subscript numbers increase with the increasing 'age' of the sub-assembly to which they refer. If there is no input on a balance period, there is a direct correspondance between subscript numbers on the progression:

$$e_{1_{k+1}}^{p\&b\&d} = \alpha_x \cdot e_{1_k}^{p\&b\&d} \quad (6.17)$$

$$e_{2_{k+1}}^{p\&b\&d} = \alpha_y \cdot e_{2_k}^{p\&b\&d} \quad (6.18)$$

$$e_{3_{k+1}}^{p\&b\&d} = \alpha_z \cdot e_{3_k}^{p\&b\&d} \quad (6.19)$$

etc.

The α terms are calculated by dividing the mass from the relevant sub-assembly present at (k+1) by the mass present at (k). Their values are all $0 \leq \alpha \leq 1$.

On a balance period in which a sub-assembly arrives as input, $e_{1_{k+1}}^{p\&b\&d}$ refers to the new input sub-assembly: there is no previous knowledge to establish its numerical value, so the Filter will make an estimate from the variance.

$$e_{1_{k+1}}^{p\&b\&d} = \beta^{p\&b\&d} \cdot \omega_{k+1}^{ip} \quad (6.20)$$

where β is the fraction of the input sub-assembly in the uncropped pins, batches in baskets and dissolver at the end of the balance period, and ω_{k+1}^{IP} is the unknown 'random' error of the input sub-assembly estimate, defined by:

$$E[\omega^{ip}] = 0 \quad E[\omega^{ip} \cdot \omega^{ip}] = \sigma^2[ip] \quad (6.21)$$

where $E[x]$ is the expected value of x

The remaining pins, batches and dissolver error terms are shifted in their correspondance with the previous balance period:

$$e_{2k+1}^{p\&b\&d} = \alpha_y \cdot e_{1k}^{p\&b\&d} \quad (6.22)$$

$$e_{3k+1}^{p\&b\&d} = \alpha_z \cdot e_{2k}^{p\&b\&d} \quad (6.23)$$

If, in this instance, a sub-assembly was also brought into the caves on the previous balance period, the state vector will contain two references to a single sub-assembly. There is thus an alternative valid recursion equation for $e_{2k+1}^{p\&b\&d}$:

$$e_{2k+1}^{p\&b\&d} = \alpha_x \cdot e_k^{ip} \quad (6.24)$$

Equation 6.22 is simpler to implement, and so is used in this application of the Filter.

The hold-all tank is reassessed when its level changes. The determination error can be expressed

$$e_{k+1}^{HAT} = \alpha^{HAT} \cdot e_k^{HAT} + \omega_{k+1}^{HAT} \quad (6.25)$$

where $\alpha^{HAT}=1$, $\omega^{HAT}=0$ if there is no level change, (6.26)

and $\alpha^{HAT}=0$, $E[\omega^{HAT}] = 0$, $E[\omega^{HAT} \cdot \omega^{HAT}] = \sigma^2(HAT)$ (6.27)

if the contents are remeasured.

The waste error term can be described by

$$e_{k+1}^{wst} = \alpha^{wst} \cdot e_k^{wst} + \omega_{k+1}^{wst} \quad (6.28)$$

where α^{wst} is the fraction of waste carried over from the previous

balance period inventory, and ω^{wst} is defined by

$$E[\omega^{wst}] = 0, \quad E[\omega^{wst} \cdot \omega^{wst}] = \sigma^2(wst) \quad (6.29)$$

Similarly, the output waste error term is written

$$e_{k+1}^{opwst} = \alpha^{opwst} \cdot e_k^{wst} + \beta^{opwst} \cdot \omega_{k+1}^{wst} \quad (6.30)$$

where α^{opwst} and β^{opwst} are the fractions of the waste from the previous balance period and the current balance period respectively leaving as output.

The input error and the dissolver heel error terms are uncorrelated variables, and do not give rise to a progression; their errors are expressed in the random noise vector.

$$e_{k+1}^{ip} = \omega_{k+1}^{ip} \quad (6.31)$$

$$e_{k+1}^{dissh} = \omega_{k+1}^{dissh} \quad (6.32)$$

$$\text{where } E[\omega^{ip}] = 0 \quad E[\omega^{ip} \cdot \omega^{ip}] = \sigma^2(ip) \quad (6.33)$$

$$E[\omega^{dissh}] = 0 \quad E[\omega^{dissh} \cdot \omega^{dissh}] = \sigma^2(dissh) \quad (6.34)$$

6.3.5 Kalman Filter equations

The Filter models for the new accountancy system are thus:

Progression model

$$\begin{pmatrix} \text{KALMUF} \\ \eta \\ e_1^{p\&b\&d} \\ e_2^{p\&b\&d} \\ e_3^{p\&b\&d} \\ e_4^{p\&b\&d} \\ e_5^{p\&b\&d} \\ e_{\text{dissh}} \\ e_{\text{HAT}} \\ e_{\text{wst}} \\ e_{\text{opwst}} \\ e_{\text{ip}} \end{pmatrix}_{k+1} = \begin{pmatrix} 1 & 0 & 0 & 0 & 0 & 0 & 0 & 0 & 0 & 0 & 0 & 0 \\ 0 & 0 & 1 & 1 & 1 & 1 & 1 & 1 & 1 & 1 & 0 & 0 \\ 0 & 0 & \alpha_{33} & 0 & 0 & 0 & 0 & 0 & 0 & 0 & 0 & 0 \\ 0 & 0 & \alpha_{43} & \alpha_{44} & 0 & 0 & 0 & 0 & 0 & 0 & 0 & 0 \\ 0 & 0 & 0 & \alpha_{54} & \alpha_{55} & 0 & 0 & 0 & 0 & 0 & 0 & 0 \\ 0 & 0 & 0 & 0 & \alpha_{65} & \alpha_{66} & 0 & 0 & 0 & 0 & 0 & 0 \\ 0 & 0 & 0 & 0 & 0 & \alpha_{76} & \alpha_{77} & 0 & 0 & 0 & 0 & 0 \\ 0 & 0 & 0 & 0 & 0 & 0 & 0 & 0 & 0 & 0 & 0 & 0 \\ 0 & 0 & 0 & 0 & 0 & 0 & 0 & 0 & \alpha_{99} & 0 & 0 & 0 \\ 0 & 0 & 0 & 0 & 0 & 0 & 0 & 0 & 0 & \alpha_{AA} & 0 & 0 \\ 0 & 0 & 0 & 0 & 0 & 0 & 0 & 0 & 0 & \alpha_{AB} & 0 & 0 \\ 0 & 0 & 0 & 0 & 0 & 0 & 0 & 0 & 0 & 0 & 0 & 0 \end{pmatrix} \begin{pmatrix} \text{KALMUF} \\ \eta \\ e_1^{p\&b\&d} \\ e_2^{p\&b\&d} \\ e_3^{p\&b\&d} \\ e_4^{p\&b\&d} \\ e_5^{p\&b\&d} \\ e_{\text{dissh}} \\ e_{\text{HAT}} \\ e_{\text{wst}} \\ e_{\text{opwst}} \\ e_{\text{ip}} \end{pmatrix}_k$$

$$+ \begin{pmatrix} 0 \\ 0 \\ \beta^{p\&b\&d} \cdot \omega_{k+1}^{ip} \\ 0 \\ 0 \\ 0 \\ 0 \\ \omega_{k+1}^{\text{dissh}} \\ \omega_{k+1}^{\text{HAT}} \\ \omega_{k+1}^{\text{wst}} \\ \omega_{k+1}^{\text{wst}} \\ \beta^{\text{opwst}} \cdot \omega_{k+1}^{\text{wst}} \\ \omega_{k+1}^{\text{ip}} \end{pmatrix}$$

(6.35)

Measurement model

$$MUF_{k+1} = (1 \quad 1 \quad -1 \quad 1) \cdot \begin{pmatrix} KALMUF \\ \eta \\ e_{p\&b\&d}^1 \\ e_{p\&b\&d}^2 \\ e_{p\&b\&d}^3 \\ e_{p\&b\&d}^4 \\ e_{p\&b\&d}^5 \\ e_{dissh} \\ e_{HAT} \\ e_{wst} \\ e_{opwst} \\ e_{ip} \end{pmatrix}_k - e_k^{op} \quad (6.36)$$

where superscripts p&b&d refers to uncropped pins, batches in baskets, and the dissolver

dissh	the dissolver heel
HAT	the hold-all tank
wst	waste in crates
opwst	output waste

and numerical subscripts relate to the source sub-assembly, '1' referring to components of the newest sub-assembly

If there is no input,

$$\alpha_{43}, \alpha_{54}, \alpha_{65}, \alpha_{76} = 0$$

$$0 \leq \alpha_{33}, \alpha_{44}, \alpha_{55}, \alpha_{66}, \alpha_{77} \leq 1$$

If there is an input,

$$\alpha_{33}, \alpha_{44}, \alpha_{55}, \alpha_{66}, \alpha_{77} = 0$$

$$0 \leq \alpha_{43}, \alpha_{54}, \alpha_{65}, \alpha_{76} \leq 1$$

It should be noted that the Kalman Filter can only produce estimates of the errors where these errors contribute to the observation of

MUF. Thus if a sub-assembly arrives as input, and its content remains in its entirety in the dismemberment caves as uncropped pins and batches in baskets awaiting dissolution, its positive error contribution to the MUF as an input is exactly cancelled by its negative contribution as an inventory. The Filter will thus estimate e^{ip} as zero.

The final Filter equations for the old accountancy system are:

Progression model

$$\begin{pmatrix} \text{KALMUF} \\ \eta \\ e_1^{p\&b\&d} \\ e_2^{p\&b\&d} \\ e_3^{p\&b\&d} \\ e_4^{p\&b\&d} \\ e_{diss} \\ e_{dissh} \\ e_{HAT} \\ e_{wst} \\ e_{opwst} \\ e^{ip} \end{pmatrix}_{k+1} = \begin{pmatrix} 1 & 0 & 0 & 0 & 0 & 0 & 0 & 0 & 0 & 0 & 0 & 0 \\ 0 & 0 & 1 & 1 & 1 & 1 & 1 & 1 & 1 & 1 & 0 & 0 \\ 0 & 0 & \alpha_{33} & 0 & 0 & 0 & 0 & 0 & 0 & 0 & 0 & 0 \\ 0 & 0 & \alpha_{43} & \alpha_{44} & 0 & 0 & 0 & 0 & 0 & 0 & 0 & 0 \\ 0 & 0 & 0 & \alpha_{54} & \alpha_{55} & 0 & 0 & 0 & 0 & 0 & 0 & 0 \\ 0 & 0 & 0 & 0 & \alpha_{65} & \alpha_{66} & 0 & 0 & 0 & 0 & 0 & 0 \\ 0 & 0 & 0 & 0 & 0 & 0 & 0 & 0 & 0 & 0 & 0 & 0 \\ 0 & 0 & 0 & 0 & 0 & 0 & 0 & 0 & \alpha_{99} & 0 & 0 & 0 \\ 0 & 0 & 0 & 0 & 0 & 0 & 0 & 0 & 0 & \alpha_{AA} & 0 & 0 \\ 0 & 0 & 0 & 0 & 0 & 0 & 0 & 0 & 0 & 0 & \alpha_{AB} & 0 \\ 0 & 0 & 0 & 0 & 0 & 0 & 0 & 0 & 0 & 0 & 0 & 0 \end{pmatrix} \cdot \begin{pmatrix} \text{KALMUF} \\ \eta \\ e_1^{p\&b\&d} \\ e_2^{p\&b\&d} \\ e_3^{p\&b\&d} \\ e_4^{p\&b\&d} \\ e_{diss} \\ e_{dissh} \\ e_{HAT} \\ e_{wst} \\ e_{opwst} \\ e^{ip} \end{pmatrix}_k$$

$$\begin{pmatrix} 0 \\ 0 \\ \beta^{p\&b\&d} \cdot \omega_{k+1}^{ip} \\ 0 \\ 0 \\ 0 \\ \omega_{k+1}^{diss} \\ \omega_{k+1}^{dissh} \\ \omega_{k+1}^{HAT} \\ \omega_{k+1}^{wst} \\ \beta^{opwst} \cdot \omega_{k+1}^{wst} \\ \omega_{k+1}^{ip} \end{pmatrix}$$

(6.37)

Measurement model

$$MUF_{k+1} = (1 \quad 1 \quad -1 \quad 1) \cdot \begin{pmatrix} KALMUF \\ \eta \\ e_{1 \text{ p&b&d}} \\ e_{2 \text{ p&b&d}} \\ e_{3 \text{ p&b&d}} \\ e_{4 \text{ p&b&d}} \\ e_{\text{diss}} \\ e_{\text{dissh}} \\ e_{\text{HAT}} \\ e_{\text{wst}} \\ e_{\text{opwst}} \\ e_{\text{ip}} \end{pmatrix}_k - e_k^{\text{op}} \quad (6.38)$$

6.4 Performance of the Kalman Filter

In addition to the KALMUF term in the state vector, a 'residual', defined as the difference between the expected MUF and the observed MUF, can also be calculated. In the terminology used in section 6.2, this is written

$$\underline{y}_k = \underline{z}_k - H_k \cdot \tilde{x}_k \quad (6.39)$$

where \underline{y}_k is the residual vector. In this case, it has a single dimension, and will be called the Kalman-residual, or KALR. If the Filter is informed that there is no material diversion (KALMUF eliminated, or initialized as zero with zero variance), the KALR sequence will be identical to the MUF-residuals sequence; this is a useful check on the accuracy of the Kalman Filter model and the calculation of the MUF covariance matrix.

Enabling the loss model in the Filter introduces another variable with

an associated error, thus increasing the variance of KALR. This may slightly reduce the power to detect an abrupt loss. Against this, the use of the KALMUF term gives an estimate of the mean, constant loss; it is a very sensitive indicator of instrument bias, or the protracted siphoning-off of small quantities of material. Theoretically, as nothing is known about KALMUF(0), it should be initialized with an infinite variance, and the Filter allowed to track down on the actual uncertainty. However, this makes the variance of the early KALR values too high to be of use in loss detection. In practice, it was found that initializing the variance of KALMUF at 40 gave sufficient sensitivity to detect small, protracted anomalies, without unduly impairing the power of KALR to identify a larger diversion.

Against a variety of simulated loss scenarios, the KALR statistic displays a very similar behaviour to MUF_R. Both are effective against abrupt and loss-with-replacement strategies, but insensitive to very small, protracted diversion. A useful advantage of the Kalman Filter approach is its adaptation to errors described in its system model; in this example, KALR shows a small but consistent superiority in detecting abrupt losses against a small negative systematic error in the transfer estimates.

The KALMUF term is blind to abrupt losses, but, as described above, very sensitive to small, protracted discrepancies. Its response has a very large time-constant - as a guide, it will take at a minimum of about 10 balance periods to show any convergence on the anomaly. This does mean that it is fairly effective against loss-on-alternate-periods, despite the fact that this scenario is not within its model.

As protracted anomalies are handled by the KALMUF term, the KALR term is less sensitive than MUF_R to background systematic errors. This aids

investigation, as the discrepancy will probably be indicated in the KALMUF statistic rather than as an unidentified alarm in KALR.

6.5 Results

The two statistics generated from the Kalman Filter, the residual KALR and the mean loss estimator KALMUF, are compared with MUF, MUFR, and CUMUF, in the threshold test and, where appropriate, Page's Test.

As described above, the Kalman-residuals sequence KALR is very similar to the MUF-residuals (MUFR) calculated from the MUF covariance matrix. Its performance is in general also very similar - in can be seen, in figure 6.1, that in detecting a 1200g abrupt loss under the old accountancy system, the two detection plots are virtually identical. Even at this late stage of the campaign, when the CUMUF variance is quite high, CUMUF detects a loss of this magnitude with 95% probability, compared to 99% for KALR/MUFR. The slow reponse of KALMUF is shown quite clearly here, the detection rate reaching 90% six balance periods after the event, and with an overall power of 98% nine periods after. The constant loss model assumed the Kalman Filter is triggered by the large, abrupt diversion; it then assumes this loss is continuing, causing later alarms. The overall power of KALMUF is thus comparable with MUFR and KALR in this scenario.

The Page's Test results shown in figure 6.2 again illustrate the closeness between KALR and MUFR. The KALMUF response is extremely slow; the KALMUF model is of constant loss, so the sequence contains a very high positive correlation between successive elements, like CUMUF values towards the end of a campaign. Like CUMUF, it is thus not a suitable statistic to use in Page's Test, as to achieve a low false alarm rate

the thresholds must be set very high.

The real benefits of the KALMUF sequence are demonstrated by its performance against a constant loss. Figure 6.3 shows the detection probability/time curve for the statistics against a constant 30g/period diversion or systematic error in the threshold test. The KALMUF sequence is slow to repond again, but offers the greatest chance of detection after 18 balance periods. Applied to Page's Test, KALMUF has slightly more overall power than Page/MUFR (figure 6.4), but is actually more effective in the threshold test.

Against a strategy of alternate diversion/fractional replacement, KALMUF performs well in the threshold test (figure 6.5), but is bettered in absolute power by Page/MUFR and Page/KALR (figure 6.6).

The absolute power curves are shown in figures 6.7 - 6.10. The best performance against the abrupt loss is given by Page/KALR, and against the protracted loss by KALMUF.

Turning to the new accountancy system, KALR again performs in a very similar fashion to MUFR. The detectable levels of abrupt losses, and losses with fractional replacement are much lower under this regime, and KALMUF performs poorly against small losses over short periods. However, the use of KALMUF with the threshold test still offers the greatest power against a protracted diversion, figure 6.11 showing the performance against a constant loss of 25g/period. Again, the response is slow; up to period 22, CUMUF has a higher power. The use of Page's Test, illustrated in figure 6.12, yields no improvement; the anomalous benefit of ITMUF in this accountancy system against protracted losses is thus nullified.

The absolute power curves for the new accountancy system are shown in figures 6.13 - 6.16. It can be seen that MUFR or KALR, used with the threshold test, offer the highest probability of detecting an abrupt diversion, while again KALMUF is the most effective against the constant loss.

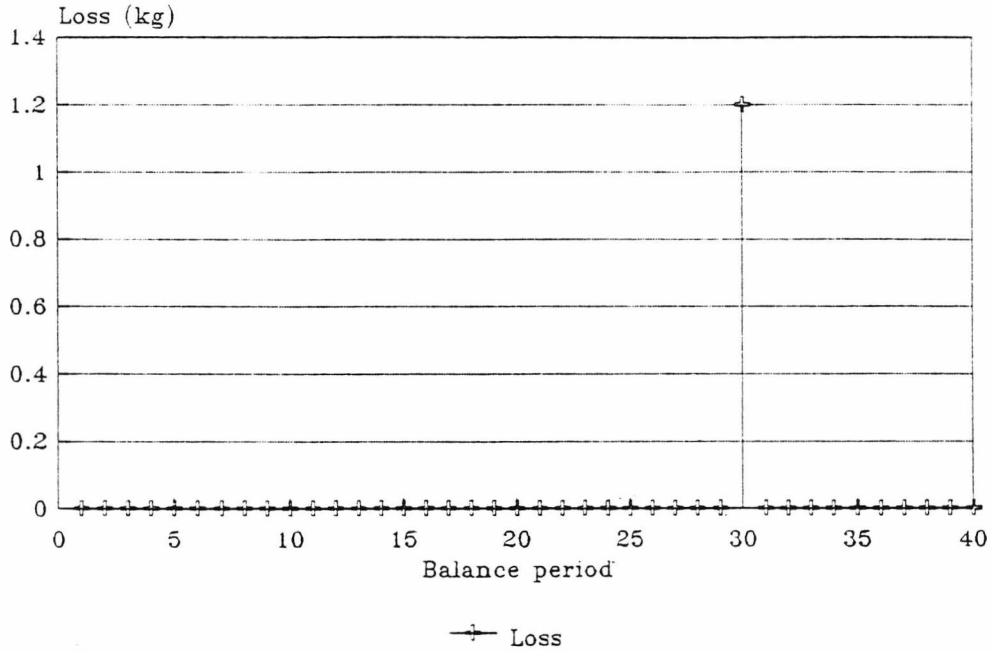
6.6 The use of a 'Twin test'

It can be seen in the absolute power against protracted loss curves for both the old (figures 6.9, 6.10) and new (figures 6.14, 6.15) that KALR is unresponsive to this scenario; this is due to the 'absorption' of the constant anomaly by the KALMUF term. This may be turned to a slight advantage where a prompt theft of material occurs against a background of negative instrument error - deliberate miscalibration being a possible strategy open to a potential diverter.

The Kalman Filter thus tends to segregate the background trend from any instantaneous anomaly. This suggests that the two statistics derived from the Kalman Filter form a complementary pair, and should be used in a twin test.

This also aids the implementation of Page's Test, as the parameters can be selected to operate over different ranges. Data from the new accountancy system is particularly sensitive to the choice of the H-K pair - the variation of power with K is illustrated for an abrupt and protracted loss in figures 6.17 and 6.18 respectively. KALMUF still provides the greatest sensitivity in a protracted loss scenario for both accountancy systems, but the use of Page's Test with $K=2$ enhances the performance of MUFR and KALR in the new system; they are now comparable with their threshold test equivalents.

Loss scenario



Cumulative alarm probabilities Independent dissolver estimate

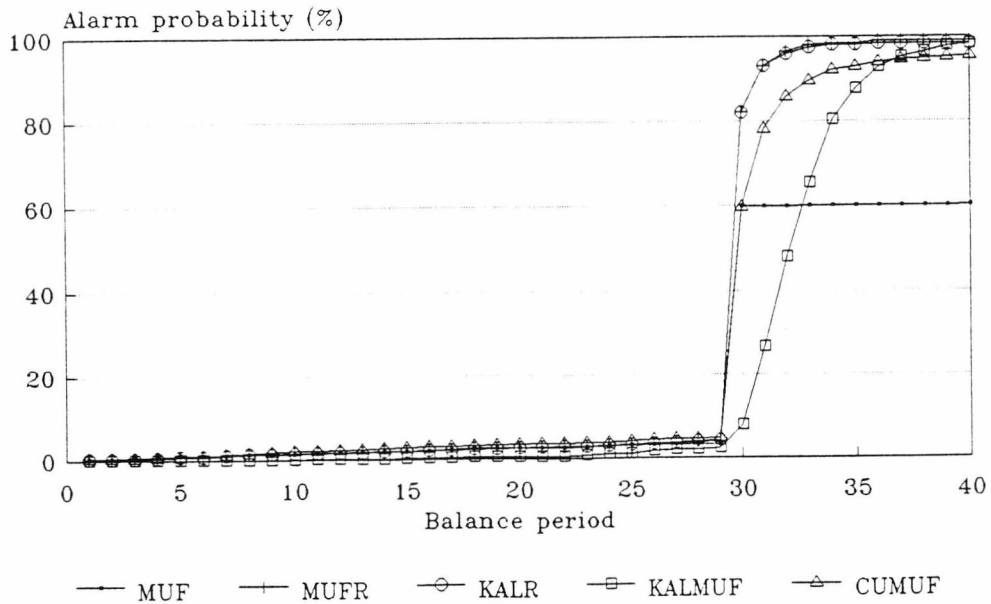
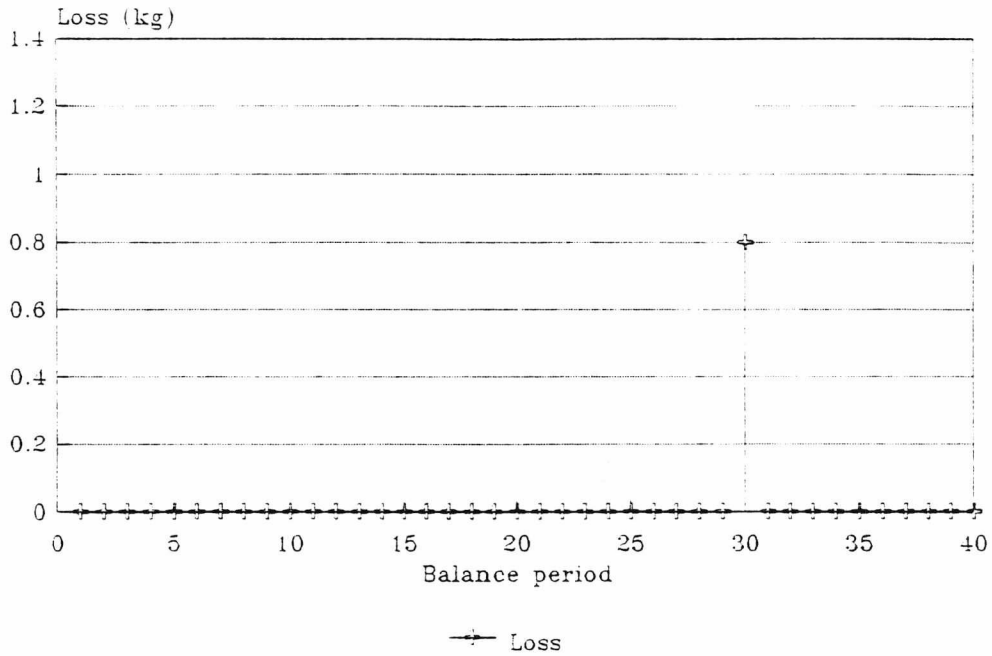


Fig 6.1 Cumulative alarm probabilities for abrupt loss, old system
Threshold test with MUF, MUFR, KALR, KALMUF, CUMUF

Loss scenario



Cumulative alarm probabilities Independent dissolver estimate

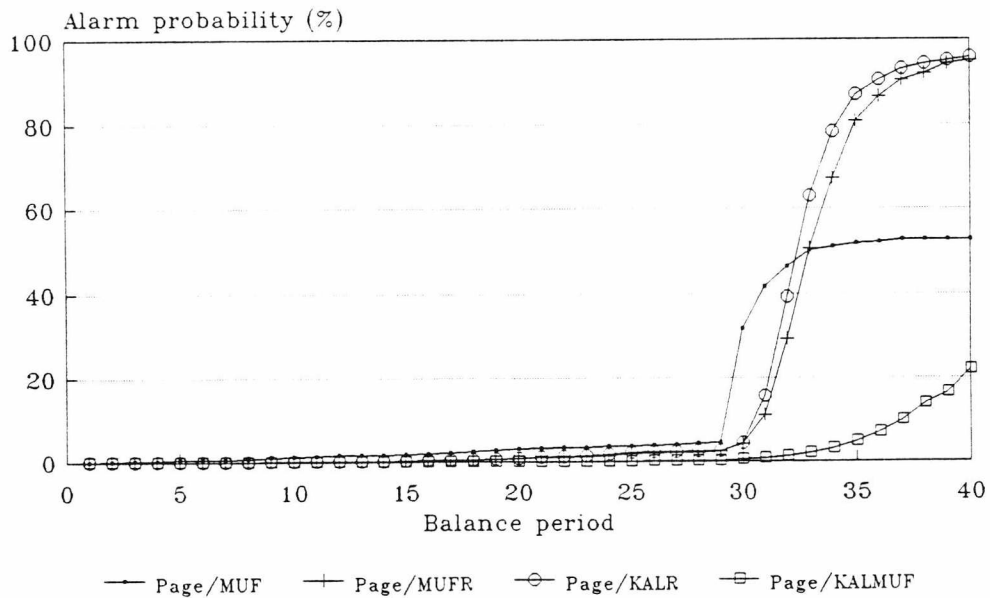
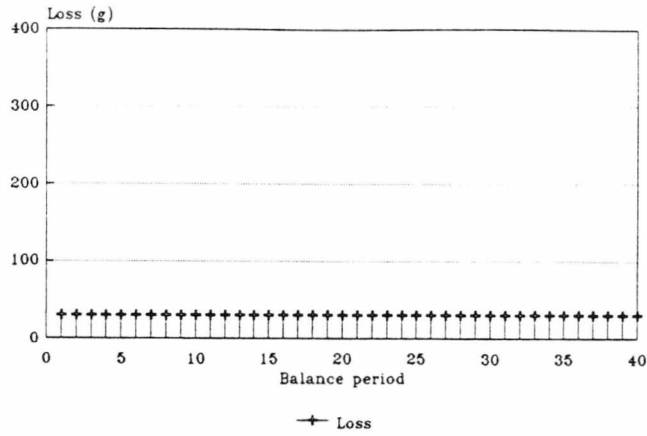


Fig 6.2 Cumulative alarm probabilities for abrupt loss, old system
Page's Test with MUF, MUFR, KALR, KALMUF

Loss scenario



Cumulative alarm probabilities
Independent dissolver estimate

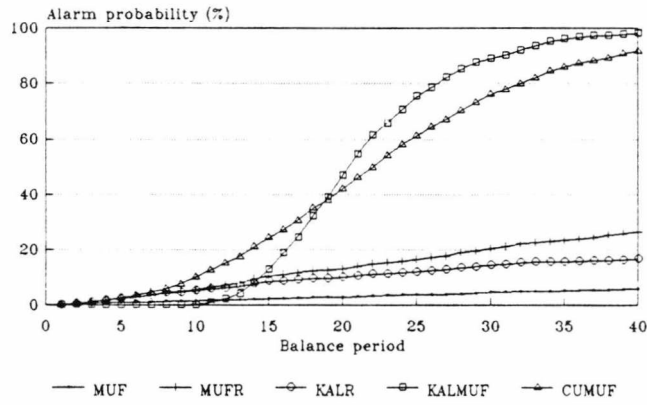


Fig 6.3 Cumulative alarm probs. for protracted loss, old system
Threshold test with MUF, MUFR, KALR, KALMUF, CUMUF

Cumulative alarm probabilities
Independent dissolver estimate

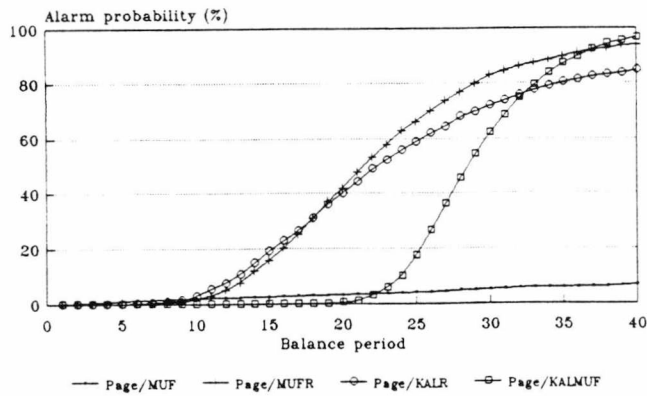
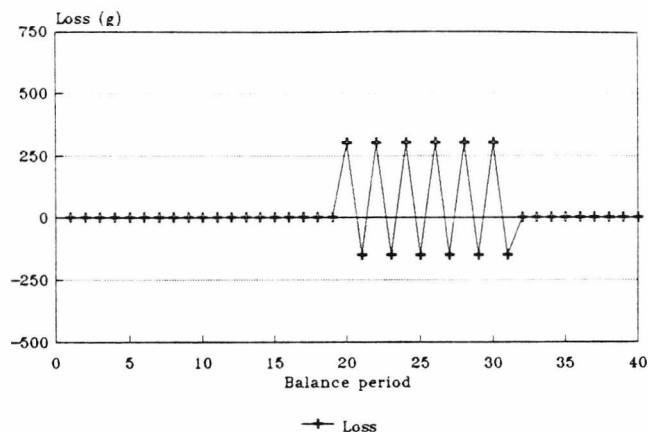


Fig 6.4 Cumulative alarm probs. for protracted loss, old system
Page's Test with MUF, MUFR, KALR, KALMUF

Loss scenario



Cumulative alarm probabilities
Independent dissolver estimate

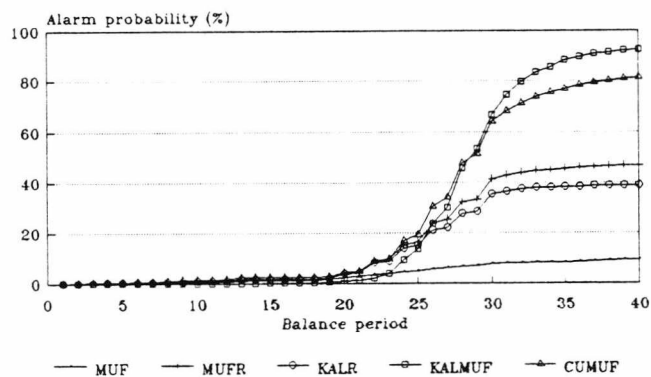


Fig 6.5 Cumulative alarm probabilities for alternate loss with fractional replacement, old system

Threshold test with MUF, MUFR, KALR, KALMUF, CUMUF

Cumulative alarm probabilities
Independent dissolver estimate

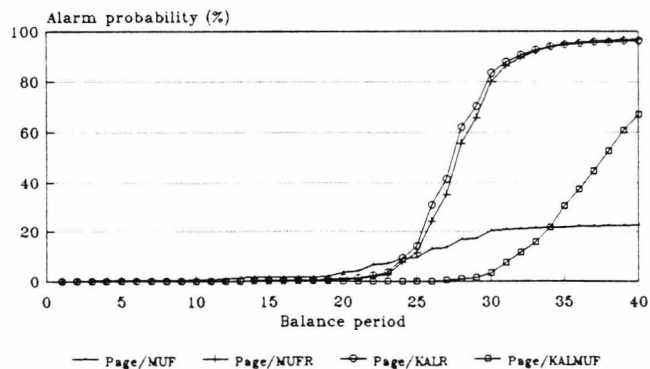


Fig 6.6 Cumulative alarm probabilities for alternate loss with fractional replacement, old system

Page's Test with MUF, MUFR, KALR, KALMUF

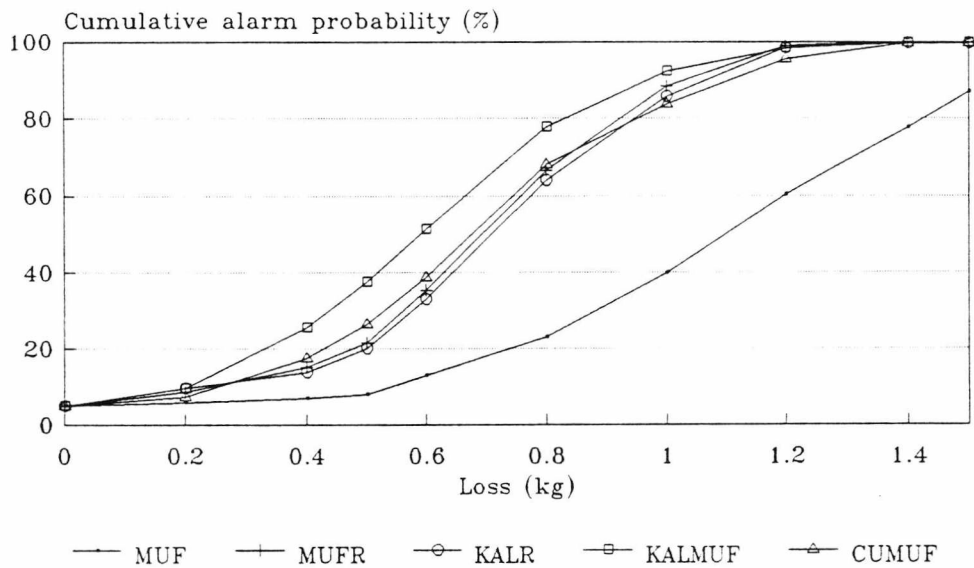


Fig 6.7 Absolute power for abrupt loss on period 30, old system
Threshold test with MUF, MUFR, KALR, KALMUF, CUMUF

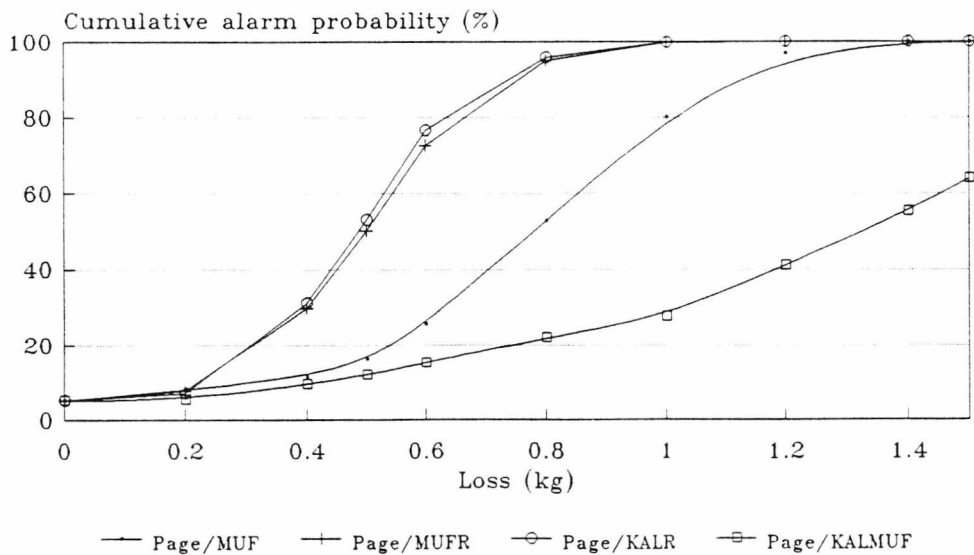


Fig 6.8 Absolute power for abrupt loss on period 30, old system
Page's Test with MUF, MUFR, KALR, KALMUF

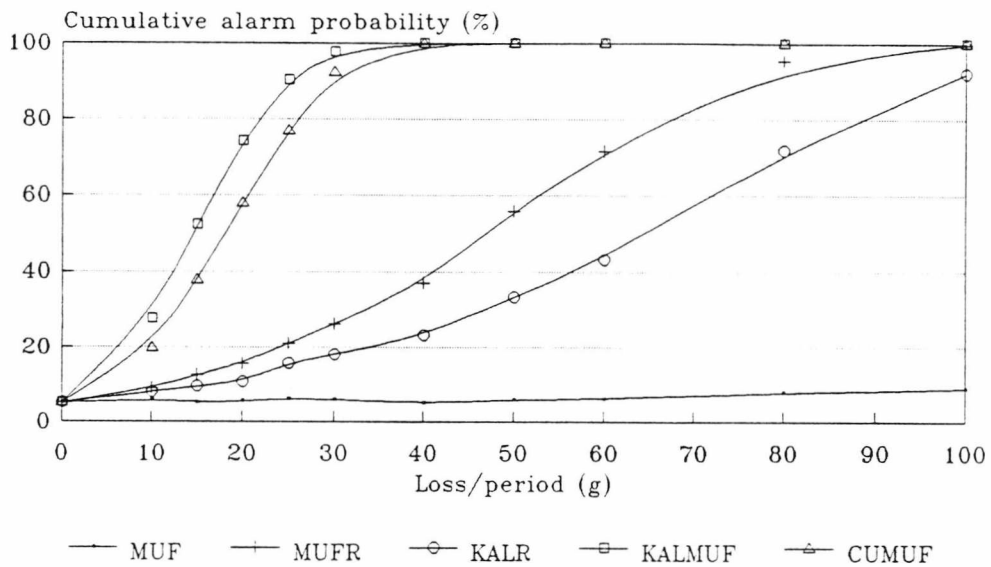


Fig 6.9 Absolute power for protracted loss, old system
 Threshold test with MUF, MUFR, KALR, KALMUF, CUMUF

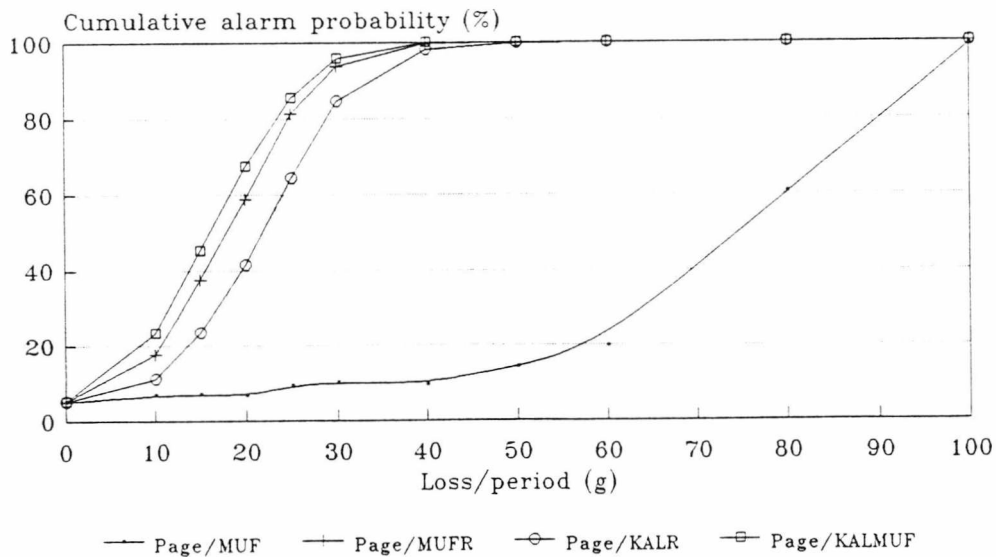
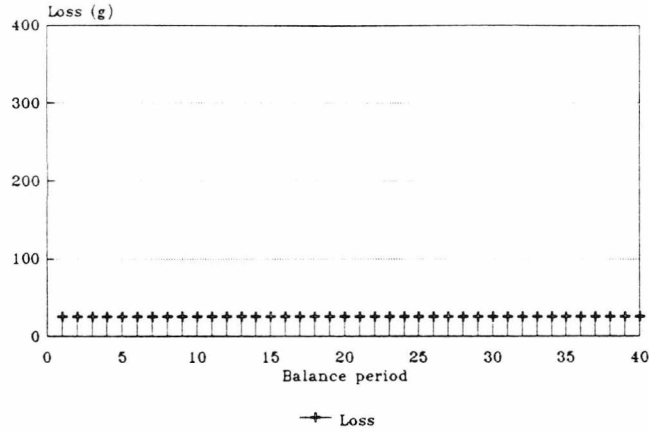


Fig 6.10 Absolute power for protracted loss, old system
 Page's Test with MUF, MUFR, KALR, KALMUF

Loss scenario



Cumulative alarm probabilities
Dissolver estimated from burn-up calculn

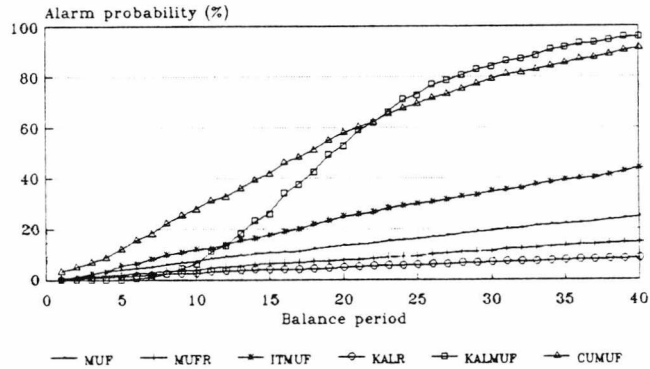


Fig 6.11 Cumulative alarm probs. for protracted loss, old system
Threshold test with MUF, MUFR, ITMUF, KALR, KALMUF, CUMUF

Cumulative alarm probabilities
Dissolver estimated from burn-up calculn

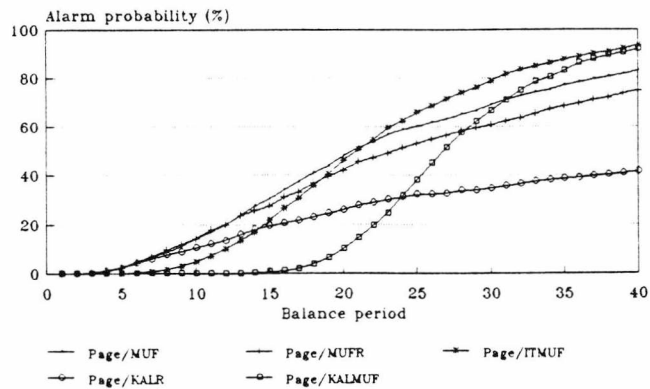


Fig 6.12 Cumulative alarm probs. for protracted loss, old system
Page's Test with MUF, MUFR, ITMUF, KALR, KALMUF

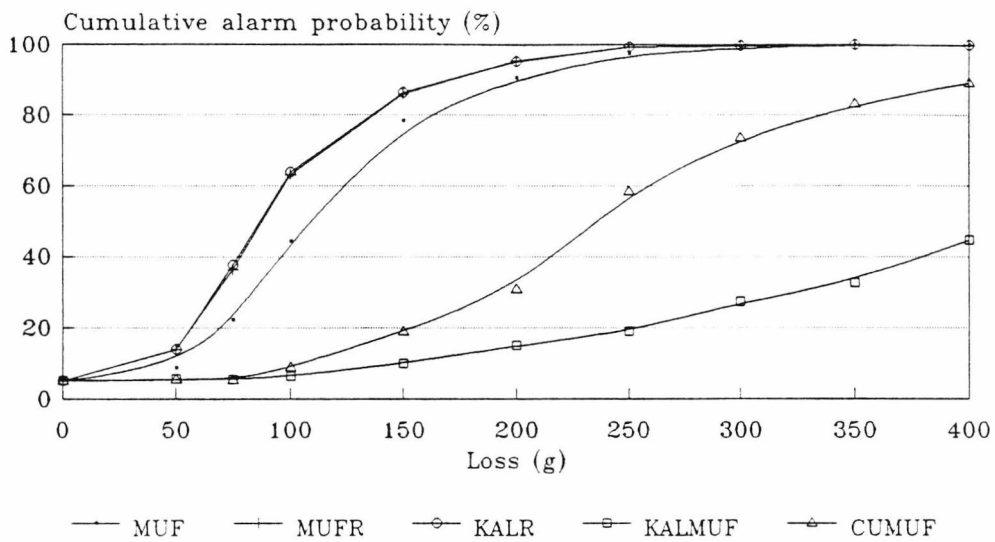


Fig 6.13 Absolute power for abrupt loss on period 30, new system
Threshold test with MUF, MUFR, KALR, KALMUF, CUMUF

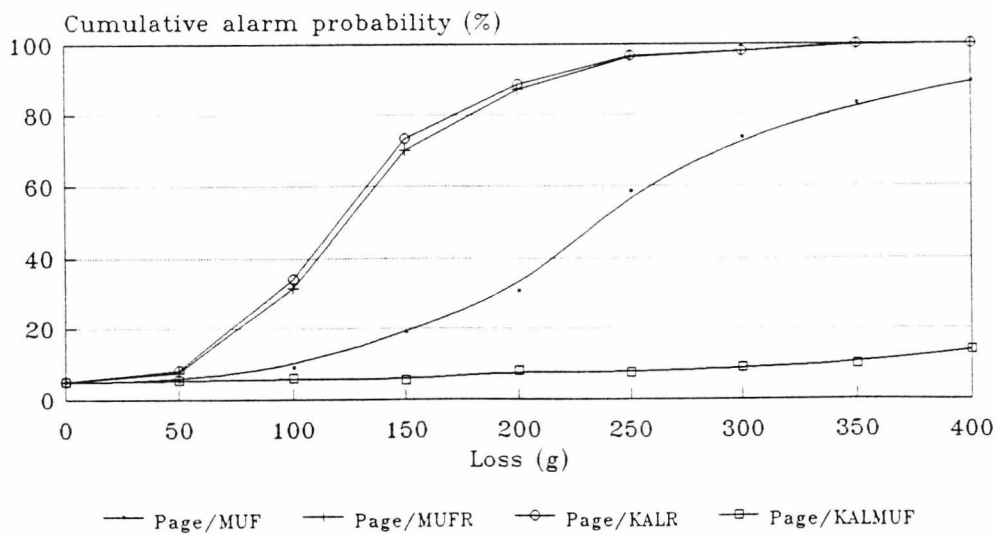


Fig 6.14 Absolute power for abrupt loss on period 30, new system
Page's Test with MUF, MUFR, KALR, KALMUF

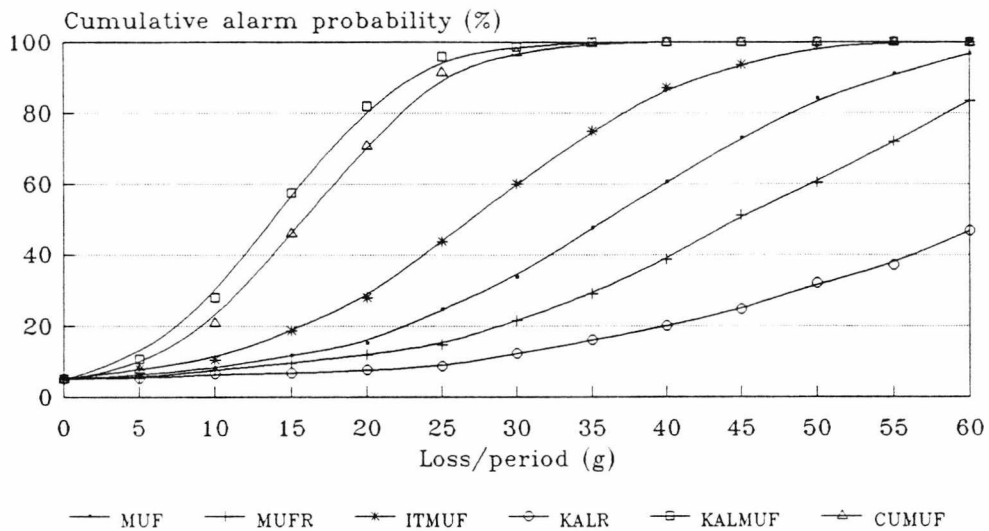


Fig 6.15 Absolute power for protracted loss, new system
 Threshold test with MUF, MUFR, KALR, KALMUF, CUMUF

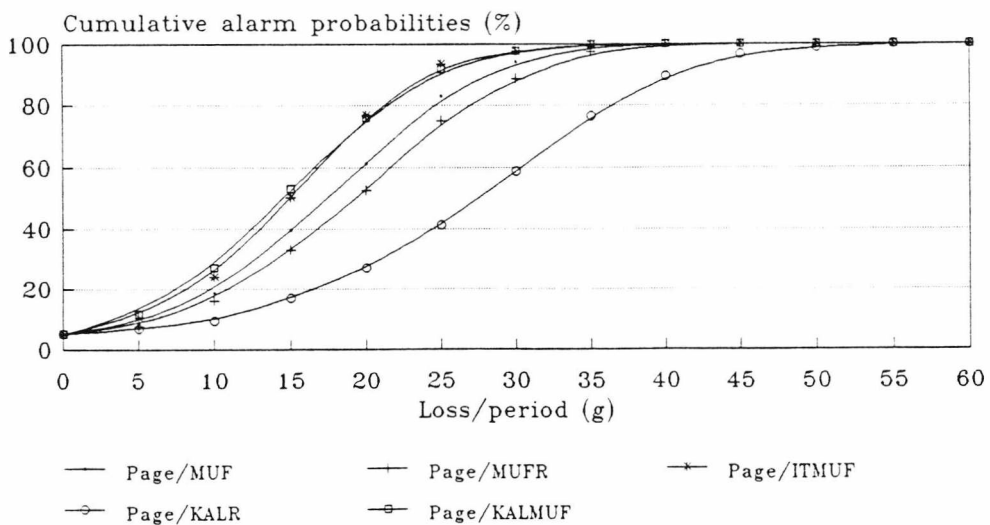


Fig 6.16 Absolute power for protracted loss, new system
 Page's Test with MUF, MUFR, KALR, KALMUF

Abrupt diversion of 200g, period 30
 Dissolver estimated from burn-up calculn

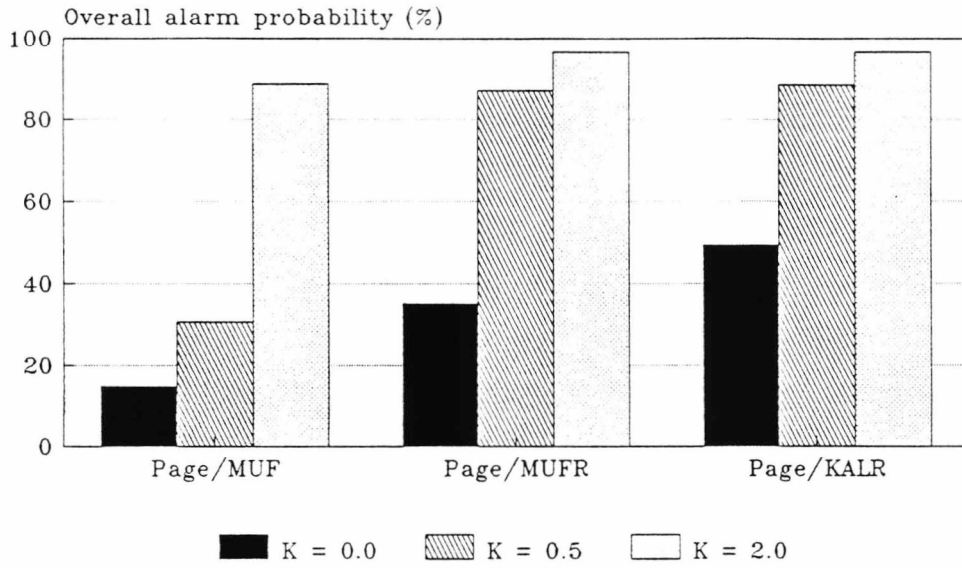


Fig 6.17 Effect of varying H-K pair in Page's Test
 Abrupt loss, new system

Protracted diversion, 30g per period
 Dissolver estimated from burn-up calculn

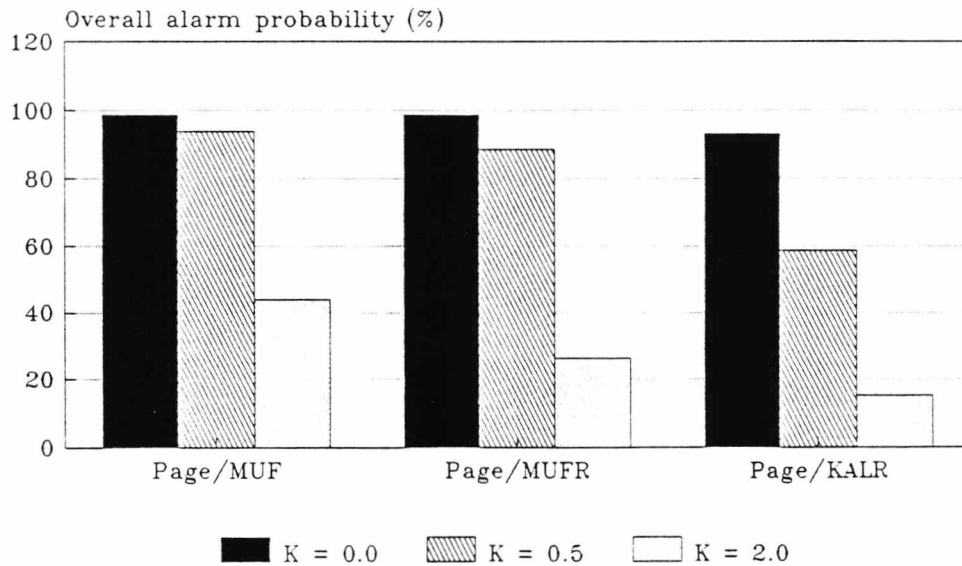


Fig 6.18 Effect of varying H-K pair in Page's Test
 Protracted loss, new system

6.7 Summary

The Kalman Filter generates two accountancy statistics, a residual very similar to MUFR, and a mean constant loss term. The latter offers the most powerful means of detecting a protracted loss or determination bias under both accountancy systems; however, it has a slow response, and is particularly unsuitable for detecting abrupt losses. The use of a twin test, using KALMUF with Page/KALR for the old accountancy system, and with KALR or Page/KALR for the new accountancy system, will give an effective 'blanket' safeguards cover.

7. Conclusions & suggestions for further work

7.1 Accountancy tank MVUE

If the highest possible accuracy of a determination is required, or if the desired accuracy cannot quite be achieved with a single set of instruments, the technique of calculating a minimum variance unbiased estimate described in chapter 4 using redundant measurements with diverse instrumentation may provide a solution. Where the errors on the component measurements are normally distributed, with known standard deviation, the benefits can be quantified by the methods of Appendix IV. If the error distributions are likely to vary significantly from the normal assumption, the reduction in the error range may have to be found by simulation.

7.2 Modelling the plant measurement system

As the research into Near Real Time Materials Accountancy has matured, there has been a growing recognition of the need to establish more sophisticated methods of statistical data conditioning to enhance the performance of decision tests. With this aim, using the head-end of the Fast Reactor Fuel Reprocessing Plant at Dounreay as an example, two methods of accurately modelling the plant measurement strategy have been developed and applied to materials accountancy.

The methods both centre on the accepted basis of materials accountancy, the 'Material Unaccounted For' or 'MUF' statistic defined in equation 2.1. Firstly, a means of calculating an accurate MUF covariance matrix, to remove the serial correlation from the MUF sequence, is described and compared with existing simple-model approaches. Secondly, the use of

state-estimation techniques in the form of a Kalman Filter is demonstrated, predicting a set of state variables through a 'progression model' and correcting the prediction with the measured MUF.

The strategies were compared with the aid of simulated data, derived from models of two different data acquisition systems on the head-end of the Fast Reactor Fuel Reprocessing Plant. The results from the performance analyses illustrate the advantages of accurate modelling of the plant measurement regime. Additionally, the modelling enables the standard deviation of the test statistics to be accurately calculated.

No single test statistic is robust enough to satisfactorily handle the conflicting requirements of powerful and credible detection against an unknown diversion scenario, with a single set of parameters. Multiple testing is impractical, as either the overall false alarm rate will get out of control, or the thresholds for each test will have to be raised, reducing their effectiveness. There is general agreement that a dual test offers the best compromise, one 'tuned' for large, abrupt losses, the other for protracted diversions.

The choice of the 'ideal' statistic for detecting abrupt losses depends to a certain extent on the accountancy regime. Where there is an independent assessment of the inventory, leading to a negative correlation between successive MUF figures, the use of Page's Test with the Kalman Filter residual KALR offers the best solution. The CUSUM technique also suppresses the effect of modelling errors.

However, if there is no satisfactory, independent determination of the inventory, and the bulk of the plant content is assumed from an input figure, the performance of Page's Test is critically dependent on the

choice of the H-K parameters. At best, the performance of Page/MUFR and Page/KALR match those of the respective threshold tests. To ensure robustness, the choice must thus fall to either MUFR or KALR with the threshold test.

The mean constant loss estimator generated by the Kalman Filter (KALMUF) is very sensitive to very protracted diversions or transfer biases under both accountancy systems. However, the slow response time means that it is ineffective until it has run for a number of balance periods. Its performance exactly complements CUMUF, which is very sensitive to early anomalies but has an excessive variance to perform well later in a campaign. Results from the simulations suggest that the switch to KALMUF should be effected after about twenty balance periods. Further research is needed to establish a theoretical basis for this decision.

MUFR, KALR and KALMUF are less readily interpretable than MUF and CUMUF. However, they offer a better and more consistent all-round performance. ITMUF is included in the analyses as an example of modelling error by over-simplification. The intention is not to discredit the concept behind ITMUF, but to indicate that, in practice, other factors than those generally considered in the calculation of ITMUF may condition the MUF sequence, and these should be accounted for. Where plant conditions approximate to the ITMUF assumptions of constant, known correlation between successive MUF estimates (as in the earlier accountancy system in the head-end of the Dounreay facility), the simple model shows a reasonably reliable performance, particularly if the data is applied to the CUSUM test. However, if the measurement regime differs substantially from this, results from the simple model are highly inaccurate. A simple ITMUF transformation on current data from the head-end of the Dounreay plant would yield grossly misleading

results.

7.3 Future work

Pike et al [35] demonstrate that the Kalman Filter is an ideal vehicle to implement a smoothing algorithm. The next stage of this work would be the extension of the Filter models to provide retrospective estimates of the plant states.

It may be useful to carry out a theoretical investigation into the convergence of the Kalman Filter, with particular regard to the settling time of the KALMUF statistic. Reference [64], published by Kalman in 1963, may be of assistance in this task.

8. References

1. IAEA Safeguards Glossary IAEA/SG/INF/1. International Atomic Energy Agency, Vienna, 1980.
2. W Bush et al; Safeguards measurement errors. IAEA-SM-231/104, 1978.
3. H Ihara et al; Development of a Near Real Time Materials Accountancy Data Processing System and evaluation of statistical analysis methods using field test data. IAEA-SM-293/33, 1986.
4. D J Pike, A J Woods; Analysis of Nuclear Material Accountancy data from the Tokai Reprocessing Plant. L T Consultants, Reading, May 1986.
5. T L Jones & D Gordon; Near Real Time Nuclear Materials Accountancy at Dounreay. IAEA-SM-293/22, 1986.
6. J Lovett et al; Near Real Time Material Accountancy - A technical status report. IAEA-SM-260/145, 1982.
7. D Gupta et al; International workshop on the Near Real Time Accountancy measure. IAEA-SM-260/29, 1982.
8. B J Jones; Comparison of Near Real Time Materials Accountancy using SITMUF and Page's Test with conventional accountancy. 9th Annual Symposium on Safeguards and Nuclear Material Management, EUR 11041 EN, ESARDA 21, 1987.
9. R Avenhaus; Safeguards Systems Analysis. Plenum Press, 1986.
10. R Beegden; Statistical considerations concerning multiple materials balance models. Los Alamos National Lab, LA-9645-MS, August 1983.
11. E Leitner et al; What is the price of timeliness? 9th Annual Symposium on Safeguards and Safeguards and Nuclear Material Management, EUR 11041 EN, ESARDA 21, 1987.
12. A Wald; Sequential analysis. John Wiley & Sons, New York,

- 1947.
13. N S Russell; A review of NRTMA Statistical Tests. SARDTAC report. SRDP - R114. (1984)
 14. N S Russell; Evaluation of multinormal probabilities using Fourier Series expansion. UKAEA Safeguards R & D Report, SRDP-R116, May 1984.
 15. W A Shewhart; Economic control of quality of manufactured products. Van Nostrand, New York, 1931.
 16. E S Page; Continuous Inspection Schemes. Biometrika 41, 1954.
 17. C S Van Dobben de Bruyn; Cumulative Sum Tests: Theory and Practice. Griffin's Statistical Monographs & Courses No. 24 1968.
 18. N L Johnson; A simple theoretical approach to Cumulative Sum Control Charts. J. Amer. Statist. Assoc, 56. 1961.
 19. N S Russell; Stochastic techniques for time series with applications to Materials Accountancy. Ph.D. Thesis, Dept. of Electrical Engineering, University of Southampton, August 1985.
 20. M R Reynolds; Approximations to the Average Run Length in Cumulative Sum Control Charts. Technometrics, Vol. 17, No. 1, February 1975.
 21. W D Ewen & K W Kemp; Sampling inspection of continuous processes with no autocorrelation between successive results. Biometrika 47, 1960.
 22. R Seifert; Application of Near Real Time Accountancy to Nuclear Material Balance data. Symposium on Computerized Material Accountancy and Information Systems, Harwell, 1988.
 23. B J Jones; Calculation of diversion detection using the SITMUF sequence and Page's Test. IAEA-SM-293/23P, 1986.
 24. B J Jones; Near Real Time Materials Accountancy using

- SITMUF and Page's Test: Comparison with MUF and CUMUF tests. ESARDA Bulletin 15, November 1988.
25. K B Stewart; B-PID and inventory estimates with minimum variance. Document HW-56536, UC34, General Electric Company Hanford Atomic Products Operation, 1958.
 26. K B Stewart; A new weighted average. Technometrics, Vol. 12, No. 2, May 1970.
 27. D J Pike, A J Woods, D M Rose; A critical appraisal of the use of estimators for the detection of loss in Nuclear Material Accountancy. Technical Report 1/80/07, University of Reading, 1980.
 28. D J Pike, A J Woods, D T Dunn; The effect of the calibration history of a measurement system on the variance-covariance matrix of a sequence of measurements. 5th Annual Symposium on Safeguards and Nuclear Material Management, ESARDA 13, 1983.
 29. R Beegden, W Golly, R Seifert; Problems in establishing a measurement model for reprocessing facilities and its use in applying sequential statistical tests. Proceedings of the RECOD '87, 1987.
 30. Leitner et al; Near Real Time Material Accountancy in an industrial scale reprocessing plant. IAEA-SM-293/55, 1986.
 31. R Seifert; The GEMUF Test: A new sequential test for detecting loss of material in a sequence of accounting periods. IAEA-SM-293/46, 1986.
 32. D Sellinschegg; A statistic sensitive to deviations from the zero-loss condition in a sequence of Material Balances. J. Nuclear Materials Management, 11, Part 4, 1982.
 33. R E Kalman; A new approach to linear filtering and prediction problems. Trans. ASME, J. Basic Eng, 82D, 1960.
 34. R E Kalman, R S Bucy; New results in linear filtering and prediction theory. Trans. ASME, J. Basic Eng, 83D, 1961.
 35. D H Pike, G W Morrison, G W Westley; Application of Kalman

- Filtering to Nuclear Material Control. ORNL/NUREG/CSD-1, Union Carbide Corporation, October 1977.
36. J P Shipley, J T Baker; DECANAL User's Manual. LA-9043-M, Los Alamos National Laboratory, April 1982.
 37. R Gale; CIMENT: An operating data management system for Near Real Time Materials Accountancy. IAEA-SM-293/171, 1986.
 38. S Nakamori, A Hataji; Relation between Filter using covariance information and Kalman Filter. Automatica, Vol.18, No. 4, 1982.
 39. N S Russell, M H Butterfield, J Howell; Comparison of Retrospective Testing with statistical tests in Near Real Time Materials Accountancy. 6th Annual Symposium on Safeguards and Nuclear Material Management, ESARDA, 1984.
 40. R Beegden, R Seifert; Statistical methods for verification of measurement models. ESARDA Bulletin 15, November 1988.
 41. R Beegden, W Golly, R Seifert; Concepts of establishing measurement models for NRTA procedures. Proceedings of the INMM, 1988.
 42. U Bicking, W Golly, R Seifert; Establishing a detailed measurement model for NRTA procedures. 11th Annual Symposium on Safeguards and Nuclear Material Management, ESARDA 22, EUR 12193 EN, 1989.
 43. P S Annibal, P D Roberts; Improvements in statistical techniques for Nuclear Material Accountancy. 11th Annual Symposium on Safeguards and Nuclear Material Management, ESARDA 22, EUR 12193 En, 1989.
 44. M Bagshaw, R A Johnson; The effect of serial correlation on the performance of CUSUM tests. Technometrics, Vol.17, No. 1, February 1975.
 45. A J Woods, D J Pike. Use of the Standardized ITMUF for choosing parameters of sequential tests for protracted and abrupt diversions. 5th Annual Symposium on Safeguards and

Nuclear Material Management, ESARDA, 1983.

46. B P Dudding, W J Jennet; Quality Control Charts. British Standard 600R, British Standards Institution, 1942.
47. L H Ford, S N Oruh, G S Coldwell; Measurement of liquid masses in accountancy tanks. IAEA-SM-293/167P, 1986.
48. P S Annibal, P D Roberts; The application of statistical techniques to Nuclear Material Accountancy. AEA Technology Safeguards R & D Report, SRDP-166, 1990.
49. F E Hunter & T H Green; UKAEA Dounreay internal report, October 1983.
50. W N Miller; UKAEA Northern Division internal report, December 1980.
51. W N Miller; UKAEA Northern Division internal report, April 1986.
52. W I Hamilton, J McQuade; UKAEA Dounreay internal report, March 1978
53. H Shimojima; A precise vessel calibration. IAEA-SM-293/98P, 1986.
54. W Davis et al; A statistical examination of the practical problems of measurement in accountancy tanks. IAEA-SM-231/57, 1978.
55. C Foggi et al; Reprocessing input tank accountancy. IAEA-SM-293/79, 1986.
56. T J Stevens; The application of diverse transfer calculations to detect erroneous inputs and systematic errors. UK Safeguards R & D Report, SRDP-R-164, AEEW-R 2575, March 1990.
57. B J Jones; Calculation of the parameters used in Page's Test. ESARDA Bulletin Number 7. Joint Research Centre, Ispra, Italy. (1984)
58. A Gelb et al; Applied Optimal Estimation. The M.I.T.

Press, Massachusetts Institute of Technology, 1974.

59. B D O Anderson, J B Moore; Optimal Filtering. Information and System Science Series, Prentice-Hall, 1979.
60. S P Banks; Control Systems Engineering. Prentice-Hall, 1986.
61. A P Sage, J L Melsa; Estimation Theory with application to communications and control. Robert E. Krieger Publishing Company, Florida, 1971.
62. A H Jazwinski; Stochastic processes and filtering theory. Vol. 64 in Mathematics in Science and Engineering, Academic Press, New York, 1970.
63. C A Brebbia, A J Ferrante; Computational methods for the solution of engineering problems. Pentech Press, 1979.
64. R E Kalman; New methods in Wiener Filtering theory. Proc. the First Symposium on Engineering Applications of Random Function Theory. John Wiley & Sons Inc, New York, 1963.

General references for statistical equations and tables

I Miller & J E Freund; Probability and Statistics for Engineers. Prentice Hall, 1977.

E Mansfield; Statistics for Business and Economics. W W Norton & Co, 1980.

M M Tatsuoka & P R Lohnes; Multivariate Analysis. Macmillan Publishing Company, 1988.

APPENDIX I - Liquor Height in a Tank from Pneumercator Readings

Figure I.1 shows schematically a pneumercator system in plant conditions and in calibration conditions.

The pressure gauge is calibrated in mm of H₂O at 20°C: this is the pressure P. The actual pressure across the gauge (in Pascals) is (referring to the inset) given by:

$$p_1 - p_2 = gh\rho_{a20} + g^P\rho_{w20} - g(P + h)\rho_{a20} \quad (\text{I.1})$$

Where ρ denotes density, subscript a denotes air and subscript 20 denotes 20°C.

Now referring to the main diagram:

$$p_1 + g(h + H)\rho_{aT} = gH\rho_{LT} + p_s \quad (\text{I.2})$$

$$p_s = p_2 + gh\rho_{aT} \quad (\text{I.3})$$

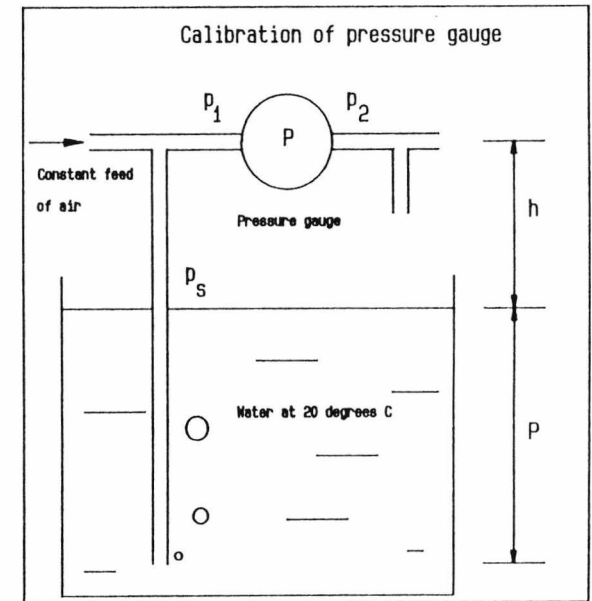
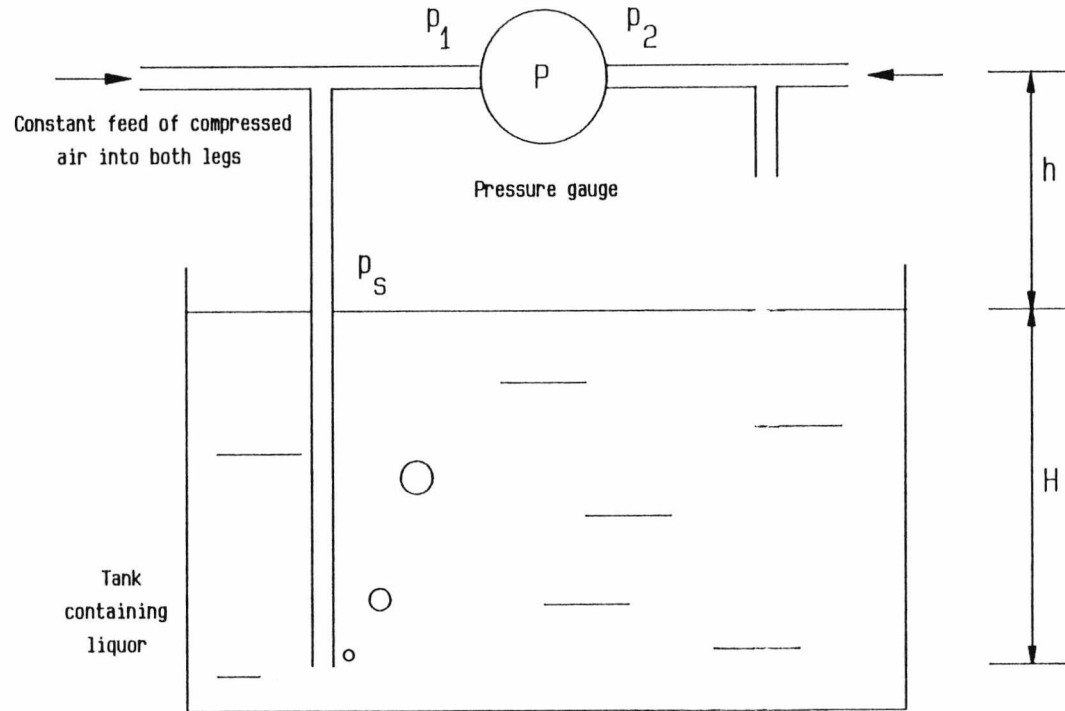
$$\therefore p_1 - p_2 = gH(\rho_{LT} - \rho_{aT}) \quad (\text{I.4})$$

Where subscript L denotes liquor and subscript T denotes tank temperature.

Equating (I.1) and (I.4) gives:

$$H = P \cdot \left(\frac{\rho_{w20} - \rho_{a20}}{\rho_{LT} - \rho_{aT}} \right) \quad (\text{I.5})$$

Figure I.1 Conversion of pneumercator readings to pressures



APPENDIX II - Derivation of the elements of Table 4.1

II.1 Tank liquor density from laboratory density measurement

$$\rho_{LT} = \left(1 + \alpha \cdot (20 - T)\right) \cdot \rho_{L20} \quad \begin{array}{l} \text{Tank density given} \\ \text{density at } 20^{\circ}\text{C} \end{array} \quad (\text{II.1})$$

$$\rho_{Lt} = \left(1 + \alpha \cdot (20 - t)\right) \cdot \rho_{L20} \quad \begin{array}{l} \text{Lab density given} \\ \text{density at } 20^{\circ}\text{C} \end{array} \quad (\text{II.2})$$

$$\therefore \boxed{\rho_{LT} = \rho_{Lt} \cdot \left(\frac{1 + \alpha \cdot (20 - T)}{1 + \alpha \cdot (20 - t)}\right)} \quad (\text{II.3})$$

II.2 Tank Liquor Density from the "In Tank S.G." Reading

Gauge S is connected between two dip tubes a nominal 1m apart (the true distance is denoted by d). At calibration time, the gauge is placed across two dip tubes placed in water at 20°C a distance 'd' apart and the gauge is marked with the value 's'. If the gauge is fitted on plant between two tubes exactly 1m apart then, calibrated in this way, (and ignoring air density correction) the gauge would read the S.G. of the tank fluid.

The relationship between reading 's' and Δp across the pressure gauge is:

$$\Delta p = (\rho_{w20} - \rho_{a20}) \cdot g \cdot s \quad (\text{II.4})$$

In the tank the same relationship is:

$$\Delta p = (\rho_{LT} - \rho_{aT}) \cdot g \cdot d \quad (\text{II.5})$$

Equating these and rearranging gives:

$$\rho_{LT} = \frac{(\rho_{w20} - \rho_{a20}) \cdot s}{d} + \rho_{aT} \quad (II.6)$$

II.3 Tank Liquor Density from the Overall and Neck Gauges

The ends of the dip-tubes connected to gauges A and P (see figure 3.3) are a distance D apart. The difference between the pressure across the gauge registering A, Δp_A , and the pressure across the gauge registering P, Δp_P , is given by:

$$\Delta p_A - \Delta p_P = D \cdot g \cdot \rho_{LT} - D \cdot g \cdot \rho_{aT} = (\rho_{LT} - \rho_{aT}) \cdot D \cdot g \quad (II.7)$$

The two gauges are calibrated with water at 20°C, ie:

$$\Delta p_A = (\rho_{w20} - \rho_{a20}) \cdot g \cdot A \quad \Delta p_P = (\rho_{w20} - \rho_{a20}) \cdot g \cdot P \quad (II.8)$$

Substituting these two results into the equation above and rearranging gives:

$$\rho_{LT} = \frac{(A - P) \cdot (\rho_{w20} - \rho_{a20})}{D} + \rho_{aT} \quad (II.9)$$

**II.4 Concentration in g/l at tank temperature given concentration
in g/l at lab temperature**

If Y_t is the concentration in g/l measured at lab temperature,
then Y_{20} , the concentration in g/l at 20°C is:

$$Y_{20} = \frac{Y_t}{1 + \alpha \cdot (20-t)} \quad (\text{II.10})$$

From this Y_T , the concentration in g/l at the tank temperature can
be calculated as:

$$Y_T = Y_t \cdot \left(\frac{1 + \alpha \cdot (20-T)}{1 + \alpha \cdot (20-t)} \right) \quad (\text{II.11})$$

II.5 Volume of Transfer using Laboratory Density Measurement

The equation for the initial volume is found by substituting
II.3 into I.1 using P, the reading from the neck level gauge,
and applying the height-to-volume calibration function, ψ :

$$\psi \left(\frac{P \cdot (\rho_{w20} - \rho_{a20})}{\rho_{Lt} \cdot \left(\frac{1 + \alpha \cdot (20-T)}{1 + \alpha \cdot (20-t)} \right) - \rho_{aT}} \right) \quad (\text{II.12})$$

Similarly the final volume of fluid (heel volume) using a, the
reading from the overall gauge after the transfer:

$$\psi \left(\frac{a \cdot (\rho_{w20} - \rho_{a20})}{\rho_{Lt} \cdot \left(\frac{1 + \alpha \cdot (20-T)}{1 + \alpha \cdot (20-t)} \right) - \rho_{aT}} \right) \quad (\text{II.13})$$

Thus the expression for the volume transferred is:

$$\psi \left(\frac{P \cdot (\rho_{w20} - \rho_{a20})}{\rho_{Lt} \cdot \left(\frac{1 + \alpha \cdot (20-T)}{1 + \alpha \cdot (20-t)} \right) - \rho_{aT}} \right) - \psi \left(\frac{a \cdot (\rho_{w20} - \rho_{a20})}{\rho_{Lt} \cdot \left(\frac{1 + \alpha \cdot (20-T)}{1 + \alpha \cdot (20-t)} \right) - \rho_{aT}} \right) \quad (\text{II.14})$$

II.6 Volume of Transfer using In Tank SG Indicator

The equation for the initial volume is found by substituting II.6 into I.1 using P, the reading from the neck level gauge, and applying the height-to-volume calibration function, ψ . Similarly, the equation for the volume of fluid remaining after the transfer (heel volume) is found by substituting II.3 into I.5 using a, the final reading from the overall gauge. The volume transferred is the difference:

$$\psi \left(\frac{P \cdot d}{s} \right) - \psi \left(\frac{a \cdot d}{s} \right) \quad (\text{II.15})$$

II.7 Volume of Transfer using In Tank Density Measurement

The equation for the volume transferred is formed in the same way as the above equation, substituting II.9 into I.1 and taking the difference between initial and final volumes:

$$\psi \left(\frac{P \cdot D}{A - P} \right) - \psi \left(\frac{a \cdot D}{A - P} \right) \quad (\text{II.16})$$

APPENDIX III - General Derivation of MVUE Coefficients

If X can be measured in n ways X_1, X_2, \dots, X_n then a linear estimator of the quantity $Y = \bar{X}$ can be formed as

$$Y = \gamma_1 X_1 + \gamma_2 X_2 + \gamma_3 X_3 + \dots + \gamma_n X_n \quad (\text{III.1})$$

The variance of Y, σ_Y is given by:

$$\sigma_Y^2 = \sum_{i=1}^n \sum_{j=1}^n \gamma_i \gamma_j \sigma_{ij} \quad (\text{III.2})$$

The condition that Y is to be an unbiased estimate of X can be expressed as:

$$\left(\sum_{i=1}^n \gamma_i \right) = 1 \quad (\text{III.3})$$

A further condition which can be imposed on Y is that it should have minimum variance; ie. the γ 's should be chosen so as to minimise σ_Y^2 . This can be achieved by setting the partial differentials of σ_Y^2 with respect to the γ 's to zero. However, in order to impose the unbiased condition a Lagrangian undetermined multiplier, λ , is introduced and the following is minimised with respect to the γ 's and to λ :

$$\sigma_Y^2 = \sum_{i=1}^n \sum_{j=1}^n \gamma_i \gamma_j \sigma_{ij} + \lambda \cdot \left(\sum_{i=1}^n \gamma_i - 1 \right) \quad (\text{III.4})$$

Differentiating the above expression with respect to n γ 's and to λ and setting the results to zero produces n + 1 equations which solve for the n γ 's and λ .

$$\frac{\partial \sigma_Y^2}{\partial \gamma_j} = 0 = 2 \sum_{i=1}^n \gamma_i \sigma_{ij} + \lambda \quad (\text{III.5})$$

$$\frac{\partial \sigma_Y^2}{\partial \lambda} = 0 = \sum_{i=1}^n \gamma_i - 1 \quad (\text{III.6})$$

Writing III.5 and III.6 in matrix format ...

$$\begin{bmatrix} 2\sigma_1^2 & 2\sigma_{12} & 2\sigma_{13} & \cdot & \cdot & \cdot & 2\sigma_{1n} & 1 \\ 2\sigma_{21} & 2\sigma_2^2 & 2\sigma_{23} & \cdot & \cdot & \cdot & 2\sigma_{2n} & 1 \\ 2\sigma_{31} & 2\sigma_{32} & 2\sigma_3^2 & \cdot & \cdot & \cdot & 2\sigma_{3n} & 1 \\ \cdot & \cdot \\ \cdot & \cdot \\ \cdot & \cdot \\ \cdot & \cdot \\ 2\sigma_{n1} & 2\sigma_{n2} & 2\sigma_{n3} & \cdot & \cdot & \cdot & 2\sigma_n^2 & 1 \\ 1 & 1 & 1 & \cdot & \cdot & \cdot & 1 & 0 \end{bmatrix} \begin{bmatrix} \gamma_1 \\ \gamma_2 \\ \gamma_3 \\ \cdot \\ \cdot \\ \cdot \\ \cdot \\ \gamma_n \\ \lambda \end{bmatrix} = \begin{bmatrix} 0 \\ 0 \\ 0 \\ \cdot \\ \cdot \\ \cdot \\ \cdot \\ 0 \\ 1 \end{bmatrix}$$

$$= \lambda \quad (\text{III.7})$$

In summary,

The Minimum Variance (Linear) Unbiased Estimator of X is:

$$Y = \gamma_1 X_1 + \gamma_2 X_2 + \gamma_3 X_3 + \dots + \gamma_n X_n$$

where the γ_i 's are the first n elements of the last column of Λ^{-1}

$$\Lambda = \begin{bmatrix} 2\sigma_1^2 & 2\sigma_{12} & 2\sigma_{13} & \cdot & \cdot & \cdot & 2\sigma_{1n} & 1 \\ 2\sigma_{21} & 2\sigma_2^2 & 2\sigma_{23} & \cdot & \cdot & \cdot & 2\sigma_{2n} & 1 \\ 2\sigma_{31} & 2\sigma_{32} & 2\sigma_3^2 & \cdot & \cdot & \cdot & 2\sigma_{3n} & 1 \\ \cdot & \cdot \\ \cdot & \cdot \\ \cdot & \cdot \\ 2\sigma_{n1} & 2\sigma_{n2} & 2\sigma_{n3} & \cdot & \cdot & \cdot & 2\sigma_n^2 & 1 \\ 1 & 1 & 1 & \cdot & \cdot & \cdot & 1 & 0 \end{bmatrix}$$

(III.8)

APPENDIX IV - Calculation of the Accountancy Tank Transfer MVUE

Coefficients

In Appendix III a method for calculating MVUE coefficients is described. It is shown that the coefficients are the first n elements of the last column of the matrix Λ^{-1} , where Λ is derived from the covariance matrix of the individual measurements. In the case of the accountancy tank transfer, MVUEs are required for the three volume expressions. To calculate the three Λ s, the concentration and volume terms are simplified to remove negligible components and keep the solution manageable. They thus become:

$$C_1 = Z \cdot \rho_{Lt} \cdot \left(\frac{1 + \alpha \cdot (20-T)}{1 + \alpha \cdot (20-t)} \right) \quad (\text{IV.1})$$

$$C_2 = Z \cdot \left(\frac{(\rho_{w20} - \rho_{a20}) \cdot s}{d} \right) \quad (\text{IV.2})$$

$$C_3 = Z \cdot \left(\frac{(A - P) \cdot (\rho_{w20} - \rho_{a20})}{D} \right) \quad (\text{IV.3})$$

$$C_4 = Y_t \cdot \left(\frac{1 + \alpha \cdot (20-T)}{1 + \alpha \cdot (20-t)} \right) \quad (\text{IV.4})$$

$$V_1 = \psi \left(\frac{P \cdot (\rho_{w20} - \rho_{a20})}{\rho_{Lt}} \right) - \psi \left(\frac{a \cdot (\rho_{w20} - \rho_{a20})}{\rho_{Lt}} \right) \quad (\text{IV.5})$$

$$V_2 = \psi \left(\frac{P \cdot d}{s} \right) - \psi \left(\frac{a \cdot d}{s} \right) \quad (\text{IV.6})$$

$$V_3 = \psi \left(\frac{P \cdot D}{A - P} \right) - \psi \left(\frac{a \cdot D}{A - P} \right) \quad (\text{IV.7})$$

For each of the equations $[L_1]$, $[L_2]$ and $[L_3]$, the variance of each (concentration \times volume) term and the covariances between the four terms are needed. To calculate these, the following identities are

useful.

Variance of a product

Two random variables x, y have mean \bar{x} , \bar{y} and error components u,v.

They form the series

$$\bar{x} + u_1, \bar{x} + u_2, \dots, \bar{x} + u_n \tag{IV.8}$$

$$\bar{y} + v_1, \bar{y} + v_2, \dots, \bar{y} + v_n \tag{IV.9}$$

The product of the jth elements is

$$p_j = (\bar{x} + u_j) \cdot (\bar{y} + v_j) = \bar{x} \cdot \bar{y} + \bar{x} \cdot v_j + \bar{y} \cdot u_j + u_j \cdot v_j \tag{IV.10}$$

with a mean value for the product series of

$$\bar{p} = \frac{\sum_{i=1}^n p_i}{n} = \bar{x} \cdot \bar{y} + \frac{\sum_{i=1}^n (u_i \cdot v_i)}{n} \tag{IV.11}$$

p_j can also be expressed

$$p_j = \bar{p} + w_j \tag{IV.12}$$

where w is the error component. Thus,

$$w_j = p_j - \bar{p} = \bar{x} \cdot v_j + \bar{y} \cdot u_j + u_j \cdot v_j - \frac{\sum_{i=1}^n (u_i \cdot v_i)}{n} \tag{IV.13}$$

The variance of p is equal to $\frac{\sum_{i=1}^n w_i^2}{n}$ (IV.14)

$$w_j^2 = \bar{x}^2 \cdot v_j^2 + \bar{y}^2 \cdot u_j^2 + u_j^2 \cdot v_j^2 + \left(\frac{\sum_{i=1}^n (u_i \cdot v_i)}{n} \right)^2 \quad (\text{IV.15})$$

$$+ 2 \cdot \bar{x} \cdot u_j \cdot \bar{y} \cdot v_j + 2 \cdot u_j^2 \cdot \bar{y} \cdot v_j - 2 \cdot u_j \cdot \bar{y} \cdot \left(\frac{\sum_{i=1}^n (u_i \cdot v_i)}{n} \right)$$

$$+ 2 \cdot \bar{x} \cdot u_j \cdot v_j^2 - 2 \cdot \bar{x} \cdot v_j \cdot \left(\frac{\sum_{i=1}^n (u_i \cdot v_i)}{n} \right) - 2 \cdot u_j \cdot v_j \cdot \left(\frac{\sum_{i=1}^n (u_i \cdot v_i)}{n} \right)$$

$$\frac{\sum_{i=1}^n w_i^2}{n} = \bar{x}^2 \sigma^2(y) + \bar{y}^2 \sigma^2(x) + \sigma^2(x) \sigma^2(y) + 2 \bar{x} \bar{y} \cdot \text{Cov}(x, y) - \{ \text{Cov}(x, y) \} \quad (\text{IV.16})$$

If x and y are accurate measurements,

$$\bar{x}^2 \cdot \sigma^2(y) \text{ or } \bar{y}^2 \cdot \sigma^2(x) \gg \sigma^2(x) \cdot \sigma^2(y) \quad (\text{IV.17})$$

and if they are uncorrelated, $\text{Cov}(x, y) = 0$ (IV.18)

The variance of the product (x.y) thus simplifies to

$$\sigma^2(x \cdot y) \approx \bar{x}^2 \cdot \sigma^2(y) + \bar{y}^2 \cdot \sigma^2(x)$$

(IV.19)

Variance of a quotient

The jth quotient of the random variables x and y is

$$q_j = \frac{\bar{x} + u_j}{\bar{y} + v_j} = \frac{\bar{x} + u_j}{\bar{y}} \cdot \left[\frac{1}{1 + v_j / \bar{y}} \right] \quad (\text{IV.20})$$

The term in brackets can be expanded by the binomial series

$$\frac{1}{1 + v_j / \bar{y}} = 1 - \left(\frac{v_j}{\bar{y}}\right) + \left(\frac{v_j}{\bar{y}}\right)^2 - \left(\frac{v_j}{\bar{y}}\right)^3 \dots \quad (\text{IV.21})$$

As $v_j \ll \bar{y}$ for an accurate measurement, this may be approximated to

$$\frac{1}{1 + v_j / \bar{y}} \approx 1 - \left(\frac{v_j}{\bar{y}}\right) \quad (\text{IV.22})$$

Thus,
$$q_j \approx \frac{(\bar{x} + u_j) \cdot (\bar{y} - v_j)}{\bar{y}^2} \quad (\text{IV.23})$$

This expression enables the variance of the quotient to be found by similar method to that described above.

$$\sigma^2(q) \approx \frac{\bar{x}^2}{\bar{y}^2} \cdot \left\{ \frac{\sigma^2(x)}{\bar{x}^2} + \frac{\sigma^2(y)}{\bar{y}^2} + \frac{\sigma^2(x) \cdot \sigma^2(y)}{\bar{x}^2 \cdot \bar{y}^2} - \frac{2 \cdot \text{Cov}(x, y)}{\bar{x} \cdot \bar{y}} - \frac{\{\text{Cov}(x, y)\}^2}{\bar{x}^2 \cdot \bar{y}^2} \right\} \quad (\text{IV.24})$$

Again, with accurate measurements and no covariance between x and y, this simplifies to:

$$\boxed{\sigma^2\left(\frac{x}{y}\right) \approx \frac{\bar{x}^2}{\bar{y}^2} \cdot \left\{ \frac{\sigma^2(x)}{\bar{x}^2} + \frac{\sigma^2(y)}{\bar{y}^2} \right\}} \quad (\text{IV.25})$$

Covariances

To evaluate product or quotient covariances, use is made of the identity

$$\sigma(x,y) = \frac{\sum_{i=1}^n x \cdot y}{n} - \frac{\sum_{i=1}^n x \cdot \sum_{i=1}^n y}{n^2} \quad (\text{IV.26})$$

For some cases, such as $\sigma\left(x, \frac{1}{x}\right)$, the expansion of the denominator requires the second order binomial term.

Sample data

The following values were used for the various plant measurements:

Plant variable		Mean	Std. dev.
T	Temperature of liquor in tank	22.68°C	0.50°C
t	Temperature of liquor in lab.	24.60°	0.05°C
P	Neck level gauge reading	1317 (mm water)	2.5 (mm)
A	Overall gauge reading	3980 (mm water)	5.0 (mm)
a	Heel level gauge reading	63 (mm water)	1.5 (mm)
s	In tank specific gravity reading	1274 (mm water)	2.5 (mm)
D	Separation of heel and overall dip-tube ends	2070 mm	
d	Separation of dip-tubes ends for 's'	990 mm	
Z	Pu concentration weight/weight	0.0220 g Pu/g	5×10^{-5} g/g
Y_t	Pu concentration weight/volume	28.2 g Pu/l	1.0 g/l
ρ_{lt}	Density of liquor at t	1282.4 g/l	1.6 g/l

The values of the constants are

Constant		Value
α	Expansion coeff. of 5M nitric acid @ 20°C	0.00057
δ	Expansion coeff. of stainless steel tank @ 20°C	0.000048
ρ_{w20}	Density of water @ 20°C	998.2 g/l
ρ_{a20}	Density of air @ 20°C	1.2 g/l
ρ_{aT}	Density of air @ tank temperature	1.2 g/l

Note: The air density term is always added to or subtracted from a water density in the formulae. Thus the variation in air density between 20°C and tank temperature has no effect on the precision of the transfer estimate.

Accountancy tank calibration models

The accountancy tank has narrowed regions at the neck and heel to improve the resolution of the height-volume conversion. Linear models of these regions were found from the tank calibration table using 'least-squares' techniques. These are:

$$\text{Filled volume} = (\text{Neck height} \times 0.017317) + 152.47 \quad (\text{IV.27})$$

$$\text{Emptied volume} = (\text{Heel height} \times 0.004651) + 0.20 \quad (\text{IV.28})$$

The neck model covers the height range 900-1100mm, and the heel model 43-64.5mm. Measurements are normally taken with the liquor level within these bands.

Results

For $[C_{1-4}] \times [V_1]$

mean: 4795.6 g

standard deviations: 11.58 g

inter-component correlations:

Between components...	1 and 2:	0.657
	1 and 3:	0.627
	1 and 4:	-0.001
	2 and 3:	0.549
	2 and 4:	0.000
	3 and 4:	-0.001

For $[C_{1-4}] \times [V_2]$

mean: 4795.6 g

standard deviations: 11.57 g

inter-component correlations:

Between components...	1 and 2:	0.641
	1 and 3:	0.634
	1 and 4:	0.001
	2 and 3:	0.531
	2 and 4:	-0.004
	3 and 4:	-0.002

For $[C_{1-4}] \times [V_3]$

mean: 4795.6 g

standard deviations: 11.56 g

inter-component correlations:

Between components...	1 and 2:	0.665
	1 and 3:	0.607
	1 and 4:	0.001
	2 and 3:	0.528
	2 and 4:	0.002
	3 and 4:	-0.005

Applying the Λ^{-1} formula for calculation of MVUE coefficients, derived in Appendix III, gives:

$$\begin{aligned}\gamma_1 &= 0.5747 \\ \gamma_2 &= 0.2019 \\ \gamma_3 &= 0.2187 \\ \gamma_4 &= 0.0047\end{aligned}$$

$$\begin{aligned}\nu_1 &= 0.4637 \\ \nu_2 &= 0.3042 \\ \nu_3 &= 0.2174 \\ \nu_4 &= 0.0047\end{aligned}$$

$$\begin{aligned}\eta_1 &= 0.4629 \\ \eta_3 &= 0.2004 \\ \eta_3 &= 0.3220 \\ \eta_4 &= 0.0047\end{aligned}$$

APPENDIX V - Comparison of the sensitivity to measurement bias of
the MVUE with the existing four methods

Table V.1

Percentage change in estimate of transfer L for a $+3\sigma$ bias

Measurement given $+3\sigma$ bias		Formula 1	Formula 2	Formula 3	Formula 4	MVUE
Pu conc (W/W)	Z	0.681	-	0.681	0.681	0.679
Pu conc (W/V)	Y_t	-	10.63	-	-	0.048
Pneumer. read.	P	0.059	0.059	0.059	-0.193	-0.001
Pneumer. read.	A	-	-	-	0.505	0.121
Pneumer. read	a	-0.010	-0.010	-0.010	-0.010	-0.010
Lab. density	ρ_{Lt}	0.336	-	-	-	0.180
Tank density	s	-	-0.064	0.528	-	0.116
Lab. temp.	t	0.008	0.009	-	-	0.004
Tank temp.	T	-0.070	-0.078	0.007	0.007	-0.034

Table V.2

Percentage change in estimate of transfer L for a +1% bias

Measurement given +1% bias		Formula 1	Formula 2	Formula 3	Formula 4	MVUE
Pu conc (W/W)	Z	1.000	-	1.000	1.000	1.000
Pu conc (W/V)	Y_t	-	1.000	-	-	0.005
Pneumer. read.	P	0.104	0.104	0.104	-0.339	-0.001
Pneumer. read.	A	-	-	-	1.339	0.321
Pneumer. read	a	-0.001	-0.001	-0.001	-0.001	-0.001
Lab. density	ρ_{Lt}	0.897	-	-	-	0.481
Tank density	s	-	-0.102	0.896	-	0.197
Lab. temp.	t	0.013	0.014	-	-	0.007
Tank temp.	T	-0.011	-0.012	0.001	0.001	-0.005

APPENDIX VI - Setting the alarm thresholds

The cost and effort involved in investigating false alarms by the diversion/no diversion decision tests demands a low false alarm rate - the IAEA suggest 5% as being an acceptable level. In terms of NRTMA, for the purpose of comparison in this thesis, this is taken to mean an average of one false alarm in twenty campaigns, 40 balance periods per campaign. This is a stringent constraint, and is obviously dependent on the number of balance periods in the campaign.

For the conditions stated above, an independent data set will give an almost equi-probable chance of false alarming on each balance period of about 0.13% with constant thresholds. This does not hold if there are strong correlations within the sequence; in particular, CUMUF will have an excessively high chance of false alarming over the first few balance periods. MUF and ITMUF suffer this to a much lesser extent, as their covariance matrices are more sparse; constant thresholds were used for these.

The only practical way of establishing thresholds for MUF, ITMUF and CUMUF over a large number of balance periods is by Monte-Carlo simulation. The models of the head-end of the reprocessing plant were used to generate MUF sequences, covariance data and state-space information, which was then used to calculate all the thresholds and Page H-K pairs for both the old and new accountancy systems. These thresholds apply to both positive and negative limits, and were calculated from 10 sets of data each comprising 1000 campaigns of 40 balance periods. The values are not exact - there is inevitably a degree of uncertainty surrounding the sampling of points in the tails of the normal distribution. From the data available, the standard deviation on each of these is about 0.05. They are tabulated below, the

CUMUF thresholds for the old and new accountancy systems being displayed graphically in figure VI.1.

	Old accountancy system	New accountancy system
MUF	3.17	3.23
MUFR	3.33	3.27
ITMUF	2.95	4.73
KALR	3.30	3.24
KALMUF	1.57	1.65

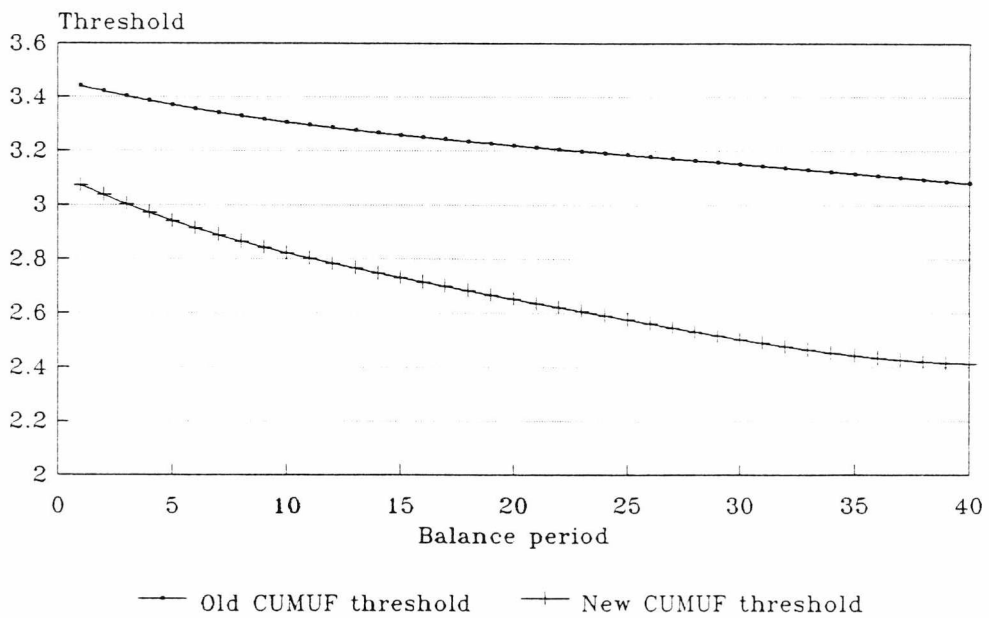


Fig VI.1 CUMUF thresholds to maintain a constant false alarm probability of 0.13% per period

It can be seen in figure VI.2 below that the KALMUF false alarm probability is not constant. This statistic takes about 10 balance periods to settle, so there is little point in adjusting the thresholds to give a constant false alarm probability over this period.

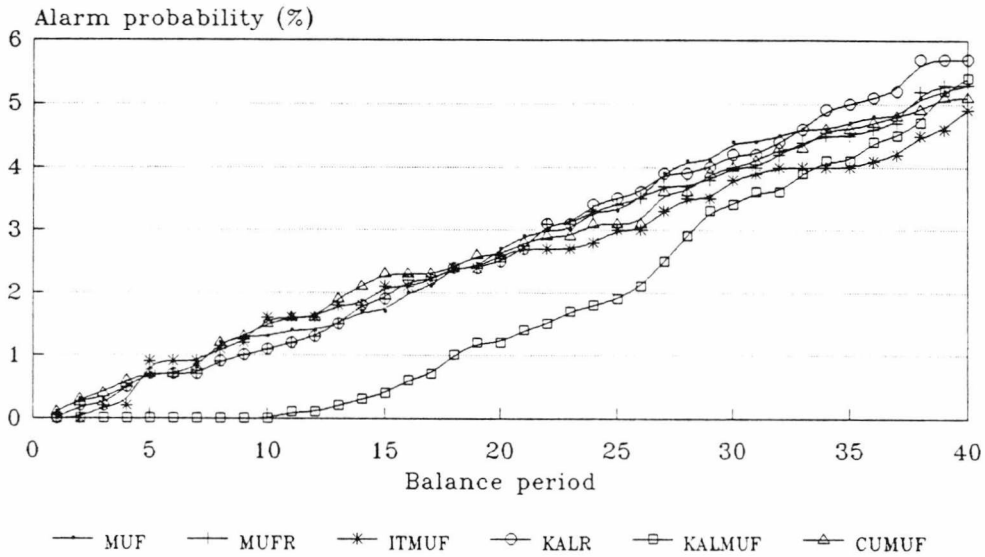


Fig VI.2 Cumulative false alarm probabilities
Varying CUMUF thresholds, new accountancy system

The H-K curves for the old and new systems are shown in figures VI.3 - VI.8. The H-K curves for MUFR and KALR are, as expected, the same for both accountancy systems.

Page's Test thresholds

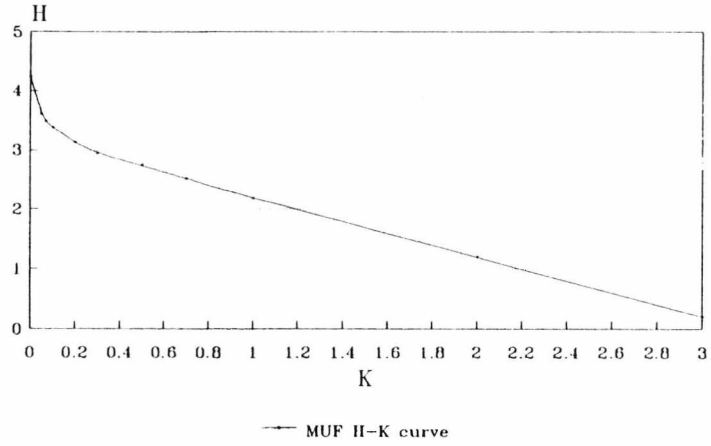


Fig. VI.3 MUF H-K curve
Old accountancy system

Page's Test thresholds

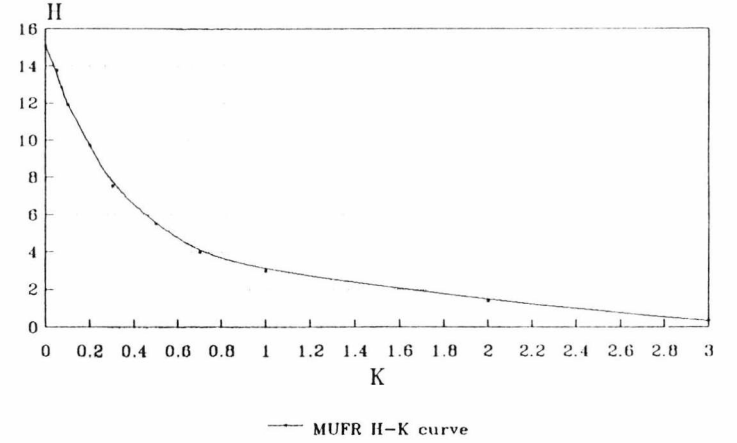


Fig. VI.4 MUFR H-K curve

Page's Test thresholds

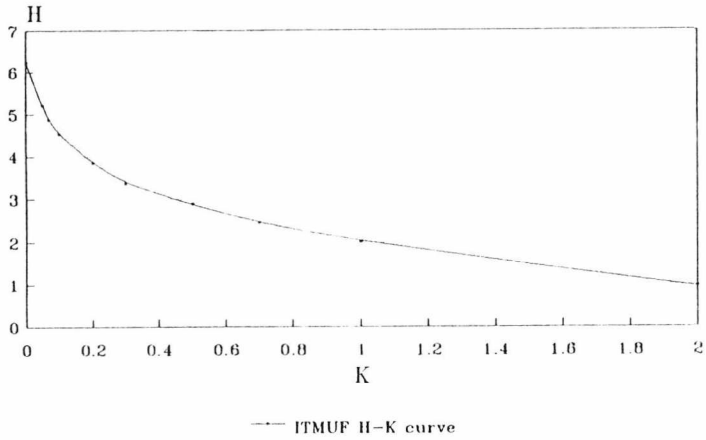


Fig. VI.5 ITMUF H-K curve
Old accountancy system

Page's Test thresholds

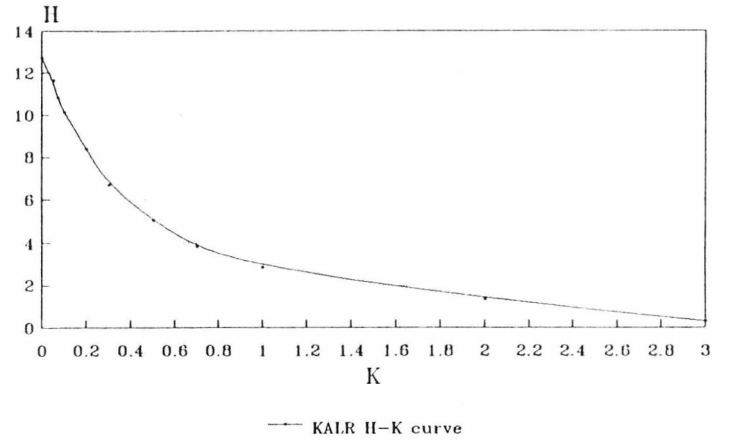


Fig. VI.6 KALR H-K curve

Page's Test thresholds

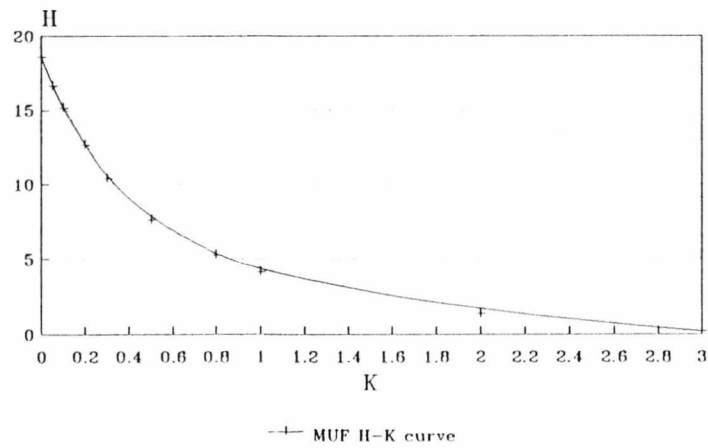


Fig. VI.7 MUF H-K curve
New accountancy system

Page's Test thresholds

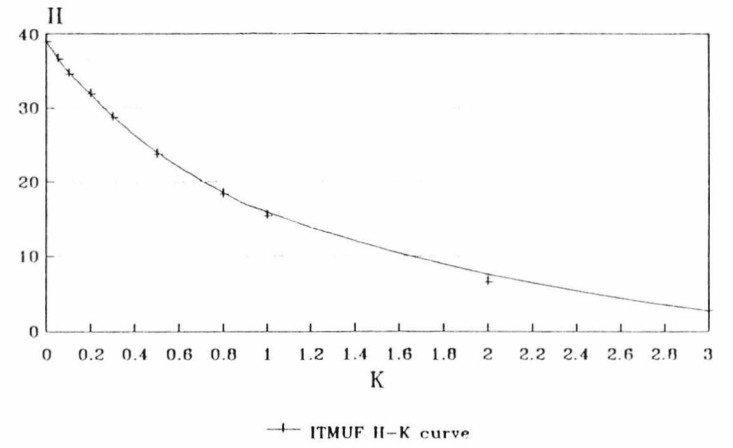


Fig. VI.8 ITMUF H-K curve
New accountancy system

APPENDIX VII – A method of calculating the residuals sequence from a general covariance matrix

Introduction

Sellinschegg [32] has described an efficient recursive algorithm for calculating the MUF-residuals transformation matrix based on conditional covariances. The algorithm proposed here is developed through a diagonalisation of the covariance matrix. In general, this requires more calculation than Sellinschegg's method; however, if the statistical test deems that a diversion has taken place (the system is 'out of control'), this offers an easier way to reset the residuals calculation at that point, ignoring previous correlations. This is particularly useful in Page's Test, where the Cusum statistic merely represents a 'score' attributed to the system performance, rather than an estimate of the loss.

Method

Given a serially correlated vector \underline{x} , representing a MUF sequence with covariance matrix T , a transformation matrix to remove the serial correlation can be calculated [13]. This matrix, B , is lower triangular with leading diagonal elements all '1'. The transformation can be stated

$$\underline{y} = B \cdot \underline{x} \quad (\text{VII.1})$$

where each element of \underline{y} is independent of the others.

The matrix B has the property that

$$D = B.T.B^T \quad (\text{VII.2})$$

is diagonal.

Calculation of the transformation matrix

$$B = \begin{bmatrix} 1 & 0 & 0 & \cdot & \cdot & 0 \\ B_{21} & 1 & 0 & & & \cdot \\ B_{31} & B_{32} & 1 & \cdot & & \cdot \\ \cdot & & & \cdot & \cdot & \cdot \\ \cdot & & & & \cdot & 0 \\ B_{n1} & \cdot & \cdot & \cdot & B_{n \ n-1} & 1 \end{bmatrix} \quad (\text{VII.3})$$

with

$$B_{ij} = \frac{\sigma_i M_{ij}}{\sigma_j M_{ii}} ; \quad i = 2, \dots, n; j = 1, \dots, i-1 \quad (\text{VII.4})$$

where M_{ij} is the (i,j) th cofactor of C_i , the correlation matrix of the set $\left(X_j \right)_{j=1}^i$ found from T.

$$\left(C_i \right)_{km} = \text{cor}(x_k, x_m) ; \quad k, m = 1, \dots, i \quad (\text{VII.5})$$

$$\text{cor}(x_k, x_k) = 1 \quad (\text{VII.6})$$

To calculate the (i) th row of B, the (i) th row of cofactors from the correlation matrix are required. The (i) th row of the inverse of C_i would contain these elements, each multiplied by the determinant of C_i . As one element is divided by another for each of the elements of B, the determinant can be ignored and the terms of

the inverse used in the expression.

Inversion of the correlation matrix

Taking advantage of the symmetric, positive definite nature of the correlation matrix, an efficient inversion can be effected using Choleski's method [63]. C_i is first expressed as the product of two triangular matrices:

$$C_i = S^T S \quad (\text{VII.7})$$

or

$$\begin{bmatrix} c_{11} & c_{12} & c_{13} & \cdot & c_{1i} \\ c_{21} & c_{22} & c_{23} & \cdot & \cdot \\ c_{31} & c_{32} & c_{33} & \cdot & \cdot \\ \cdot & \cdot & \cdot & \cdot & \cdot \\ c_{ii} & \cdot & \cdot & \cdot & c_{ii} \end{bmatrix} = \begin{bmatrix} s_{11} & 0 & 0 & \cdot & 0 \\ s_{12} & s_{22} & 0 & \cdot & \cdot \\ s_{13} & s_{23} & s_{33} & 0 & \cdot \\ \cdot & \cdot & \cdot & \cdot & 0 \\ s_{1i} & \cdot & \cdot & \cdot & s_{ii} \end{bmatrix} \begin{bmatrix} s_{11} & s_{12} & s_{13} & \cdot & s_{1i} \\ 0 & s_{22} & s_{23} & \cdot & s_{2i} \\ 0 & 0 & s_{33} & \cdot & \cdot \\ \cdot & \cdot & \cdot & \cdot & \cdot \\ 0 & \cdot & \cdot & \cdot & s_{ii} \end{bmatrix} \quad (\text{VII.8})$$

This is achieved using the relationships

$$s_{xx} = \left(c_{xx} - \sum_{z=1}^{x-1} s_{zx}^2 \right)^{1/2} ; \quad s_{xy} = \frac{c_{xy} - \sum_{z=1}^{y-1} s_{zx} s_{zy}}{s_{xx}} , \quad y > x \quad (\text{VII.9})$$

S can be inverted to give the matrix A using the algorithm

$$a_{xy} = -\frac{1}{s_{xx}} \sum_{z=x+1}^{x+w} s_{zx} a_{zy}, \quad y = x + w \quad (\text{VII.10})$$

A is a lower triangular matrix.

Thus

$$C_i^{-1} = A A^T \quad (\text{VII.11})$$

Only the i th row of C_i^{-1} is required; as the i th row of A contains only the element a_{ii} , this can be found from

$$C_i^{-1}(i,j) = |C_i| \cdot M_{ij} = a_{ii} \times a_{ji} \quad (\text{VII.12})$$

Thus

$$B_{ij} = \frac{\sigma_i a_{ji}}{\sigma_j a_{ii}}; \quad i = 2, \dots, n; \quad j = 1, \dots, i-1 \quad (\text{VII.13})$$

Conclusions

This technique enables the residuals sequence of an 'out of control' sequence to be reset merely by moving the start point of the transformation calculation to the period after the statistical test has signalled a fault.

Compared to general matrix inversion techniques, the utilisation of the properties of the covariance matrix enable substantial savings in calculation times, typically quartering the time required to carry out the full set of inversions for a one hundred balance period campaign without diversion alarm.

APPENDIX VIII - Derivation of the Kalman Filter

The Kalman Filter calculates a set of optimal estimates for the state variables from a prediction and an observation, each weighted according to their relative accuracy. The prediction is found from a 'progression model', in which the values of the variables at (k+1) are expressed in terms of those at (k). There will be an uncertainty in the prediction - if the step was completely determinate, no filter would be required - which must be quantified in terms of an error vector of standard deviations (expandable to an error covariance matrix).

Progression model

$$\underline{x}_{k+1} = A_k \cdot \underline{x}_k + \underline{u}_k + \underline{\omega}_k \quad (\text{VIII.1})$$

where \underline{x} = State vector, dimension n

A = Progression matrix

\underline{u} = Input vector

$\underline{\omega}$ = Random error vector of uncertainties in A and \underline{u}

The observation consists of a set of measurements which may or may not correspond to the state variables; the relationship between the two is expressed in the 'measurement model'. Again, there will be uncertainties which must be explicitly quantified.

Measurement model

$$\underline{z}_k = H_k \cdot \underline{x}_k + \underline{v}_k \quad (\text{VIII.2})$$

where \underline{z} = Measurement vector, dimension m
 H = Observation matrix
 \underline{v} = Random measurement noise vector

The variances and covariances between the elements of the noise vectors \underline{w} and \underline{v} are summarized in the covariance matrices Q and R respectively:

$$Q_{ij} = \text{Cov}(\omega_i, \omega_j) \quad (\text{VIII.3})$$

$$R_{ij} = \text{Cov}(v_i, v_j) \quad (\text{VIII.4})$$

The derivation assumes that the noise vectors are zero-mean, and there is no covariance between the progression noise and the measurement noise.

The optimal linear estimate based on the prediction and the observation can be expressed:

$$\hat{\underline{x}}_k = K'_k \cdot \tilde{\underline{x}}_k + K_k \cdot \underline{z}_k \quad (\text{VIII.5})$$

where $\hat{\underline{x}}$ = Estimated state vector
 $\tilde{\underline{x}}$ = Predicted state vector
 K' , K are the weighting matrices

As the estimate must be unbiased, K' and K are related. By analysis of the error terms, these can be reduced to a single variable.

$$\hat{\underline{x}}_k = \underline{x}_k + \hat{\underline{e}}_k \quad (\text{VIII.6})$$

$$\tilde{\underline{x}}_k = \underline{x}_k + \tilde{\underline{e}}_k \quad (\text{VIII.7})$$

where $\hat{\underline{e}} =$ estimation error
 $\tilde{\underline{e}} =$ prediction error

Substituting identity (VIII.7) into the measurement equation (VIII.2), and replacing z_k in equation (VIII.5) with the new definition gives:

$$\hat{\underline{x}}_k = K'_k \cdot \tilde{\underline{x}}_k + K_k \cdot H_k \cdot \tilde{\underline{x}}_k - K_k \cdot H_k \cdot \tilde{\underline{e}}_k + K_k \cdot \underline{v}_k \quad (\text{VIII.8})$$

Applying the identities (VIII.6) and (VIII.7) leads to the result:

$$\hat{\underline{e}}_k = [K'_k + K_k \cdot H_k - I] \cdot \underline{x}_k + K_k \cdot \tilde{\underline{e}}_k + K_k \cdot \underline{v}_k \quad (\text{VIII.9})$$

Taking expectations:

$$\text{If the measurement noise is unbiased, } E[\underline{v}_k] = 0 \quad (\text{VIII.10})$$

$$\text{If the prediction is unbiased, } E[\tilde{\underline{e}}_k] = 0 \quad (\text{VIII.11})$$

$$\text{Thus for the estimate to be unbiased, } [K'_k + K_k \cdot H'_k - I] = 0 \quad (\text{VIII.12})$$

$$\text{Hence, } K'_k = I - K_k \cdot H_k \quad (\text{VIII.13})$$

and the estimate can now be written

$$\hat{\underline{x}}_k = \tilde{\underline{x}}_k + K_k \cdot [z_k - H_k \cdot \tilde{\underline{x}}_k] \quad (\text{VIII.14})$$

where K_k is termed the Kalman gain matrix

Calculation of the error covariance matrix of the estimate

The variance of \hat{x}_k , termed G_k , is defined by

$$G_k = E[\hat{e}_k \cdot \hat{e}_k^T] \quad (\text{VIII.15})$$

From (VIII.14), using (VIII.2), (VIII.6) and (VIII.7), the estimation error term is

$$\hat{e}_k = [I - K_k \cdot H_k] \tilde{e}_k + K_k \cdot v_k \quad (\text{VIII.16})$$

enabling the error covariance matrix to be expressed

$$G_k = E\{(I - K_k \cdot H_k) \tilde{e}_k \cdot [\tilde{e}_k^T \cdot (I - K_k \cdot H_k)^T + v_k^T \cdot K_k^T] + K_k \cdot v_k \cdot [\tilde{e}_k^T \cdot (I - K_k \cdot H_k)^T\} \quad (\text{VIII.17})$$

The error covariance matrices of the prediction and the observation are termed P_k and R_k respectively:

$$P_k = E[\tilde{e}_k \cdot \tilde{e}_k^T] \quad (\text{VIII.18})$$

$$R_k = E[v_k \cdot v_k^T] \quad (\text{VIII.19})$$

As there is no correlation between the error sources,

$$E[\tilde{e}_k \cdot v_k^T] = E[v_k \cdot \tilde{e}_k^T] = 0 \quad (\text{VIII.20})$$

reducing the estimation error covariance matrix to

$$G_k = (I - K_k \cdot H_k) \cdot P_k \cdot (I - K_k \cdot H_k)^T + K_k \cdot R_k \cdot K_k^T \quad (\text{VIII.21})$$

Choice of the Kalman gain matrix

The Kalman gain matrix K_k is chosen to minimize the variance of \hat{x} , which translates to minimizing the trace of G_k , termed J_k . The value of K_k that fulfils this requirement is found by setting the partial derivative of J_k with respect to K_k equal to zero:

$$J_k = \text{trace}[G_k] = \sum_{i=1}^n G_k(i,i) \quad (\text{VIII.22})$$

$$\frac{\partial J_k}{\partial K_k} = \frac{\partial}{\partial K_k} \text{trace} \left((I - K_k \cdot H_k) \cdot P_k \cdot (I - K_k \cdot H_k)^T + K_k \cdot R_k \cdot K_k^T \right) = 0 \quad (\text{VIII.23})$$

Using the identity (with matrix B symmetric)

$$\frac{\partial}{\partial A} [\text{trace}(A \cdot B \cdot A^T)] = 2 \cdot A \cdot B \quad (\text{VIII.24})$$

the differentiation is solved as

$$- 2 \cdot (I - K_k \cdot H_k) \cdot P_k \cdot H_k^T + 2 \cdot K_k \cdot R_k = 0 \quad (\text{VIII.25})$$

(P_k is a covariance matrix and is thus symmetric)

Thus the Kalman gain matrix is isolated as

$$K_k = P_k \cdot H_k^T \cdot [H_k \cdot P_k \cdot H_k^T + R_k]^{-1} \quad (\text{VIII.26})$$

To ensure that this is indeed a minimum, the Hessian of J_k must be positive semidefinite, ie.

$$\frac{\partial^2 J_k}{\partial^2 K_k} \geq 0 \quad (\text{VIII.27})$$

$$\frac{\partial^2 J_k}{\partial^2 K_k} = 2 \cdot H_k \cdot P_k \cdot H_k^T + 2 \cdot R_k \quad (\text{VIII.28})$$

P_k and R_k are both covariance matrices, and so are positive semidefinite. Thus, provided H_k is of full rank (non-singular), the Hessian will be positive semidefinite.

Substitution of the optimizing Kalman gain (VIII.26) into the estimate covariance expression (VIII.21) gives

$$G_k = P_k - P_k \cdot H_k^T \cdot [H_k \cdot P_k \cdot H_k^T + R_k]^{-1} \cdot H_k \cdot P_k \quad (\text{VIII.29})$$

$$= [I - K_k \cdot H_k] \cdot P_k \quad (\text{VIII.30})$$

Calculation of the error covariance matrix of the prediction

The prediction error covariance matrix is defined by

$$P_k = E[\tilde{e}_k \cdot \tilde{e}_k^T] \quad (\text{VIII.31})$$

which, from (VIII.6), expands to

$$P_k = E[(\tilde{x}_k - \hat{x}_k) \cdot (\tilde{x}_k - \hat{x}_k)^T] \quad (\text{VIII.32})$$

By definition,

$$\tilde{x}_k = A_{k-1} \cdot \hat{x}_{k-1} + u_{k-1} \quad (\text{VIII.33})$$

and from (VIII.1),

$$\hat{x}_k = A_{k-1} \cdot \hat{x}_{k-1} + u_{k-1} + \omega_{k-1} \quad (\text{VIII.34})$$

Thus,

$$\tilde{\underline{e}}_k = A_{k-1} \cdot \hat{\underline{x}}_{k-1} - A_{k-1} \cdot \underline{x}_{k-1} - \underline{\omega}_{k-1} \quad (\text{VIII.35})$$

$$= A_{k-1} \cdot \hat{\underline{e}}_{k-1} - \underline{\omega}_{k-1} \quad (\text{VIII.36})$$

Substituting in (VIII.31) gives the prediction error covariance matrix as:

$$P_k = A_{k-1} \cdot G_{k-1} \cdot A_{k-1} + Q_{k-1} \quad (\text{VIII.37})$$